## ABSTRACT

MARZOLF, NICHOLAS S. Drivers and Consequences of $CO_2$ Inputs to Lowland Neotropical Streams. (Under the direction of Dr. Marcelo Ardón).

Carbon (C) cycling in inland waters is recognized as a globally relevant flux, but contributions from terrestrial ecosystems, $CO_2$ evasion to the atmosphere, and internal C processing remain poorly constrained. While the number of C flux estimates in inland waters is increasing, tropical headwater streams remain understudied despite being hotspots of carbon evasion. In this dissertation, I explore C cycling in tropical streams and rivers and evaluate C fluxes as a driver of disturbances in headwater streams. My objectives were: 1) synthesize estimates of gross primary production (GPP) and ecosystem respiration (ER) from streams and rivers in the global tropics and examine drivers of these rates; 2) estimate input and export C fluxes into a headwater tropical stream and evaluate episodic and seasonal rainfall as a driver of carbon fluxes; and 3) determine the effect of episodic acidification on individual, community, and ecosystem scale processes in headwater tropical streams across a range of acidification frequency. I determined: 1) GPP and ER are similar in magnitude to estimates from temperate streams; 2) terrestrial $CO_2$ inputs in groundwater are a greater C source than in-stream NEP and hydrologic export and $CO_2$ evasion are important losses of C; 3) experimentally altering the acidification frequency in a tropical headwater stream had little effect at individual, assemblage or ecosystem scales and suggesting that biota in streams with frequent acidification are adapted to periods of low pH. My research advances understanding of the sources of C to headwater tropical streams, the consequences of C driven changes in stream water pH, and the large-scale patterns in C metabolism across tropical and temperate streams.

Drivers and Consequences of $CO_2$ Inputs to Lowland Neotropical Streams

by
Nicholas Scott Marzolf

A dissertation submitted to the Graduate Faculty of
North Carolina State University
in partial fulfillment of the
requirements for the degree of
Doctor of Philosophy

Forestry and Environmental Resources

Raleigh, North Carolina

2021

APPROVED BY:

| | |
|---|---|
| Marcelo Ardón<br>Chair of Advisory Committee | Alonso Ramírez |
| David Genereux | Diana Oviedo-Vargas<br>External Member |
| Diego Riveros-Iregui | |

## DEDICATION

To my wife: Emma. Without her constant love, patience, kindness, laughter, and support, this document does not exist.

To my large family: who I did not see as much as we all would have wanted since this journey took me across the globe, but who know better than most what graduate school requires. I cannot wait to spend more time with you all.

## BIOGRAPHY

Nicholas (Nick) Marzolf was born in Sacramento, California, the son of Dr. Erich Marzolf and Cheryl Scott. Soon after, the family moved to Knoxville, Tennessee, where a sister, Aliah Marzolf, was born. The family soon moved to Gainesville, Florida where they made home base for the next 20 years. Nick played soccer and was a member of various bands, ensembles, and orchestras throughout high school, while in the International Baccalaureate program at Eastside High School.

Nick attended the University of Florida and received a Bachelor of Science in Biology. He attended a study abroad to the Yucatán peninsula, Mexico, focused on water resources and anthropology, and planting the seed of working in the tropics. Nick then pursued a Master of Science degree at the University of Georgia, in partnership with the Joseph W. Jones Ecological Research Center. His research documented the expansion of invasive apple snails (*Pomacea maculata*) and the consequences of population growth in Lake Seminole, Georgia. He stayed in southwest Georgia as a research technician in the Aquatic Biology lab at the Jones Center before starting a Ph.D. at North Carolina State University in Raleigh, NC. His research, as described in this document, measures carbon fluxes and cycling in headwater tropical streams and the consequences of episodic acidification events.

## ACKNOWLEDGMENTS

To my advisor, Dr. Marcelo Ardón: for being encouraging, caring, inspiring, and wise when I needed it, and more importantly, when I didn't know I needed it.

To my committee: Drs. Alonso Ramírez, David Genereux, Diana Oviedo-Vargas, and Diego Riveros-Iregui: for pushing me on what I know and showing me all that I need to learn.

To my REU students: Terrius Bruce, Dominic Baca, Mariely Vega-Gomez, Yessica Jimenez, and Breann Benitez: for keeping me organized and teaching me more about field work, lab work, writing, statistics, and natural history than I surely taught you all.

To the STREAMS project team: Minor Hidalgo, Dr. Carissa Ganong, Dr. Chip Small, Ana Meza-Salazar, Dr. Pablo Gutierrez, Dr. Alan Jackman, Dr. John Duff, and Dr. Cathy Pringle: for helping a graduate student with too many questions.

To the Ardón Lab members: Melinda, Matt, Steve, Kelsey, and Pete: for weekly support sessions during lab meetings and being willing to get ice cream/burritos/coffee at the drop of a hat.

## TABLE OF CONTENTS

## LIST OF TABLES

## LIST OF FIGURES

# Chapter 1: Introduction

The carbon (C) cycle of inland waters has undergone rapid reassessment and determined their contributions are relevant at global scales. Early global climate models (GCM) identified biologically active 'boxes' for terrestrial ecosystems and the ocean (Siegenthaler and Sarmiento 1993). However, as GCM became more sophisticated, inland waters (streams, rivers, lakes, reservoirs, and wetlands) remained 'passive' players, transporting C from the land to the ocean without substantially transforming C (Cramer et al. 2001). However, numerous studies now refute the 'passivity' of inland waters. In a seminal paper, Cole et al. (2007) challenge the 'passive pipe' assessment with C flux data from inland waters and argue that, rather than pipes connecting the land to the ocean, inland waters integrate terrestrial processes and are 'active bioreactors'. Subsequent reviews have documented large C fluxes between inland waters and terrestrial ecosystems and the atmosphere (Drake et al. 2018; Tank et al. 2018).

In this dissertation, I study C fluxes in tropical streams and rivers. In Chapter 2, I collect and synthesize internal C fluxes from tropical streams and rivers and explore hierarchical control of in-stream processes. In Chapter 2, I use aquatic sensors to estimate C input and export fluxes from a headwater tropical stream, and examine episodic and seasonal rainfall as a driver of C fluxes. In Chapter 4, I explore how the frequency of stream acidification events affects individual, assemblage, and ecosystem scale processes using an *in situ* manipulative experiment.

## 1.1 Carbon cycling in inland waters

### 1.1.1 Terrestrial carbon inputs to inland waters

Carbon enters the biosphere through gross primary production (GPP) as fixation of atmospheric $CO_2$ into autotrophic biomass (Schlesinger and Bernhardt 2013). This C then fuels ecosystem respiration (ER), as the sum of all autotrophic and heterotrophic respiration. The

difference between GPP and ER is net ecosystem production (NEP) and is either stored within the ecosystem (e.g. burial in sediments and soils), respired to $CO_2$, incorporated into food webs, or exported (Schlesinger and Bernhardt 2013). A large fraction of C is exported via fluvial processes, including C as dissolved inorganic C (DIC), dissolved organic C (DOC), or particulate organic C (POC). Fluvial C exports from terrestrial ecosystems become C inputs to inland waters in either organic or inorganic forms. In addition to biogenic C, inorganic C from terrestrial ecosystems stem from weathering of carbonate and aluminosilicate minerals to $HCO_3^-$ through dissolution by carbonic acid (Gaillardet et al. 1999). Terrestrial C export to inland waters is estimated to be similar in magnitude to terrestrial NEP (2 Pg C $yr^{-1}$, Cole et al. 2007; Battin et al. 2009; Aufdenkampe et al. 2011). However, this estimate was recently updated to 5.1 Pg C $yr^{-1}$ (Sawakuchi et al. 2017; Drake et al. 2018), suggesting inland waters are disproportionately active participants in C fluxes between the land and the atmosphere (Raymond et al. 2013).

Estimating terrestrial C flux to inland waters began with a mass balance approach (Cole et al. 2007). Early terrestrial flux to inland waters was estimated as the difference between inputs (e.g. terrestrial NEP) and losses (e.g. sum of hydrologic export, storage, and evasion to the atmosphere). As a result, the balance is susceptible to changes in the constituent fluxes, notably evasion due to new empirical measurements and estimates of spatial extent of water (Allen and Pavelsky 2018). Empirical approaches to estimate C flux to inland waters use a variety of techniques to identify and quantify subsurface flowpaths and the C being transported. Infrared gas analyzers (IRGA) are now adapted to deploy in aquatic settings (Johnson et al. 2010), including in subsurface wells. Sensors deployed in riparian wells measure $CO_2$ inputs at the terrestrial-aquatic interface and reflect high $CO_2$ concentrations from soil respiration (Leith et al. 2015). However, simultaneously estimating the volumetric groundwater discharge is required to

calculate this flux and is a limitation of this approach. Coupling $CO_2$ IRGA sensors with $O_2$ sensors to estimate stream ecosystem metabolism allows partitioning of the internal flux of C (see section 1.1.2) and can solve the external C flux by mass balance at the reach scale (Hotchkiss et al. 2015; Lupon et al. 2019; Rocher-Ros et al. 2019). Isotopic signatures of subsurface C (for DOC or DIC as $^{14}C$ and $^{13}C$) can help determine the age and source material of groundwater C that discharges into surface waters (Campeau et al. 2018, 2019).

In Chapter 3, I combine IRGA $CO_2$ sensors in both the stream and a riparian well with an in-stream $O_2$ sensor to simultaneously estimate internal and external fluxes of $CO_2$. Using stream discharge from a V-notch weir and conservative solute tracer injections to calculate groundwater discharge, I estimate terrestrial $CO_2$ flux in a headwater tropical stream.

### 1.1.2 Internal carbon cycling in inland waters

While inland waters receive substantial C from terrestrial ecosystems in organic and inorganic forms, in-stream GPP and ER contribute to net C fluxes. In general, most streams, rivers, lakes, and reservoirs are net heterotrophic (GPP < ER, Odum 1956; Hoellein et al. 2013). Estimates of GPP and ER in inland waters have increased study due to methodological advances (Marzolf et al. 1994; Holtgrieve et al. 2010; Appling et al. 2018), though disentangling the spatiotemporal, geomorphological, and physicochemical variability on GPP and ER remains under scrutiny (Bernot et al. 2010; Finlay 2011; Hoellein et al. 2013; Bernhardt et al. 2018).

Fluvial GPP is hypothesized to increase with longitudinal position (Vannote et al. 1980). Empirical studies have demonstrated this transition as a shift in metabolic processes from the benthos to pelagic zone in intermediate rivers (Hall et al. 2016; Reisinger et al. 2021). Temperate streams exhibit seasonal shifts in GPP and ER, related to terrestrial canopy cover (Roberts et al.

2007), stressing the importance of light in predicting GPP and ER (Finlay 2011). Stream flow influences GPP and ER, though there are few examples of correlating metabolic rates across a range of discharge. In temperate peatland streams, storms pulse labile DOC that stimulate ER during flow events (Demars 2019). At high flows, stream turbidity increases and acts to attenuate light in the water column (Reisinger et al. 2021) and high flows can scour benthic primary producers (Grimm and Fisher 1989), thereby inhibiting GPP. Nutrients often have a stimulatory effect on biota in inland waters, but there is limited evidence of a stimulatory effect of nutrients, primarily nitrogen (N) and phosphorus (P), on GPP and ER (Mulholland et al. 2001; Bernot et al. 2006, 2010). Despite widespread evidence of nutrients on ecosystem-scale processes, there is strong evidence for the stimulatory effect of N and P on processes that contribute to GPP and ER in tropical streams (Rosemond et al. 2002; Ramírez et al. 2003; Ardón et al. 2006), suggesting hierarchal mediation of GPP and ER.

In Chapter 2, I review and synthesize published estimates of GPP and ER from tropical streams and rivers, evaluate relevant drivers of in-stream C fluxes, and compare the drivers between temperate and tropical biomes. In Chapter 3, I estimate six months of in-stream NEP from a headwater tropical stream and assess the temporal variability across precipitation-driven seasonality.

### 1.1.3 Carbon evasion to the atmosphere from inland waters

Carbon inputs from terrestrial ecosystems and internal production result in inland waters supersaturated with $CO_2$, and therefore a source of C to the atmosphere (Raymond et al. 2013). Early estimates of C evasion reported 0.5 Pg C $yr^{-1}$ from Amazon basin alone, and led to global reassessment of evasion from inland waters (Richey et al. 2002). The first global study of $CO_2$

concentration, gas exchange, and evasion estimated 2.1 Pg C $yr^{-1}$ (Raymond et al. 2013) and provided a model for future studies. Current global estimates of $CO_2$ evasion are 3.88 Pg C $yr^{-1}$ (Sawakuchi et al. 2017, Drake et al. 2018). However, headwater and tropical streams remain understudied and under accounted in updated estimates and continued study from these streams will increase estimates of global C emissions from inland waters (Borges et al. 2019).

Fluvial $CO_2$ evasion is a large and important flux but attributing inputs of $CO_2$ to evasion remains difficult. Contributions of in-stream NEP to fluvial $CO_2$ (~28%) remains constant across headwaters to large rivers, though the relative contribution of in-stream NEP increases compared to external inputs in larger rivers (Hotchkiss et al. 2015). Headwater streams are disproportionate areas of C evasion, due to larger external terrestrial inputs that are quickly evaded to the atmosphere and high surface area to water volume ratio (Hotchkiss et al. 2015; Campeau et al. 2019). In tundra-dominated headwater streams, stream ecosystem NEP drives $CO_2$ evasion (Rocher-Ros et al. 2019). In the Amazon basin, $CO_2$ evasion is driven by in-stream respiration of young (<5 y) organic matter (Mayorga et al. 2005). In lowland streams in Costa Rica, inputs of $CO_2$ supersaturated inter-basin groundwater result in spatial variation in evasion between adjacent watersheds and changes the forest from a net C sink to a net C source to the atmosphere when properly accounted for (Genereux et al. 2013; Oviedo-Vargas et al. 2015).

In Chapter 3, I compare two sources of C inputs, in-stream NEP and groundwater $CO_2$, to daily estimates of $CO_2$ evasion and explore hydrologic drivers of these fluxes in a headwater tropical stream. Simultaneous measurement of these fluxes allowed for partitioning of relative C inputs to C evasion across the precipitation-driven seasonality.

### 1.1.4 Fluvial carbon export from inland waters

Estimates of total C export from streams and rivers is 0.95 Pg C $yr^{-1}$. Unlike the terrestrial C flux to inland waters and C evasion, estimates of fluvial C export has varied little (Cole et al. 2007; Drake et al. 2018). Export from inland waters is in the range of terrestrial NEP estimates (1 – 4 Pg C $yr^{-1}$, Randerson et al. (2002)), suggesting terrestrial NEP contributes to fluvial export. Reliability in river discharge estimates, stability in the chemical constituents of major rivers, and river-basin models for nutrients has maintained precise and robust estimates of C export to the ocean (Mayorga et al. 2010; Drake et al. 2018)

Hydrologic C export includes organic or inorganic forms. Global DOC exports increase with discharge in large rivers (Clair and Ehrman 1996; Freeman et al. 2004) and is predictive at multiple time scales (Raymond and Saiers 2010; Tank et al. 2018). Storms exert some regulation of DOC export (Raymond et al. 2016). In paired lowland watersheds, Costa Rica, DOC export as stormflow had similar quantity and quality despite inputs of inter-basin groundwater into only one watershed (Osburn et al. 2018). In temperate peatland streams, storm pulses through organic soils transport DOC to streams that is respired by stream microbes, representing an increase in DOC export that is offset as $CO_2$ export or as $CO_2$ evasion (Tank et al. 2018).

DIC export speciates according the carbonate equilibrium and is pH dependent (Stumm and Morgan 1996a). DIC speciates into the dominant forms of $H_2CO_3$*, or $CO_2$, at low pH (pH < 6.25), $HCO_3^-$ at intermediate pH (6.25 < pH < 10.3), or $CO_3^{2-}$ at high pH (pH > 10.3). Elevated DIC export can result from weathering of silicates and carbonates and accelerated from biogenic carbonic acid production from soil respiration (Gislason et al. 2009; Beaulieu et al. 2012). Around 75% of the DIC from soil respiration is never measured as soil respiration (globally ~91 Pg C $yr^{-1}$, Hashimoto et al. (2015)), but is hidden as the $HCO_3^-$ ion and protected against evasion

to the atmosphere, and more likely to be exported to the ocean (Cole et al. 2007). Groundwater is an important abiotic source of DIC to surface waters and relevant to C budgets, particularly groundwater that flows through carbonate-rich lithologies, where biogenic contribution decreases and $HCO_3^-$ contributions increase (Stoddard et al. 1999). Magmatic and geogenic sources of DIC in groundwater can increase DIC flux into surface waters (Genereux et al. 2013).

In Chapter 3, I combine sensor measurements of $CO_2$ and pH with discharge measured at a V-notch weir to estimate hydrologic export of $CO_2$ and $HCO_3^-$ from a headwater tropical stream. I compare this loss to estimates of C export from similarly sized streams in the tropics.

## 1.2 Disturbance ecology

Ecosystems are subject to disturbances that change their abiotic and biotic composition. Disturbances are defined along a spectrum. Discrete events shift ecosystems from equilibria and have biological consequences on structure and function (Sousa 1984; Resh et al. 1988; Townsend 1989; Poff 1992; Stanley et al. 2010). Conversely, disturbances are processes that exhibit legacy effects with a recurrence interval and influences ecosystem succession (Grimm et al. 2017; Graham et al. 2020). Disturbances vary over temporal and spatial scales (Lake 2000), from high frequency-low magnitude events to low frequency-high magnitude events (Sousa 1984). For example, infrequent and large magnitude events can be floods caused by hurricanes with low recurrence intervals while frequent and low magnitude events are seasonal floods or episodic acidification events with high recurrence intervals (Lake 2000). High frequency, low magnitude events can be interpreted, rather than disturbances, but as features of the ecosystem to which the biota have developed adaptions (Lytle and Poff 2004). Examples include snowmelt

high flows mountain streams (Poff 1992), tidal changes (Sousa 1984), and fire in longleaf pine ecosystems (Palik et al. 2002).

In stream ecosystems, the definition of disturbance has evolved to account for spatial, temporal, and ecological variability (Pickett and White 1985; Resh et al. 1988; Poff 1992; Lake 2000; Stanley et al. 2010). Disturbances in streams are defined by 1) quantifiable metrics of the disturbance (e.g. intensity, frequency, and duration); and 2) biological consequences. Disturbances in streams centered around changes in flow as either discrete events that alter ecosystem function (e.g. flooding from hurricanes, (Poff et al. 1997; Pickett and White 2013), or across a continuum of disturbances to incorporate spatial and temporal variability as pulses (e.g. seasonal floods), presses (e.g. barrier effects of dams), and ramps (e.g. droughts) (Lake 2000; Graham et al. 2020). Changes in stream physicochemistry across temporal and spatial scales may also be disturbances with better understanding of the temporal and spatial variability and effect on biota. Non-hydrologic disturbance events in streams (Lake 2000, Stanley et al. 2010) include temperature (Harper and Peckarsky 2006), incident light (Steinman et al. 1991), and pollutants or chemicals (Steinman et al. 1992; Harper and Peckarsky 2005).

Stream pH, which varies as a result of concentrations of dissolved solutes, inorganic carbon, and rainfall chemistry (Stumm and Morgan 1996b), is a parameter with biological consequences, particularly under acidic conditions. We define acidification events as periods of rapid and temporary pH declines or loss of acid neutralizing capacity (Laudon et al. 2004), resulting in a wide range of consequences on stream ecosystem structure and function. In temperate streams, low pH (<6) streams had slower rates of leaf litter decomposition, microbial respiration, and bacterial production in streams compared to streams with higher pH (>6) (Mulholland et al. 1987). Long-term stream and lake acidification due to acid-rain inputs and

reduced acid neutralizing capacity had detrimental effects on fish, macroinvertebrate, and algal assemblages (Bernard et al. 1990; Baker et al. 1996). In tropical streams in Costa Rica, there is a linkage between acidification events and rainfall variability, partly driven by El Niño Southern Oscillation (Small et al. 2012). In these streams in Costa Rica, macroinvertebrate drift increased in response to experimental acidification (Ardón et al. 2013), supporting acidification events as disturbances.

In Chapter 4, I explore the effects of episodic acidification in headwaters streams at La Selva Biological Station, Costa Rica. Acidification frequency varies due to inputs of inter-basin groundwater inputs with high buffering capacity. Streams with low buffering capacity experience episodic and seasonal acidification due to terrestrial $CO_2$ and Fe inputs (Chapter 3, Small et al. 2012; Ganong 2015). I experimentally increased the buffering capacity of a low buffering capacity stream and measured structural and functional metrics at individual, assemblage, and ecosystem scales to determine where acidification effects occur and if the effects propagate through the ecosystem hierarchy.

1.3 References


Allen, G. H., and T. M. Pavelsky. 2018. Global extent of rivers and streams. Science (80-. ). **361**: 585–588.

Appling, A. P., R. O. Hall, C. B. Yackulic, and M. Arroita. 2018. Overcoming Equifinality: Leveraging Long Time Series for Stream Metabolism Estimation. J. Geophys. Res. Biogeosciences **123**: 624–645. doi:10.1002/2017jg004140

Ardón, M., J. H. Duff, A. Ramírez, G. E. Small, A. P. Jackman, F. J. Triska, and C. M. Pringle. 2013. Experimental acidification of two biogeochemically-distinct neotropical streams: buffering mechanisms and macroinvertebrate drift. Sci. Total Environ. **443**: 267–277. doi:10.1016/j.scitotenv.2012.10.068

Ardón, M., L. A. Stallcup, and C. M. Pringle. 2006. Does leaf quality mediate the stimulation of leaf breakdown by phosphorus in Neotropical streams? Freshw. Biol. **51**: 618–633. doi:10.1111/j.1365-2427.2006.01515.x

Aufdenkampe, A. K., E. Mayorga, P. A. Raymond, J. M. Melack, S. C. Doney, S. R. Alin, R. E. Aalto, and K. Yoo. 2011. Riverine coupling of biogeochemical cycles between land, oceans, and atmosphere. Front. Ecol. Environ. **9**: 53–60. doi:10.1890/100014

Baker, J. P., J. Van Sickle, C. J. Gagen, and others. 1996. Episodic Acidification of Small Streams in the Northeastern United States: Effects on Fish Populations. Ecol. Appl. **6**: 422–437. doi:10.2307/2269380

Battin, T. J., S. Luyssaert, L. A. Kaplan, A. K. Aufdenkampe, A. Richter, and L. J. Tranvik. 2009. The boundless carbon cycle. Nat. Geosci. **2**: 598–600. doi:10.1038/ngeo618

Beaulieu, E., Y. Goddéris, Y. Donnadieu, D. Labat, and C. Roelandt. 2012. High sensitivity of the continental-weathering carbon dioxide sink to future climate change. Nat. Clim. Chang. **2**: 346–349.

Bernard, D. P., W. E. Neil, and L. Rowe. 1990. Impact of mild experimental acidification on short term invertebrate drift in a sensitive British Columbia stream. Hydrobiologia **203**: 63–72. doi:10.1007/BF00005614

Bernhardt, E. S., J. B. Heffernan, N. B. Grimm, and others. 2018. The metabolic regimes of flowing waters. Limnol. Oceanogr. **63**: S99–S118. doi:10.1002/lno.10726

Bernot, M. J., D. J. Sobota, R. O. Hall, and others. 2010. Inter-regional comparison of land-use effects on stream metabolism. Freshw. Biol. **55**: 1874–1890. doi:10.1111/j.1365-2427.2010.02422.x

Bernot, M. J., J. L. Tank, T. V. Royer, and M. B. David. 2006. Nutrient uptake in streams draining agricultural catchments of the midwestern United States. Freshw. Biol. **51**: 499–509. doi:10.1111/j.1365-2427.2006.01508.x

Borges, A. V, F. Darchambeau, T. Lambert, and others. 2019. Variations in dissolved greenhouse gases (CO2, CH4, N2O) in the Congo River network overwhelmingly driven by fluvial-wetland connectivity. Biogeosciences **16**: 3801–3834.

Campeau, A., K. Bishop, N. Amvrosiadi, M. F. Billett, M. H. Garnett, H. Laudon, M. G. Öquist, and M. B. Wallin. 2019. Current forest carbon fixation fuels stream CO2 emissions. Nat. Commun. **10**. doi:10.1038/s41467-019-09922-3

Campeau, A., K. Bishop, M. B. Nilsson, L. Klemedtsson, H. Laudon, F. I. Leith, M. Öquist, and M. B. Wallin. 2018. Stable Carbon Isotopes Reveal Soil-Stream DIC Linkages in Contrasting Headwater Catchments. J. Geophys. Res. Biogeosciences **123**: 149–167. doi:10.1002/2017JG004083

Clair, T. A., and J. M. Ehrman. 1996. Variations in discharge and dissolved organic carbon and nitrogen export from terrestrial basins with changes in climate: a neural network approach. Limnol. Oceanogr. **41**: 921–927.
Cole, J. J., Y. T. Prairie, N. F. Caraco, and others. 2007. Plumbing the Global Carbon Cycle: Integrating Inland Waters into the Terrestrial Carbon Budget. Ecosystems **10**: 172–185. doi:10.1007/s10021-006-9013-8
Cramer, W., A. Bondeau, F. I. Woodward, and others. 2001. Global response of terrestrial ecosystem structure and function to CO2 and climate change: results from six dynamic global vegetation models. Glob. Chang. Biol. **7**: 357–373.
Demars, B. O. L. 2019. Hydrological pulses and burning of dissolved organic carbon by stream respiration. Limnol. Oceanogr. **64**: 406–421. doi:10.1002/lno.11048
Drake, T. W., P. A. Raymond, and R. G. M. Spencer. 2018. Terrestrial carbon inputs to inland waters: A current synthesis of estimates and uncertainty. Limnol. Oceanogr. Lett. **3**: 132–142. doi:10.1002/lol2.10055
Finlay, J. C. 2011. Stream size and human influences on ecosystem production in river networks. Ecosphere **2**: art87. doi:10.1890/es11-00071.1
Freeman, C., N. Fenner, N. J. Ostle, and others. 2004. Export of dissolved organic carbon from peatlands under elevated carbon dioxide levels. Nature **430**: 195–198.
Gaillardet, J., B. Dupré, P. Louvat, and C. J. Allegre. 1999. Global silicate weathering and CO2 consumption rates deduced from the chemistry of large rivers. Chem. Geol. **159**: 3–30.
Ganong, C. N. 2015. Effects of Precipitation Regime on Neotropical Streams: Biogeochemical Drivers of Stream Physicochemistry and Macroinvertebrate Tolerance to pH Shifts. University of Georgia.
Genereux, D. P., L. A. Nagy, C. L. Osburn, and S. F. Oberbauer. 2013. A connection to deep groundwater alters ecosystem carbon fluxes and budgets: Example from a Costa Rican rainforest. Geophys. Res. Lett. **40**: 2066–2070. doi:10.1002/grl.50423
Gislason, S. R., E. H. Oelkers, E. S. Eiriksdottir, and others. 2009. Direct evidence of the feedback between climate and weathering. Earth Planet. Sci. Lett. **277**: 213–222.
Graham, E., C. Averill, B. Bond-Lamberty, and others. 2020. Towards a generalizable framework of disturbance ecology through crowdsourced science. Front. Ecol. Evol. **9**: 76. doi:10.32942/osf.io/mxkgz
Grimm, N. B., and S. G. Fisher. 1989. Stability of periphyton and macroinvertebrates to disturbance by flash floods in a desert stream. J. North Am. Benthol. Soc. **8**: 293–307.
Grimm, N. B., S. T. A. Pickett, R. L. Hale, and M. L. Cadenasso. 2017. Does the ecological concept of disturbance have utility in urban social–ecological–technological systems? Ecosyst. Heal. Sustain. **3**: 1–18. doi:10.1002/ehs2.1255
Hall, R. O., J. L. Tank, M. A. Baker, E. J. Rosi-Marshall, and E. R. Hotchkiss. 2016. Metabolism, Gas Exchange, and Carbon Spiraling in Rivers. Ecosystems **19**: 73–86. doi:10.1007/s10021-015-9918-1
Harper, M. P., and B. L. Peckarsky. 2005. Effects of pulsed and pressed disturbances on the benthic invertebrate community following a coal spill in a small stream in northeastern USA. Hydrobiologia **544**: 241–247. doi:10.1007/s10750-005-0862-5
Harper, M. P., and B. L. Peckarsky. 2006. Emergence cues of a mayfly in a high-altitude stream ecosystem: Potential response to climate change. Ecol. Appl. **16**: 612–621. doi:10.1890/1051-0761(2006)016[0612:ECOAMI]2.0.CO;2
Hashimoto, S., N. Carvalhais, A. Ito, M. Migliavacca, K. Nishina, and M. Reichstein. 2015.

Global spatiotemporal distribution of soil respiration modeled using a global database. Biogeosciences **12**: 4121–4132.
Hoellein, T. J., D. A. Bruesewitz, and D. C. Richardson. 2013. Revisiting Odum (1956): A synthesis of aquatic ecosystem metabolism. Limnol. Oceanogr. **58**: 2089–2100. doi:10.4319/lo.2013.58.6.2089
Holtgrieve, G. W., D. E. Schindler, T. A. Branch, and Z. Teresa A'Mar. 2010. Simultaneous quantification of aquatic ecosystem metabolism and reaeration using a Bayesian statistical model of oxygen dynamics. Limnol. Oceanogr. **55**: 1047–1063. doi:10.4319/lo.2010.55.3.1047
Hotchkiss, E. R., R. O. Hall, R. A. Sponseller, D. Butman, J. Klaminder, H. Laudon, M. Rosvall, and J. Karlsson. 2015. Sources of and processes controlling CO2 emissions change with the size of streams and rivers. Nat. Geosci. **8**: 696–699. doi:10.1038/ngeo2507
Johnson, M. S., M. F. Billett, K. J. Dinsmore, M. Wallin, K. E. Dyson, and R. S. Jassal. 2010. Direct and continuous measurement of dissolved carbon dioxide in freshwater aquatic systems-method and applications. Ecohydrology 68–78. doi:10.1002/eco.95
Lake, P. S. 2000. Disturbance, patchiness, and diversity in streams. J. North Am. Benthol. Soc. **19**: 573–592. doi:10.2307/1468118
Laudon, H., P. J. Dillon, M. C. Eimers, R. G. Semkin, and D. S. Jeffries. 2004. Climate-induced episodic acidification of streams in central Ontario. Environ. Sci. Technol. **38**: 6009–6015. doi:10.1021/es049165o
Leith, F. I., K. J. Dinsmore, M. B. Wallin, M. F. Billett, K. V. Heal, H. Laudon, M. G. Öquist, and K. Bishop. 2015. Carbon dioxide transport across the hillslope-riparian-stream continuum in a boreal headwater catchment. Biogeosciences **12**: 1881–1902. doi:10.5194/bg-12-1881-2015
Lupon, A., B. A. Denfeld, H. Laudon, J. Leach, J. Karlsson, and R. A. Sponseller. 2019. Groundwater inflows control patterns and sources of greenhouse gas emissions from streams. Limnol. Oceanogr. doi:10.1002/lno.11134
Lytle, D. A., and N. L. R. Poff. 2004. Adaptation to natural flow regimes. Trends Ecol. Evol. **19**: 94–100. doi:10.1016/j.tree.2003.10.002
Marzolf, E. R., P. J. Mulholland, and A. D. Steinman. 1994. Improvements to the diurnal upstream-downstream dissolved oxygen change technique for determining whole stream metabolism in small streams. Can. J. Fish. Aquat. Sci. **51**: 1591–1599.
Mayorga, E., A. K. Aufdenkampe, C. A. Masiello, A. V. Krusche, J. I. Hedges, P. D. Quay, J. E. Richey, and T. A. Brown. 2005. Young organic matter as a source of carbon dioxide outgassing from Amazonian rivers. Nature **436**: 538–541. doi:10.1038/nature03880
Mayorga, E., S. P. Seitzinger, J. A. Harrison, and others. 2010. Global Nutrient Export from WaterSheds 2 (NEWS 2): Model development and implementation. Environ. Model. Softw. **25**: 837–853. doi:10.1016/j.envsoft.2010.01.007
Mulholland, P. J., C. S. Fellows, J. L. Tank, and others. 2001. Inter-biome comparison of factors controlling stream metabolism. Freshw. Biol. **46**: 1503–1517.
Mulholland, P. J., A. V Palumbo, J. W. Elwood, and A. D. Rosemond. 1987. Effects of acidification on leaf decomposition in streams. J. North Am. Benthol. Soc. **6**: 147–158.
Odum, H. T. 1956. Primary production in flowing waters. Limnol. Oceanogr. **1**: 102–117.
Osburn, C. L., D. Oviedo-Vargas, E. Barnett, D. Dierick, S. F. Oberbauer, and D. P. Genereux. 2018. Regional groundwater and storms are hydrologic controls on the quality and export of dissolved organic matter in two tropical rainforest streams, Costa Rica. J. Geophys. Res.

Biogeosciences. doi:10.1002/2017JG003960
Oviedo-Vargas, D., D. P. Genereux, D. Dierick, and S. F. Oberbauer. 2015. The effect of regional groundwater on carbon dioxide and methane emissions from a lowland rainforest stream in Costa Rica. J. Geophys. Res. Biogeosciences **120**: 2579–2595. doi:10.1002/
Palik, B. J., R. J. Mitchell, and J. K. Hiers. 2002. Modeling silviculture after natural disturbance to sustain biodiversity in the longleaf pine (Pinus palustris) ecosystem : balancing complexity and implementation. For. Ecol. Manage. **155**: 347–356.
Pickett, S. T. A., and P. S. White. 1985. The ecology of natural disturbance and patch dynamics, Aca.
Pickett, S. T. A., and P. S. White. 2013. The ecology of natural disturbance and patch dynamics, Elsevier.
Poff, N. L. 1992. Why Disturbances Can Be Predictable : A Perspective on the Definition of Disturbance in Streams Author ( s ): N . LeRoy Poff Source : Journal of the North American Benthological Society , Vol . 11 , No . 1 ( Mar ., 1992 ), Published by : The University of. J. North Am. Benthol. Soc. **11**: 86–92.
Poff, N. L., J. D. Allan, M. B. Bain, J. R. Karr, K. L. Prestegaard, B. D. Richter, R. E. Sparks, and J. C. Stromberg. 1997. The natural flow regime. Bioscience **47**: 769–784. doi:10.1007/s11277-014-1857-1
Ramírez, A., C. M. Pringle, and L. Molina. 2003. Effects of stream phosphorus levels on microbial respiration. Freshw. Biol. **48**: 88–97.
Randerson, J. T., F. S. Chapin Iii, J. W. Harden, J. C. Neff, and M. E. Harmon. 2002. Net ecosystem production: a comprehensive measure of net carbon accumulation by ecosystems. Ecol. Appl. **12**: 937–947.
Raymond, P. A., J. Hartmann, R. Lauerwald, and others. 2013. Global carbon dioxide emissions from inland waters. Nature **503**: 355–359. doi:10.1038/nature12760
Raymond, P. A., and J. E. Saiers. 2010. Event controlled DOC export from forested watersheds. Biogeochemistry **100**: 197–209.
Raymond, P. A., J. E. Saiers, and W. V Sobczak. 2016. Hydrological and biogeochemical controls on watershed dissolved organic matter transport: pulse-shunt concept. Ecology **97**: 5–16.
Reisinger, A. J., J. L. Tank, R. O. Hall, E. J. Rosi, M. A. Baker, and L. Genzoli. 2021. Water column contributions to the metabolism and nutrient dynamics of mid-sized rivers. Biogeochemistry. doi:10.1007/s10533-021-00768-w
Resh, V. H., A. V Brown, A. P. Covich, and others. 1988. The Role of Disturbance in Stream Ecology Journal of the North American Benthological Society. J. North Am. Benthol. Soc. **7**: 263–288.
Richey, J. E., J. M. Melack, A. K. Aufdenkampe, V. M. Ballestter, and L. L. Hess. 2002. Outgassing from Amazonian rivers and wetlands as a large tropical source of atmospheric CO2. Nature **416**: 617–620.
Roberts, B. J., P. J. Mulholland, and W. R. Hill. 2007. Multiple scales of temporal variability in ecosystem metabolism rates: results from 2 years of continuous monitoring in a forested headwater stream. Ecosystems **10**: 588–606.
Rocher-Ros, G., R. A. Sponseller, A. Bergstr, M. Myrstener, and R. Giesler. 2019. Stream metabolism controls diel patterns and evasion of CO2 in Arctic streams. Glob. Chang. Biol. 0–3. doi:10.1111/gcb.14895
Rosemond, A. D., C. M. Pringle, A. Ramírez, M. J. Paul, and J. L. Meyer. 2002. Landscape

variation in phosphorus concentration and effects on detritus-based tropical streams. Limnol. Oceanogr. **47**: 278–289.
Sawakuchi, H. O., V. Neu, N. D. Ward, and others. 2017. Carbon Dioxide Emissions along the Lower Amazon River. Front. Mar. Sci. **4**. doi:10.3389/fmars.2017.00076
Schlesinger, W. H., and E. S. Bernhardt. 2013. The Biosphere: the Carbon Cycle of Terrestrial Ecosystems, p. 135–172. *In* Biogeochemistry: An analysis of global change. Elsevier Oxford.
Siegenthaler, U., and J. L. Sarmiento. 1993. Atmospheric carbon dioxide and the ocean. Nature **365**: 119–125.
Small, G. E., M. Ardón, A. P. Jackman, J. H. Duff, F. J. Triska, A. Ramírez, M. Snyder, and C. M. Pringle. 2012. Rainfall-driven amplification of seasonal acidification in poorly buffered tropical streams. Ecosystems **15**: 974–985.
Sousa, W. P. 1984. The role of disturbance in natural communities. Annu. Rev. Ecol. Syst. Vol. 15 353–391. doi:10.1146/annurev.ecolsys.15.1.353
Stanley, E. H., S. M. Powers, and N. R. Lottig. 2010. The evolving legacy of disturbance in stream ecology: Concepts, contributions, and coming challenges. J. North Am. Benthol. Soc. **29**: 67–83. doi:10.1899/08-027.1
Steinman, A. D., P. J. Mulholland, A. V. Palumbo, D. L. DeAngelis, and T. E. Flum. 1992. Lotic ecosystem response to a chlorine disturbance. Ecol. Appl. **2**: 341–355.
Steinman, A. D., P. J. Mulholland, A. V Palumbo, T. F. Flum, and D. L. DeAngelis. 1991. Resilience of lotic ecosystems to a light-elimination disturbance. Ecology **72**: 1299–1313.
Stoddard, J. L., D. S. Jeffries, A. Lükewille, and others. 1999. Regional trends in aquatic recovery from acidification in North America and Europe. Nature **401**: 575–578.
Stumm, W., and J. J. Morgan. 1996a. Dissolved Carbon Dioxide, *In* Aquatic chemistry: chemical equilibria and rates in natural waters. Wiley.
Stumm, W., and J. J. Morgan. 1996b. Acids and Bases, p. 172–177. *In* Aquatic chemistry: chemical equilibria and rates in natural waters. Wiley.
Tank, S. E., J. B. Fellman, E. Hood, and E. S. Kritzberg. 2018. Beyond respiration: Controls on lateral carbon fluxes across the terrestrial-aquatic interface. Limnol. Oceanogr. Lett. **3**: 76–88. doi:10.1002/lol2.10065
Townsend, C. R. 1989. The Patch Dynamics Concept of Stream Community Ecology. North Am. Benthol. Soc. **8**: 36–50.
Vannote, R. L., G. W. Minshall, K. W. Cummins, J. R. Sedell, and C. E. Cushing. 1980. The river continuum concept. Can. J. Fish. Aquat. Sci. **37**: 130–137.

## Chapter 2: Ecosystem metabolism in tropical streams and rivers: a review and synthesis

This chapter has been published in the journal *Limnology and Oceanography:*

Marzolf, N. S., and M. Ardón. 2021. Ecosystem metabolism in tropical streams and rivers: a review and synthesis. Limnology and Oceanography. doi:10.1002/lno.11707.

### 2.1 Introduction

For over six decades, measuring and estimating primary productivity and ecosystem respiration in freshwater ecosystems (i.e. streams, rivers, lakes, and wetlands) has been a complex theoretical and empirical task (Odum 1956). Beneath the theoretical and data collection approach first developed by Odum (1956) is a complex interaction of climate, hydrologic, geologic, and terrestrial influences on in-stream processes. The basic stream ecosystem metabolism calculation is an oxygen mass balance that informs carbon (C) fixation and mineralization within the stream ecosystem in terms of oxygen concentration in the water:

$$\frac{dO_2}{dt} = G + R + D$$

where the change in $O_2$ (g $m^{-3}$) is a balance of production during photosynthesis (G) during day light hours, consumption during aerobic heterotrophic respiration (R), and $O_2$ diffusion exchange based on the $O_2$ partial pressure gradient between water and atmosphere (D). Each of these volumetric $O_2$ fluxes (G, R, D) are scaled to the area of benthos for a particular time period, and estimates of gross primary productivity (GPP), ecosystem respiration (ER), and net ecosystem production (NEP) are derived using a variety of quantitative approaches (Marzolf et al. 1994; Holtgrieve et al. 2010; Grace et al. 2015; Hall and Hotchkiss 2017; Appling et al. 2018). Data collection for stream ecosystem metabolism depends on $O_2$ sensor quality and accurate understanding of gas exchange (Raymond et al. 2012; Hall and Ulseth 2020). Each component driving the oxygen mass balance is mediated by a variety of geomorphological and hydrological

factors, and the existing methods and theory have been developed primarily from temperate streams in North America and Europe.

There have been persistent arguments discussing what fundamental differences, or lack thereof, exist between tropical and temperate ecosystems (Hawkins 2001), including streams and rivers (Boulton et al. 2008; Dodds et al. 2019). Tropical streams, defined here as streams between 0° and 23.5° North and South latitude, experience a different climatic regime than temperate streams, which potentially influences metabolism in freshwaters (Lewis 2008). Tropical forests experience diverse climate, geology, and high taxonomic diversity of organisms (Townsend et al. 2008). For example, canopy cover and temporal availability of light to the stream bed are more variable in temperate stream ecosystems than tropical ecosystems (Davies et al. 2008; Dodds et al. 2019). In forested temperate streams, canopy closure following seasonal spring leaf-out resulted in reduced GPP due to light limitation, and canopy opening due to leaf abscission stimulated ER from leaf material inputs in the fall (Roberts et al. 2007), whereas tropical streams and rivers can have closed canopies year-round. In tropical streams, the seasonal variation of canopy closure may not be as strong or canopy closure may persist year-round, leaving streams light limited and with high continuous inputs of terrestrial organic matter (Townsend et al. 2011). In tropical streams where light availability to the benthos is high, GPP is among the highest rates measured, up to 10-times greater than comparable temperate streams (Davies et al. 2008). However, no previous reviews or syntheses of tropical stream metabolic rates has allowed for a comparison to their temperate counter parts.

Seasonal temperature variation in the tropics span a narrower range than that of temperate streams (Janzen 1967). Temperature regulates biological metabolism (Brown et al. 2004) and infrequent low temperatures in tropical streams, particularly in the lowland tropics, should drive

higher respiration year-round (Song et al. 2018). Temperature variability due to elevation are stronger than temporal variation in tropical streams compared to temperate streams (Janzen 1967; Polato et al. 2018). At the organismal level, the response of heterotrophic metabolism to increases in temperature is exponential for terrestrial tropical taxa (Dillon et al. 2010), suggesting that increases in metabolism per unit temperature increase will be higher in the tropics. As a result, faster metabolic rates at the organismal level due to warming temperatures associated with climate change should result in elevated rates at the ecosystem level in the tropics (Dillon et al. 2010). However, warmer water has lower gas solubility, and combined with high metabolic rates, can lead to low dissolved oxygen and difficulties in estimating stream ecosystem metabolism (Lewis 2008). Further, temperature patterns vary across elevation and land-use types, and the responses of ecosystem metabolism to temperature will vary depending on a suite of climatic and site specific characteristics (Dodds et al. 2019). An improved understanding of how temperature affects both GPP and ER in tropical streams will help forecast possible feedbacks to climate change associated with a warmer world.

In addition to temperature differences between temperate and tropical streams and their effects on stream metabolism, a range of abiotic drivers are of interest in tropical streams. Generally, rainfall is greater in the tropics due to the inter-tropical convergence zone (ITCZ), which distributes heat and water across the tropics. Increased rainfall causes greater solid and solute fluxes through streams and rivers from weathered soils (Lewis 2008), structures the stream benthos and primary producer assemblages (Pringle and Hamazaki 1997), and delivers terrestrial organic matter and nutrients downstream to the ocean (Mayorga et al. 2010). Seasonal flooding associated with rainfall contributes to higher turbidity, which attenuates light penetration to the benthos and in water column. Flooding can also structure primary producer assemblages, shifting

dominance from diatoms and blue-green algae in headwater streams (Pringle and Hamazaki 1997) and transporting producers from upstream reaches in larger rivers and their floodplains (Lewis 1988).

Nutrients also influence biological processes in streams. Nitrogen (N) and phosphorus (P) are limiting elements in freshwaters (Dodds and Smith 2016; Paerl et al. 2016) and their availability in tropical streams may regulate both GPP and ER. Increased N and P can result in small increases in both GPP and ER across different stream types and latitudes, (Mulholland et al. 2001, Bernot et al. 2006, Bernot et al. 2010). Specific to the effects of phosphorus in the tropics, a number of studies have reported increased heterotrophic activity (microbes, macroinvertebrates, and fungi) with elevated P (Rosemond et al. 2002; Ramírez et al. 2003; Ardón et al. 2006), suggesting a stimulatory effect of P on ER. Studies from streams across nutrient gradients have concluded light limitation is a stronger effect on GPP than nutrients (Pringle et al. 1986; Paaby and Goldman 1992), and as is reported in temperate streams (Hill et al. 2001; Roberts et al. 2007; Finlay 2011). However, greater study of the combined effects of limitations from light and nutrients on primary producers and the food webs they support is needed.

In this paper, we review and synthesize stream ecosystem metabolism measurements made in the tropics. Reviews on C processing in streams, rivers, lakes, and estuaries (Bernot et al. 2010; Marcarelli et al. 2011; Hoellein et al. 2013) and on whole stream metabolism (Finlay 2011) have been completed, though focused on temperate ecosystems. Greater number of studies of freshwater metabolism from streams and rivers is part of a growing literature in tropical ecology (Ramírez et al. 2015; Riveros-Iregui et al. 2018) and an important contribution to the field as there are increasing threats to tropical freshwater ecosystems, including reduced

hydrologic connectivity, pollution, hydropower development, and biodiversity loss (Encalada et al. 2019). Specifically, we evaluated the effect of watershed area, nutrients, rainfall, and temperature on stream ecosystem metabolism, evaluated potentially associated physical and chemical parameters, and use a structural equation model to explore how multiple variables control GPP and ER. We hypothesized that 1) as watershed area increases and incident light increases in wider rivers, GPP will increase due to alleviation of light limitation; 2) streams with higher nutrient concentrations will have greater GPP and ER due to nutrient stimulation of photosynthesis and respiration; 3) streams that receive higher rainfall will have lower GPP and ER as a result of scouring and elevated turbidity; and 4) GPP and ER will be greater in streams with warmer temperatures. Further, we also explored the upscaling of daily metabolic estimates to annual C fluxes and light mediation of GPP and ER.

## 2.2 Methods

### 2.2.1 Data selection and extraction

Our review began with a literature search in Web of Science, using key words "tropical" in each search, either "stream" or "river", and "gross primary producti*", "ecosystem respiration", or "metabolism" as different search words, yielding a total of 257 articles published before September 2019. Each of these papers was assessed for inclusion of 1) stream location identified by latitude and longitude; 2) text, graphical, and/or tabular presentation of GPP and ER, and 3) open channel methods used to measure metabolism (e.g. single station or two-station), and 4) dates of the measurements, resulting in 18 articles with available data. Graphically presented data were extracted using WebPlotDigitizer for each measurement (Rohatgi 2019). We amended the dataset from published research with unpublished data from

our own research in Costa Rica and from publicly available metabolism data from Rio Icacos and Quebrada Sonadora in Puerto Rico through the StreamPULSE project (Appling et al. 2018; Vlah and Berdanier 2020). The data in this study are available online at: https://aslopubs.onlinelibrary.wiley.com/doi/abs/10.1002/lno.11707.

We expanded the data extraction from each reference for relevant hydrological, geomorphological, physical, and chemical parameters (Table 2.1). Metabolism estimates are integrative at the ecosystem level and influenced by climate, geology, hydrology, chemistry, and biota; therefore, we compiled parameters relevant to each of these potential drivers. Units were standardized to those shown in Table 1 and conversions of stream ecosystem metabolism expressed as g C $m^{-2}$ $d^{-1}$ were converted to units of $O_2$ using a 1:1 molar respiratory quotient (Demars et al. 2016). Dissolved inorganic nitrogen (DIN), if not explicitly reported, was calculated as the sum of nitrate ($NO_3^-$-N) and ammonium ($NH_4^+$-N). In studies where GPP was low, many authors report GPP as <0.01 g $O_2$ $m^{-2}$ $d^{-1}$, and we report those data as 0.01 g $O_2$ $m^{-2}$ $d^{-1}$ as a minimum threshold; studies that quantitatively report GPP <0.01 g $O_2$ $m^{-2}$ $d^{-1}$ are compiled as reported.

**Table 2.1** Parameters extracted from each reference, if available, with associated units and percentage of whole-stream metabolism measurements for each parameter.

| Parameter | Units | % of measurements filled |
|---|---|---|
| Latitude | Decimal degree | 99.1 |
| Longitude | Decimal degree | 99.1 |
| Elevation | Meters above sea level | 43.6 |
| Annual Rainfall[1] | mm | 100 |
| %For | % forested area in watershed | 84.7 |
| %Ag | % agricultural area in watershed | 84.7 |
| %Urb | % urban area in watershed | 84.7 |
| Canopy[2] | Categorical: Open, Closed | 83.0 |
| Canopy Cover | % canopy cover | 62.9 |
| PAR | $\mu mol\ m^{-2}\ s^{-1}$ | 100 |
| Strahler order | Integer | 72.3 |
| Stream width | m | 82.7 |
| Stream depth | m | 50 |
| Velocity | $m\ s^{-1}$ | 46 |
| Slope | $m\ m^{-1}$ | 44.1 |
| Watershed area | $km^2$ | 74.8 |
| Discharge | $m^3\ s^{-1}$ | 79.7 |
| Temperature | ˚C | 77.7 |
| DO | $mg\ L^{-1}$ | 30.7 |
| pH | unit | 39.6 |

**Table 2.1** (Continued)

| | | |
|---|---|---|
| Conductivity | $\mu S\ cm^{-1}$ | 48.5 |
| $NO_3^-$-N | $\mu g\ L^{-1}$ | 55 |
| $NH_4^+$-N | $\mu g\ L^{-1}$ | 21.3 |
| Dissolved inorganic nitrogen (DIN) | $\mu g\ L^{-1}$ | 24.3 |
| Total nitrogen (TN) | $\mu g\ L^{-1}$ | 23.3 |
| Total phosphorus (TP) | $\mu g\ L^{-1}$ | 23.3 |
| Soluble reactive phosphorus (SRP) | $\mu g\ L^{-1}$ | 60.9 |
| TN:TP | molar | 23.3 |
| DIN:SRP | molar | 10.4 |
| Gas exchange ($K_{600}$)[4] | $d^{-1}$ | 86.6 |
| GPP | $g\ O_2\ m^{-2}\ d^{-1}$ | 100 |
| ER | $g\ O_2\ m^{-2}\ d^{-1}$ | 100 |

[1] If not reported in the study, annual rainfall at the given coordinates was extracted from the TerraClimate dataset

[2] 'Closed' canopy is classified as %canopy cover >= 70% or >= 90% forested land-cover; 'Open' is %canopy cover < 50% or stream width > 5 m

[3] Taken for the given coordinates from the CFS Reanalysis dataset for the year of study

[4] Standardized all reported gas exchange coefficients to a Schmidt number of 600, following Raymond et al. (2012).

### 2.2.2 Climate data collection

Rainfall was collected as total annual rainfall for the year of the GPP and ER measurements. If not reported in the papers, location and date specific annual rainfall totals were extracted from the TerraClimate dataset (Abatzoglou et al. 2018), which yields total annual rainfall within a 4000 m buffer around a given location (i.e. the coordinates of the stream extracted from the paper). Incident downward radiation was extracted using the CFS Reanalysis dataset (Saha et al. 2014), specific to the coordinates and year of the metabolism estimates. We extracted mean daily radiation (W $m^{-2}$) for the year of the measurements. Radiation values were converted to PAR fluxes following Sager and McFarlane (1997). Each of the climate datasets were accessed through the Climate Engine data portal (Huntington et al. 2017).

### 2.2.3 Analysis and synthesis

Based on our hypotheses and the availability of data collected in the review, we examined the drivers of GPP and ER from tropical streams and rivers. We evaluated metabolic space to visualize patterns in productivity, similar to previous studies (Odum 1956; Hoellein et al. 2013). We used Student's t-test to evaluate GPP and ER under closed or open canopies. We used linear regression to evaluate the effects of watershed area, soluble reactive phosphorus (SRP), rainfall (mm), and stream temperature (ºC), which were $\log_{10}$ transformed to meet assumptions of normality and better visualize the variation across the range of conditions represented in our dataset.

For parameters that were not commonly reported in our review (less than 50% in Table 2.1), we used a pairwise correlation matrix for chemical and geomorphological variables. We evaluated correlation of incomplete data using the Kendall tau statistic, using only complete pairs

in our limited dataset, which is a rank-based measure of association and are more robust for datasets with few complete cases.

We constructed a structural equation model (SEM) to better understand multiple controls of GPP and ER in tropical streams and rivers. These models allow for testing of causal hypotheses and evaluation of multiple, simultaneous influences. There are many drivers of both GPP and ER, often with high co-linearity, and the SEM approach allows for *a priori* evaluation of a potentially interrelated drivers and is more robust compared to other multivariate approaches (Bernot et al. 2010; Lefcheck 2019). Using the SEM in Bernot et al. (2010) as a template to evaluate controls of GPP and ER within a hierarchy, we constructed an *a priori* meta-model based on the data we compiled (Appendix 1). Our model incorporated hierarchical structure, attempting to separate drivers at the regional (watershed area, land cover, rainfall) and local (temperature, discharge, SRP, DIN, width, and depth) levels. We hypothesized that correlated errors would exist at the two levels. At regional level, we modeled temperature and rainfall with correlated errors, as warmer temperatures correlate with wetter conditions (Collins et al. 2013). At the local level, we correlated errors between SRP and DIN to reflect nutrient increases particularly from non-forested lands (Allan 2004), and between width and depth which increase predictably with stream size (Raymond et al. 2012).

To provide close approximation to daily metabolism estimates, rainfall in the SEM was converted to mean daily rainfall by dividing annual rainfall by 365. The SEM was fit with $\log_{10}$ transformed metabolic and chemical data and arcsin transformed land cover data, averaged for each stream, using the psem() function in the piecewiseSEM R package (Lefcheck 2016). The psem() function returns standardized and unstandardized path coefficients (ß) for all pathways and coefficient of determination ($r^2$) for endogenous variables. We evaluated the goodness of fit

of the SEM using the Fisher's C statistic, which assess the fit of the data to the model structure and ensures no missing paths were excluded. Fisher's C is $\chi^2$ distributed with degrees of freedom equal to 2 times the number of independence claims and a model-wide *p* value can be determined where $p > 0.05$ indicates the data support the model structure. Further details on SEM methods are in the supplementary material.

2.2.4 Light influence on annual GPP and ER

We upscaled median GPP and ER from each stream to annual rates of C fixation and respiration (g C $m^{-2}$ $y^{-1}$). Metabolic rates were converted from $O_2$ to C using a molar respiratory quotient of 1:1 (Demars et al. 2016). As temperatures in the tropics are less variable over time and space (Janzen 1967), we hypothesize the upscaling of metabolic rates to annual rates is less dependent on changes in temperature than similar estimates from temperate and Arctic streams and represent changes as a result seasonality driven by rainfall. Annual estimates of GPP and ER from tropical streams will be useful in understanding the importance of in-stream processes in the tropics.

Using upscaled annual rates, we evaluated the dependence of fixation and respiration on mean daily light availability. We evaluated annual metabolic rates as a function of PAR assuming linear and non-linear (e.g. logarithmic, logistic, or Michaelis-Menten) saturation equations. Linear and logarithmic models were fit using lm() in R (R Core Team 2019). Logistic and Michaelis-Menten models were fit using the drc R package (Ritz et al. 2015), using the L.3() and MM.2() self-starter functions, respectively, within the drm() function. The four models for each GPP and ER were compared using AIC and AIC weights, $w_i$. Comparing model fits allows interpretation of the effect of light directly on GPP and indirectly on ER, through GPP.

## 2.3 Results

From the published studies and publicly available data, we extracted 202 GPP and ER measurements from 83 streams and rivers across the global tropics (Fig 2.1 a, 2.2 a). Metabolism data publicly available through the StreamPULSE data portal (https://data.streampulse.org/) provided continuous data for 11 months in two streams in Puerto Rico (Rio Icacos and Quebrada Sonadora) and our own unpublished data from Costa Rica (Taconazo) were the three sources of continuous data, in contrast to most articles that presented a few days of data for each stream. The most daily measurements came from the Daly River, Australia (n = 16), followed by two streams from Puerto Rico: Puente Roto (n = 12) and Quebrada Bisley (n = 10) (Fig 2.2b), spanning multiple publications and study years. The most measurements were made in 1995 (n = 25) and 2016 (n = 24) (Fig 2.1, b). The majority of measurements were made in headwater or first order streams (54.9%), followed by third order (13.7%), fourth order (9.1%), and second order (5.1%); 17% of measurements did not report stream position data.

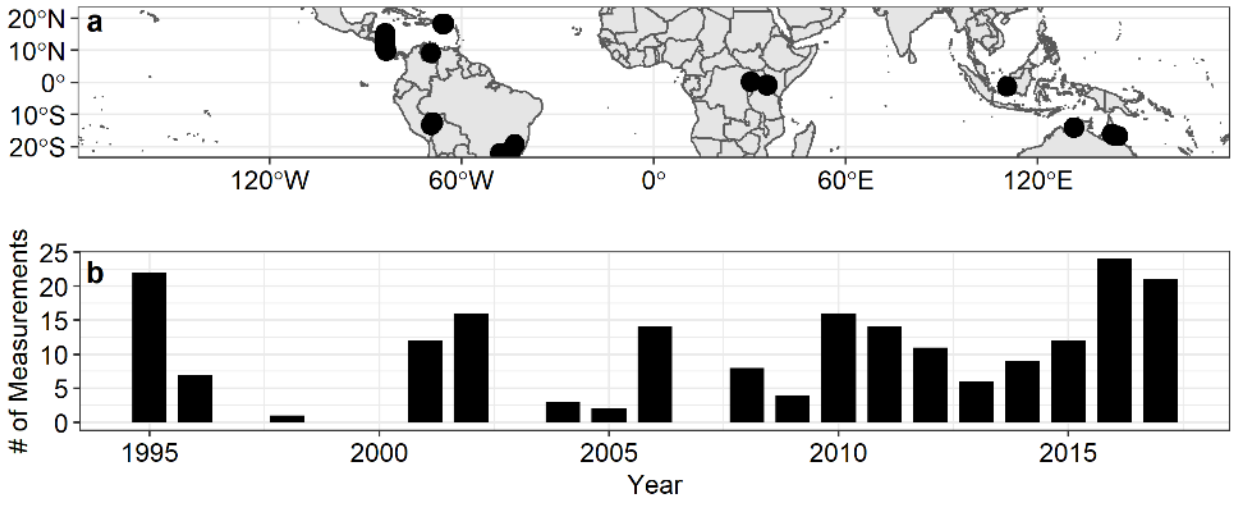


**Figure 2.1** Map of the tropics (|latitude| < 23.5˚) and metabolism measurements in this study; b) number of metabolism measurements made by year compiled in this review.

Streams were predominately heterotrophic (GPP < ER) across all regions and stream sizes (Fig 2.2). Across all measurements, median GPP was 0.4 g $O_2$ $m^{-2}$ $d^{-1}$ (range 0.01 to 11.7 g $O_2$ $m^{-2}$ $d^{-1}$) and median ER was -4.30 g $O_2$ $m^{-2}$ $d^{-1}$ (range -0.1 to -42.1 g $O_2$ $m^{-2}$ $d^{-1}$). Only 13 measurements (6.3%) occurred where GPP:ER > 1. Ecosystem respiration significantly increased with GPP, but with little explanatory power ($R^2 = 0.05$, $p < 0.01$).

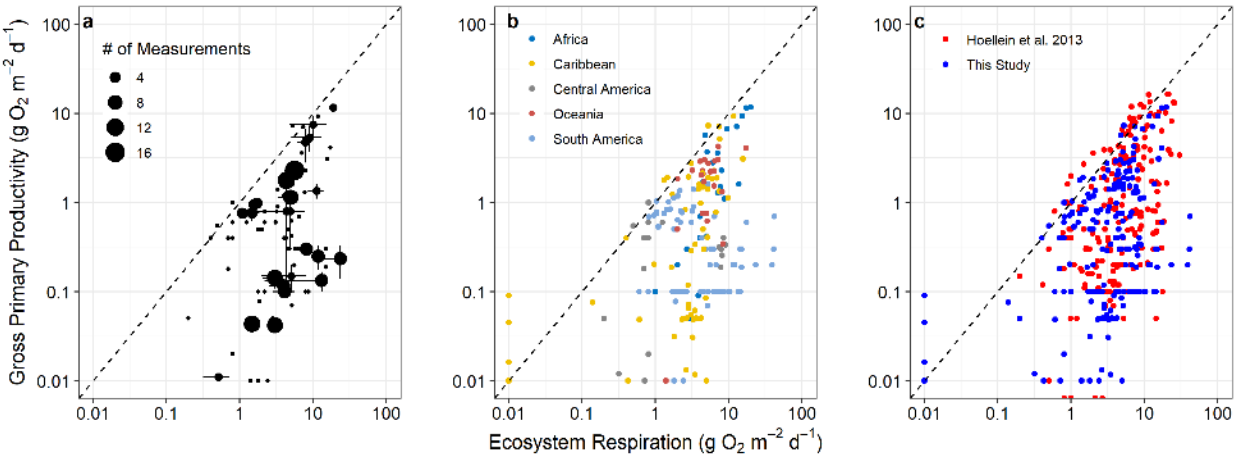


**Figure 2.2** a) Median GPP and ER from each stream, with error lines showing 95% confidence intervals; b) All metabolic rates collected in the review, colored by global region; c) All GPP and ER data compiled in this review (blue) plotted against stream data reviewed in Hoellein et al. (2013) (red). Point size in a) is scaled by the number of measurements in each stream. The dashed black lines are 1:1 lines in all panels. Note log axes.

Hypothesized drivers explained some of the variation in GPP and ER. Watershed area was weakly related with GPP ($R^2 = 0.07$, $p = 0.08$) (Fig 3a, Table 2.2), while ER showed no relation with watershed area ($R^2 = 0.01$, $p = 0.56$) (Fig 3b, Table 2.2). Ecosystem respiration decreased at higher SRP ($R^2 = 0.29$, $p < 0.01$), while GPP showed no relationship ($R^2 < 0.01$, $p = 0.74$) (Table 2, Fig 2.3b, f). Total annual rainfall showed no relationship with GPP ($R^2 = 0.02$, $p$

= 0.19) but a negative relationship with ER ($R^2$ = 0.07, $p$ = 0.01) (Fig 2.3 c, g, Table 2). Neither GPP ($R^2$ = 0.01, $p$ = 0.29) nor ER ($R^2$ < 0.01, $p$ = 0.68) were related with temperature (Fig 3d, h). Gross primary productivity was 2.6-times greater under open (mean GPP = 2.09 g $O_2$ $m^{-2}$ $d^{-1}$) canopies compared to closed (mean GPP = 0.57 g $O_2$ $m^{-2}$ $d^{-1}$) canopies ($t$ = -4.7, p < 0.01, Fig 2.4), while ER in open (-4.74 g $O_2$ $m^{-2}$ $d^{-1}$) or closed canopies (-6.33 g $O_2$ $m^{-2}$ $d^{-1}$) showed less variation ($t$ = -1.77, $p$ = 0.08).

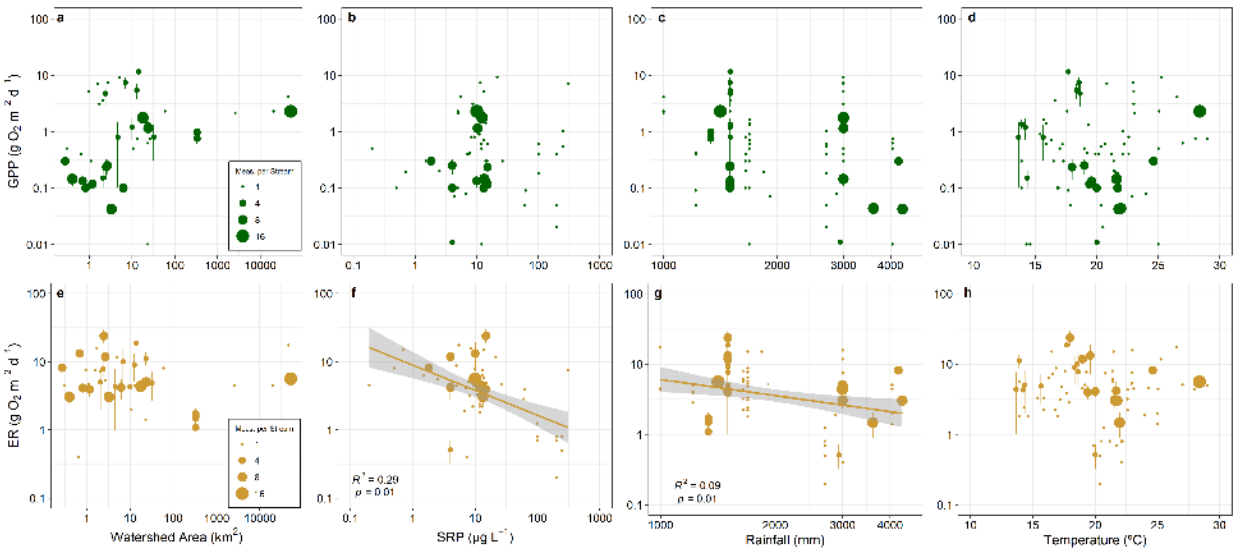


**Figure 2.3** Predicted drivers of mean GPP (a-d) and mean ER (e-h) in each stream. Point size in each panel shows the number of metabolism measurements from a single stream contributing to calculate the average. Error bars are standard error. Lines represent best-fit lines with 95% confidence intervals. Note log10 transformation of y-axes and x-axes in a, b, c, e, f, and g.

**Table 2.2** Results of linear regression between GPP and ER, and the hypothesized drivers. Values in parentheses for Intercept and Estimate are 95% confidence intervals.

| Rate | Driver | Intercept | Estimate | *F* value | *p* value | $R^2$ |
|---|---|---|---|---|---|---|
| $\log_{10}$ (GPP) | $\log_{10}$(Area) | -0.22 (-0.50 – 0.05) | 0.14 (-0.02 – 0.30) | $F_{1,41} = 3.30$ | 0.08 | 0.07 |
| $\log_{10}$ (GPP) | $\log_{10}$(SRP) | -0.49 (-0.84 - -0.14) | 0.04 (-0.23 – 0.32) | $F_{1,59} = 0.11$ | 0.75 | <0.01 |
| $\log_{10}$ (GPP) | $\log_{10}$(Rainfall) | 1.69 (-1.37 – 4.75) | -0.62 (-1.55 – 0.31) | $F_{1,81} = 1.76$ | 0.19 | 0.02 |
| $\log_{10}$ (GPP) | Temperature | -0.85 (-1.76 – 0.06) | 0.02 (-0.02 – 0.07) | $F_{1,75} = 1.11$ | 0.29 | 0.01 |
| $\log_{10}$ (ER) | $\log_{10}$(Area) | 0.73 (0.59 – 0.88) | -0.02 (-0.11 – 0.06) | $F_{1,41} = 0.34$ | 0.56 | 0.01 |
| $\log_{10}$ (ER) | $\log_{10}$(SRP) | 0.95 (0.75 – 1.14) | -0.37 (-0.52 - -0.22) | $F_{1,59} = 23.6$ | <0.01 | 0.29 |
| $\log_{10}$ (ER) | $\log_{10}$(Rainfall) | 3.06 (1.32 – 4.79) | -0.76 (-1.29 - -0.23) | $F_{1,81} = 8.23$ | 0.01 | 0.09 |
| $\log_{10}$ (ER) | Temperature | 0.69 (0.16 – 1.22) | -0.01 (-0.03 – 0.02) | $F_{1,75} = 0.18$ | 0.68 | <0.01 |

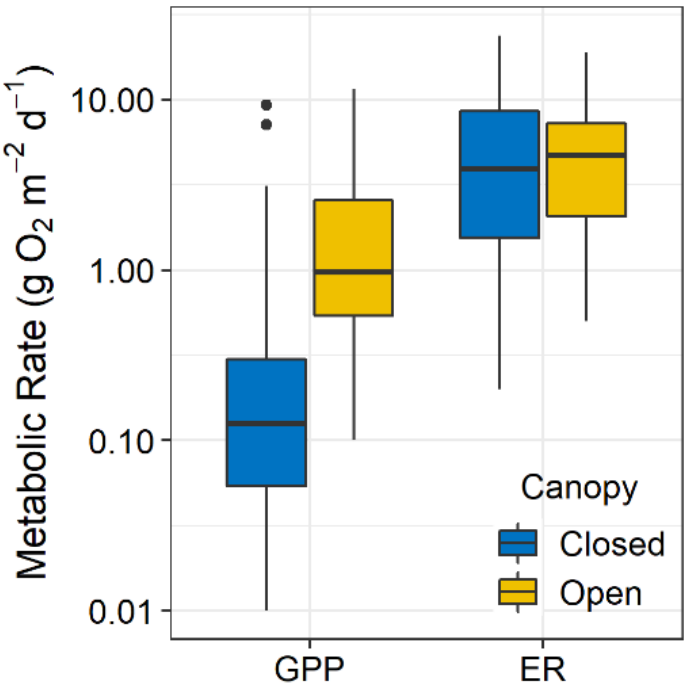


**Figure 2.4** Metabolic rates under closed (in blue) and open (yellow) canopies. Boxplots show the median, 25th and 75 quartiles, with outliers at >90 and <10 percentiles. Note log y axis.

Less commonly reported variables reveal potential drivers of both GPP and ER as indicated by the Kendall τ correlation coefficient. Strongest physical and chemical relationships (Fig 5, a) for ER were pH (τ = 0.52), TN:TP (τ = -0.41), and conductivity (τ = 0.40), while GPP had strongest associations with TN (τ = -0.42), TP (τ = -0.37), and $NO_3^-$ (τ = -0.12) (Fig 2.5a). Geomorphological variables related (Fig 2.5, b) with ER were strongest with velocity (τ = 0.33), canopy cover (τ = -0.26), and elevation (τ = 0.26), while GPP was associated with %canopy cover (τ = -0.67), elevation (τ = -0.45), and stream order (τ = 0.42).

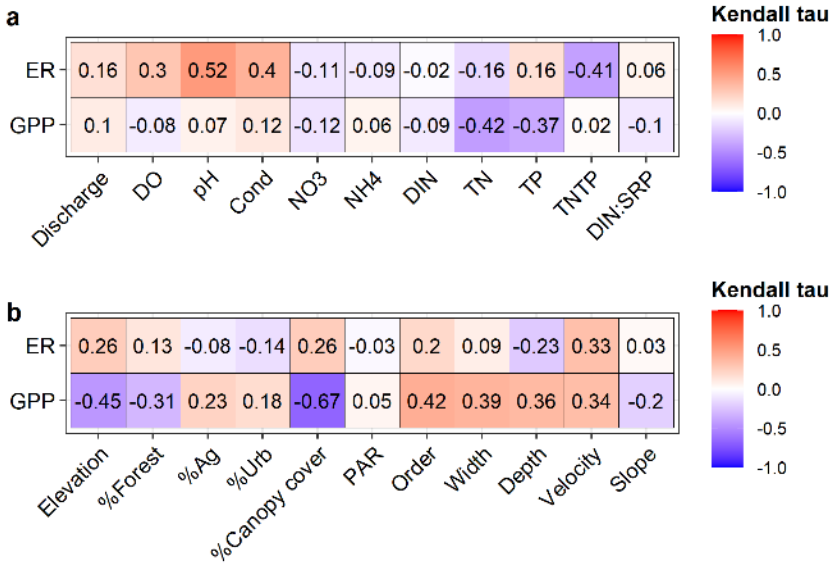


**Figure 2.5** Cross-correlation matrix of a) chemical and b) geomorphological drivers of GPP and ER. Values and colors in each box are Kendall tau, with stronger trends in richer colors and positive associations in red and negative associations in blue. Chemical and geomorphological drivers are described with units in Table 1.

We explored both regional and site level controls of both GPP and ER with a structural equation model (Fig 2.6). From the meta-model, a model was fit with strong support of the

hypothesized structure with no missing pathways (Fisher's $C = 31.6$, $p = 0.39$). The model explained more variation in ER ($r^2 = 0.74$) than GPP ($r^2 = 0.26$). Strongest pathways, as measured by the standardized coefficient, for GPP was %non-forested land area (ß = 0.51) and discharge (ß = 0.30), whereas ER was driven by SRP (ß = -0.76) and GPP (ß = 0.46). Phosphorus ($r^2 = 0.46$) was linked to watershed area (ß = 2.10) and mean daily rainfall (ß = -0.66). The SEM explained most variation in discharge ($r^2 = 0.84$), and less for temperature ($r^2 = 0.19$), DIN ($r^2 = 0.30$), and SRP ($r^2 = 0.28$).

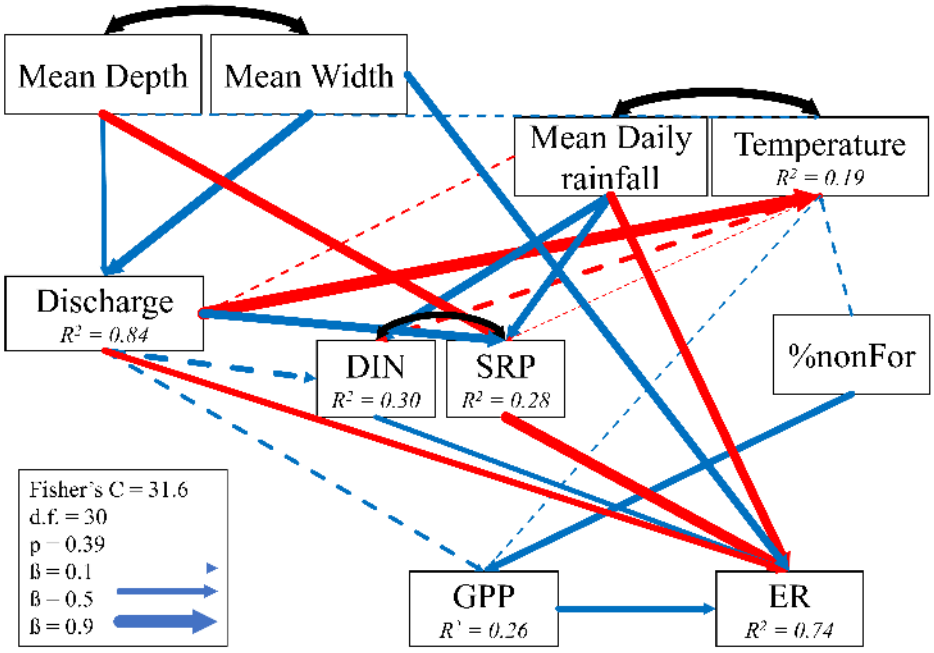


**Figure 2.6** Structural equation model examining the drivers of GPP and ER in tropical streams and rivers. Blue arrows indicate ß > 0 and red arrows ß < 0. Arrow size are proportional are standardized path coefficients, as indicated in the caption. Fisher C and p value refer to model-wide goodness of fit, where p > 0.05 indicates the data fit the model structure. Solid lines represent significant (p < 0.05) pathways and dashed lines refer to pathways with p > 0.05. See Appendix 2 for standardized and unstandardized coefficients, standard errors, sample size, and p values for each pathway.

Annual estimates of ER ranged from 27.4 to 3250 g C $m^{-2}$ $yr^{-1}$ and GPP ranged from 1.4 to 1587.8 g C $m^{-2}$ $yr^{-1}$ (Fig 2.7). Among the various models fitted, GPP was best explained by a logistic model ($w_i$ = 0.98) and ER was best fit by a logarithmic ($w_i$ = 0.38) and linear ($w_i$ = 0.35) models (Table 3).

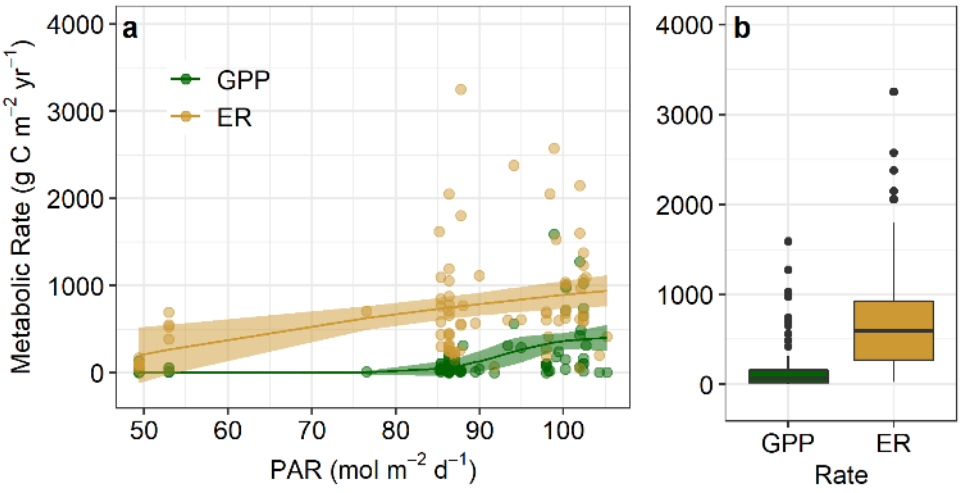


**Figure 2.7** a) Scaled metabolic rates plotted against daily mean annual PAR for each stream in the review. Brown points are ER and green are GPP, both units as kg C m-2 yr-1. Best fit lines represent the model with greatest AIC weight (Table 3), with 95% confidence intervals. b) Boxplots of mean GPP and ER from each stream. Boxplots are median with IQR (25th to 75th percentile), and outliers are >90th or <10th percentiles.

**Table 2.3** Saturation model fits for light on GPP and ER. Models are briefly summarized in each row and 'Met' represents both GPP and ER as described by PAR. Models were selected by comparing AIC scores, via AIC weights. Asterisks (*) designate the best model for each GPP and ER.

| Model | GPP | | ER | |
|---|---|---|---|---|
| | AIC | $w_i$ | AIC | $w_i$ |
| Logistic: Met ~ $1/(1 + e^{PAR})$ | 1169.5 | 0.98* | 1299.5 | 0.13 |
| Logarithmic: Met ~ $\log_{10}$(PAR) | 1180.3 | 0.00 | 1297.4 | 0.38* |
| Linear: Met ~ PAR | 1178.3 | 0.01 | 1297.6 | 0.35 |
| Michaelis-Menten: Met ~ $Met_{max}PAR/PAR$ | 1182.8 | 0.00 | 1299.3 | 0.14 |

## 2.4 Discussion

Our main finding is the similarity of metabolic rates between tropical streams (Fig 2.2, c) and temperate streams (Finlay 2011, Marcarelli et al. 2011, Hoellein et al. 2013). Specifically, Hoellein et al. (2013) found 87% (189 of 217 measurements in that study) of streams with GPP:ER < 1, compared to 97% in tropical streams, based on our analyses. In tropical streams, GPP and ER were less related ($R^2$ = 0.05) than temperate streams ($R^2$ = 0.23, Hoellein et al. 2013), though regression equations had similar slopes and intercepts (this study: ER = 0.82GPP + 4.63; Hoellein et al. 2013: ER = 0.78GPP + 4.8). Streams are predominately heterotrophic, following theory that a majority of streams rely on allochthonous inputs to fuel heterotrophic food webs (Fisher and Likens 1973; Webster and Meyer 1997). Our synthesis across the tropics showed that open canopies above streams drove greater GPP (Fig 2.4), as has been shown in Costa Rican streams (Ortega-Pieck et al. 2017) while ER was similar across open and closed

canopy types. While the relationship between seasonal inputs of organic matter during the fall leaf abscission and ER in temperate streams has been established (Hill et al. 2001), exploration of this relationship in tropical streams is needed.

Temperature may also explain some of the differences between temperate and tropical streams. Our review spans a wide range of temperature (12.9° – 34° C) and warmer temperatures than from temperate streams (3.8° – 27.1° C, Hoellein et al. 2013). While there was no relationship between temperature and GPP or ER (Fig 2.3d, h), the SEM revealed a positive effect of temperature on GPP (ß = 0.16) but no linkage between temperature and ER. The limited weak effect of temperature (Fig 2.3h, $R^2 < 0.01$) is in contrast to biological theory (Brown et al. 2004; Yvon-Durocher et al. 2012; Williamson et al. 2016) and from a study reporting non-linear increases as a result of warming temperatures on metabolic rates of tropical taxa (Dillon et al. 2010). In a cross-biome study of stream ecosystem metabolism, there was a weak pathway between ER and temperature (Bernot et al. 2010). The SEM identified a positive linkage between GPP and temperature (ß = 0.16). This relationship was not evaluated in other reviews (Bernot et al. 2010, Hoellein et al. 2013), but there is evidence for higher GPP as a result of higher N fixation caused by warmer stream temperature (Welter et al. 2015), and we suggest these indirect and multi-faceted interactions may be similarly true in tropical streams. Climate change predicts warmer stream temperatures in the tropics (0.9 – 3.3 ºC), and while we see no direct effect of temperature, there is growing evidence of shifts in productivity under warmer conditions (Padfield et al. 2017; Hood et al. 2018).

Watershed area did not drive increases in GPP as strongly as found in temperate streams (Finlay 2011; Hall et al. 2016). There was weak relationship of watershed area and GPP (Fig 2.3, a, Table 2.2). Further, the SEM identified a positive linkage of GPP to discharge (ß = 0.30),

suggesting GPP increases with stream or river size and position downstream in a watershed, though regression analysis do not reflect this point (Fig 2.3, a). However, we reviewed data from primarily small streams and a few from large rivers (Fig 2.3, a). In temperate streams, Finlay (2011) and Hoellein et al. (2013) showed increasing GPP and ER with watershed area, across a similar range of watershed area (0.01 – 10,000 $km^2$) to this study (0.3 – 53,000 $km^2$). There were strong correlations with GPP from variables including elevation, stream order, channel width, depth, and water velocity (Fig 2.5), which further support a causal relationship with river size and ecosystem metabolism, as hypothesized in the River Continuum Concept (Vannote et al. 1980) and shown empirically (Hall et al. 2016).

Stream hydrology explained some variation in GPP and ER. Annual rainfall was negatively related to ER and a negative pathway in the SEM (ß = -0.65), but not GPP (Fig 2.3, c and f). The SEM identified a strong linkage between mean daily rainfall to both discharge and temperature, as we expected. The linkage between discharge and GPP (ß = 0.30) may reflect the increase of GPP in larger rivers, also supported by the positive relationship between discharge and watershed area. However, these data are snapshots of measurements, and generally at low flows, when the data collection for stream ecosystem metabolism is easier. Metrics like days since last rainfall or short-term rainfall will capture rainfall driven processes (e.g. scouring, organic matter loading, turbidity) more accurately at the stream level and help resolve the relationship between rainfall and metabolism. Rainfall will likely have different effects on ecosystem metabolism depending on position in the watershed between mountainous streams (e.g. greater scouring) versus lowland rivers (e.g. greater organic matter loading and turbidity). Turbidity was not collected in this review and is important to consider as it relates to light penetration of the water column of streams and rivers. Rainfall and precipitation regimes,

including frequency and magnitude of extreme events, are expected to change under climate change, highlighting the need to better understand the relationships between rainfall, discharge, and stream ecosystem metabolism.

We did not find support for our second hypothesis that higher nutrients would lead to higher GPP and ER. First, we observed no relationship of GPP with SRP (Fig 2.3, b) and a negative relationship between SRP and ER (Fig 2.3, e). The highest SRP concentrations (250 µg $L^{-1}$) came from an agriculturally influenced streams in Costa Rica (Ortega-Pieck et al. 2017), where low ER (-0.5 and -0.8 g $O_2$ $m^{-2}$ $d^{-1}$) were measured relative to the overall mean ER (ER = -6.01 g $O_2$ $m^{-2}$ $d^{-1}$) in this review. The negative relationship of ER and SRP counters research from lowland forested streams in Costa Rica, where SRP is a driver of microbial respiration (Ramírez et al. 2003), macroinvertebrate abundance (Rosemond et al. 2002), and leaf litter decomposition rates (Ardón et al. 2006) across similar hydrologic and light conditions. As each of these responses to SRP contribute to integrative ER, we would hypothesize ER to increase with SRP in these streams, but conflicts with results from agriculturally influenced streams (Ortega-Pieck et al. 2017). Decreased ER in streams with higher SRP may be the result of loading of agriculturally derived chemicals (e.g. pollutants, pesticides) and obscuring a presumed stimulatory effect of SRP. Further resolution of the relationship of SRP and ER is needed. Previous studies have had difficulty in relating stream ecosystem metabolism with nutrients (Mulholland et al. 2001, Bernot et al. 2010, Finlay 2011), in part due to small sample sizes and short temporal measurements. Empirical tests of the effects of nutrients on GPP and ER are needed in both tropical and temperate streams, and the rapid increase in the number of metabolism measurements should allow for resolution of this effect and the effects of nutrients compared to effects of hydrology and light. In a recent meta-analysis, integrated ecosystem

responses (which include whole-stream measurements of GPP and ER, but also leaf decomposition rates) increased by 139% in response to N and P additions (Ardón et al. 2020).

Scaling of GPP and ER to annual rates of C fixation and respiration were similar to previous estimates from streams and rivers. The annual estimates of GPP are greater than reference streams compiled in Finlay (2011), where maximum GPP was ~100 g C $m^{-2}$ $d^{-1}$, in contrast to the maximum GPP in tropical streams of 1600 g C $m^{-2}$ $d^{-1}$, a 16-times increase. This increase is greater than the 10-fold difference between tropical and temperate stream GPP stated in Davies et al. (2008). In fact, the highest rates of GPP from tropical streams are greater than GPP reported from human-dominated (e.g. agricultural and urban) streams (~750 g C $m^{-2}$ $d^{-1}$, Finlay 2011). Respiration followed a similar pattern, with tropical ER rates >$75^{th}$ quartile (>970 g C $m^{-2}$ $d^{-1}$) from temperate streams and comparable to ER from human-dominated streams (>1000 g C $m^{-2}$ $d^{-1}$, Finlay 2011). Gross primary productivity was best explained using a logistic saturation model, whereas ER was best fit by a logarithmic model, though a linear model was similarly weighted (Table 3). This model indicates that high light conditions leads to GPP of around 550 g C $m^{-2}$ $yr^{-1}$ though several instances of GPP greater than this prediction are present in the data. Variance around the GPP-PAR curve is driven by site characteristics, including canopy shading of the stream surface, turbidity, nutrient limitation, and primary producer communities. The difference in model fits between GPP and ER reflect the influence of allochthonous material to fuel stream food webs. Light data in this study was collected as downward shortwave radiation and not PAR incident at the stream surface or benthos, similar to the approach of Savoy et al. (2019). Measuring light at these two scales is a fundamental difference to results from Finlay (2011), where a PAR had a linear relationship with GPP, and PAR was the main driver of GPP in those streams. While the upscaled annual rates are less

dependent on differences in temperature, we note that seasonality in the tropics is dictated by rainfall, and predominance of field work during the dry season may bias our values towards those periods. Further, several streams only report one day of GPP and ER estimates and should further be extrapolated with caution.

While this review includes a wide range of stream measurements, large areas of the tropics remain unstudied or unpublished (Fig 2.1, a). Specifically, metabolism data from the Amazon basin is unrepresented, despite a large field of study on C fluxes in the Amazon (Richey et al. 2002). While this review focused on studies using the open channel methods using a one- or two-station approach, we acknowledge a wide literature of respiration estimates using bottle incubations and $^{18}O$ fractionation from the Amazon basin (Quay et al. 1995; Ward et al. 2013) and Australia (Bunn et al. 1999). Bunn et al. (1999) report a range of GPP (2.7 to 6.3 g $O_2$ $m^{-2}$ $d^{-1}$) and ER (-5.4 to -12.2 g $O_2$ $m^{-2}$ $d^{-1}$) that are similar to the estimates using open channel methods summarized in this study. Previous studies have measured $CO_2$ fluxes from headwater in the Amazon (Richey et al. 2002; Johnson et al. 2008), and a large fraction of $CO_2$ generated is from in-stream respiration (Mayorga et al. 2005), suggesting that ER in these sites could be a large flux. The threats to the Amazon basin from climate change, land use change, and dam construction in montane rivers (Anderson et al. 2018; Encalada et al. 2019) all have the potential to drive changes in ecosystem structure and function in the Amazon, and changes in metabolic rates can be potentially used as a monitoring diagnostic to indicate changes in freshwater ecosystems with greater understanding of the drivers of GPP and ER (Palmer and Febria 2012). Beyond the forested sites, more study from a broad range of urban, agricultural, montane, lowland, seasonally wet, and desert streams and rivers in the tropics will be valuable additions.

An interesting component to the studies in this review are the connection of whole-stream processes with animals. In several studies, the experimental removal of fishes and loss of tadpole populations due to fungal diseases had effects that manifested at the ecosystem level. The loss of tadpoles in headwater streams in Panama stimulated GPP 10x (0.001 to 0.012 g $O_2$ $m^{-2}$ $d^{-1}$, though these values are near the measurement limits of GPP) while decreasing ER 50% (-0.71 to -0.32 g $O_2$ $m^{-2}$ $d^{-1}$) , and altered N uptake and cycling in the stream (Whiles et al. 2013). Experimental removal of a commonly harvested fish in Venezuela resulted in higher GPP and ER, but the increase in ER was greater than the increase in GPP and the ecosystem became more heterotrophic (Taylor et al. 2006). While these studies explicitly measured changes in metabolism due to the changes in stream biota, several studies have documented changes in C cycling and top-down control of benthic organic matter, nutrients, and algal communities in tropical streams (Pringle and Hamazaki 1997, 1998; Davies et al. 2008). We suggest merging metabolism measurements with consumer and food web studies can be a fruitful area of research (Rüegg et al. 2020), particularly in the tropics.

Our review suggests that tropical stream ecosystem metabolism is driven by similar processes as temperate streams and supports findings from previous reviews though have similar limitations of small sample sizes and coarse temporal resolution. Our data collection shows there is a growing body of metabolism data from the tropics including headwater streams to large rivers and should be included into global assessments of the effect of temperature. Climate change has the potential to affect metabolic rates in tropical streams. With predicted warmer temperatures from 0.9 – 3.3 ºC and wetter and more extreme seasonal rainfall in the tropics (Collins et al. 2013), it remains unclear how metabolic rates will respond. Our results suggest the

rapid depletions in forest cover across the tropics in favor of open canopy agriculture or grazing land suggest faster C release (ER) compared to C capture (GPP) from tropical streams.

2.5 References

Abatzoglou, J. T., S. Z. Dobrowski, S. A. Parks, and K. C. Hegewisch. 2018. TerraClimate, a high-resolution global dataset of monthly climate and climatic water balance from 1958-2015. Sci. Data 5: 1–12. doi:10.1038/sdata.2017.191

Allan, J. D. 2004. Landscapes and Riverscapes: The Influence of Land Use on Stream Ecosystems. Annu. Rev. Ecol. Evol. Syst. 35: 257–284. doi:10.1146/annurev.ecolsys.35.120202.110122

Anderson, E. P., C. N. Jenkins, S. Heilpern, and others. 2018. Fragmentation of Andes-to-Amazon connectivity by hydropower dams. Sci. Adv. 4: 1–8. doi:10.1126/sciadv.aao1642

Appling, A. P., R. O. Hall, C. B. Yackulic, and M. Arroita. 2018. Overcoming Equifinality: Leveraging Long Time Series for Stream Metabolism Estimation. J. Geophys. Res. Biogeosciences 123: 624–645. doi:10.1002/2017jg004140

Ardón, M., L. H. Meglin, R. M. Utz, and others. 2020. Experimental nitrogen and phosphorus enrichment stimulates multiple trophic levels of algal and detrital-based food webs: A global meta-analyses from streams and rivers. Biol. Rev. doi:10.1111/brv.12673

Ardón, M., L. A. Stallcup, and C. M. Pringle. 2006. Does leaf quality mediate the stimulation of leaf breakdown by phosphorus in Neotropical streams? Freshw. Biol. 51: 618–633. doi:10.1111/j.1365-2427.2006.01515.x

Bernot, M. J., D. J. Sobota, R. O. Hall, and others. 2010. Inter-regional comparison of land-use effects on stream metabolism. Freshw. Biol. 55: 1874–1890. doi:10.1111/j.1365-2427.2010.02422.x

Bernot, M. J., J. L. Tank, T. V. Royer, and M. B. David. 2006. Nutrient uptake in streams draining agricultural catchments of the midwestern United States. Freshw. Biol. 51: 499–509. doi:10.1111/j.1365-2427.2006.01508.x

Boulton, A. J., L. Boyero, A. P. Covich, M. Dobson, S. Lake, and R. Pearson. 2008. Are tropical streams ecologically different from temperate streams?, p. 257–284. In Tropical stream ecology. Elsevier.

Brown, J. H., J. F. Gillooly, A. P. Allen, V. M. Savage, and G. B. West. 2004. Toward a metabolic theory of ecology. Ecology 85: 1771–1789.

Bunn, S. E., P. M. Davies, and T. D. Mosisch. 1999. Ecosystem measures of river health and their response to riparian and catchment degradation. Freshw. Biol. 41: 333–345.

Collins, M., R. Knutti, J. Arblaster, and others. 2013. Long-term climate change: Projections, commitments and irreversibility, In T.F. Stocker, D. Qin, G.-K. Plattner, et al. [eds.], Climate Change 2013 the Physical Science Basis: Working Group I Contribution to the Fifth Assessment Report of the Intergovernmental Panel on Climate Change. Cambridge University Press.

Davies, P. M., S. E. Bunn, S. K. Hamilton, and D. David. 2008. Primary production in tropical streams and rivers, p. 23–42. In D. Dudgeon [ed.], Tropical stream ecology. Elsevier.

Demars, B. O. L., G. M. Gíslason, J. S. Ólafsson, J. R. Manson, N. Friberg, J. M. Hood, J. J. D. Thompson, and T. E. Freitag. 2016. Impact of warming on CO 2 emissions from streams countered by aquatic photosynthesis. Nat. Geosci. 9: 758–761.

Dillon, M. E., G. Wang, and R. B. Huey. 2010. Global metabolic impacts of recent climate warming. Nature 467: 704–706. doi:10.1038/nature09407

Dodds, W. K., L. Bruckerhoff, D. Batzer, and others. 2019. The freshwater biome gradient framework: Predicting macroscale properties based on latitude, altitude, and precipitation. Ecosphere 10. doi:10.1002/ecs2.2786

Dodds, W. K., and V. H. Smith. 2016. Nitrogen, phosphorus, and eutrophication in streams. Inl. Waters 6: 155–164. doi:10.5268/IW-6.2.909

Encalada, A. C., A. S. Flecker, N. L. Poff, and others. 2019. A global perspective on tropical montane rivers. Science (80-. ). 365: 1124–1129. doi:10.1126/science.aax1682

Finlay, J. C. 2011. Stream size and human influences on ecosystem production in river networks. Ecosphere 2: art87. doi:10.1890/es11-00071.1

Fisher, S. G., and G. E. Likens. 1973. Energy flow in Bear Brook, New Hampshire: An integrative approach to stream ecosystem metabolism. Ecol. Monogr. 43: 421–439.

Grace, M. R., D. P. Giling, S. Hladyz, V. Caron, R. M. Thompson, and R. Mac Nally. 2015. Fast processing of diel oxygen curves: Estimating stream metabolism with base (BAyesian single-station estimation). Limnol. Oceanogr. Methods 13: 103–114. doi:10.1002/lom.10011

Hall, R. O., and E. R. Hotchkiss. 2017. Stream Metabolism, p. 219–233. In G.A. Lamberti and F.R. Hauer [eds.], Methods in Stream Ecology, Vol 2: Ecosystem Function, 3rd Edition. Academic Press Ltd-Elsevier Science Ltd.

Hall, R. O., J. L. Tank, M. A. Baker, E. J. Rosi-Marshall, and E. R. Hotchkiss. 2016. Metabolism, Gas Exchange, and Carbon Spiraling in Rivers. Ecosystems 19: 73–86. doi:10.1007/s10021-015-9918-1

Hall, R. O., and A. J. Ulseth. 2020. Gas exchange in streams and rivers. Wiley Interdiscip. Rev. Water 7: e1391.

Hawkins, B. A. 2001. Ecology's oldest pattern? Trends Ecol. Evol. 16: 470. doi:10.1016/s0169-5347(01)02197-8

Hill, W. R., P. J. Mulholland, and E. R. Marzolf. 2001. Stream ecosystem responses to forest leaf emergence in spring. Ecology 82: 2306–2319.

Hoellein, T. J., D. A. Bruesewitz, and D. C. Richardson. 2013. Revisiting Odum (1956): A synthesis of aquatic ecosystem metabolism. Limnol. Oceanogr. 58: 2089–2100. doi:10.4319/lo.2013.58.6.2089

Holtgrieve, G. W., D. E. Schindler, T. A. Branch, and Z. Teresa A'Mar. 2010. Simultaneous quantification of aquatic ecosystem metabolism and reaeration using a Bayesian statistical model of oxygen dynamics. Limnol. Oceanogr. 55: 1047–1063. doi:10.4319/lo.2010.55.3.1047

Hood, J. M., J. P. Benstead, W. F. Cross, and others. 2018. Increased resource use efficiency amplifies positive response of aquatic primary production to experimental warming. Glob. Chang. Biol. 24: 1069–1084. doi:10.1111/gcb.13912

Huntington, J. L., K. C. Hegewisch, B. Daudert, C. G. Morton, J. T. Abatzoglou, D. J. McEvoy, and T. Erickson. 2017. Climate Engine: cloud computing and visualization of climate and remote sensing data for advanced natural resource monitoring and process understanding. Bull. Am. Meteorol. Soc. 98: 2397–2410.

Janzen, D. H. 1967. Why Mountain Passes are Higher in the Tropics. Am. Nat. 101: 233–249.
Johnson, M. S., J. Lehmann, S. J. Riha, A. V Krusche, J. E. Richey, J. P. H. B. Ometto, and E. G. Couto. 2008. CO2 efflux from Amazonian headwater streams represents a significant fate for deep soil respiration. Geophys. Res. Lett. 35: L17401. doi:10.1029/2008gl034619

Lefcheck, J. S. 2016. piecewiseSEM: Piecewise structural equation modelling in r for ecology, evolution, and systematics. Methods Ecol. Evol. 7: 573–579. doi:10.1111/2041-210X.12512

Lefcheck, J. S. 2019. Structural Equation Modeling in R for Ecology and Evolution,.

Lewis, W. M. 1988. Primary production in the Orinoco River. Ecology 69: 679–692.

Lewis, W. M. 2008. Physical and chemical features of tropical flowing waters, p. 1–21. In Tropical Stream Ecology. Academic Press.

Marcarelli, A. M., C. V Baxter, M. M. Mineau, and R. O. Hall. 2011. Quantity and quality: unifying food web and ecosystem perspectives on the role of resource subsidies in freshwaters. Ecology 92: 1215–1225.

Marzolf, E. R., P. J. Mulholland, and A. D. Steinman. 1994. Improvements to the diurnal upstream-downstream dissolved oxygen change technique for determining whole stream metabolism in small streams. Can. J. Fish. Aquat. Sci. 51: 1591–1599.

Mayorga, E., A. K. Aufdenkampe, C. A. Masiello, A. V. Krusche, J. I. Hedges, P. D. Quay, J. E. Richey, and T. A. Brown. 2005. Young organic matter as a source of carbon dioxide outgassing from Amazonian rivers. Nature 436: 538–541. doi:10.1038/nature03880

Mayorga, E., S. P. Seitzinger, J. A. Harrison, and others. 2010. Global Nutrient Export from WaterSheds 2 (NEWS 2): Model development and implementation. Environ. Model. Softw. 25: 837–853. doi:10.1016/j.envsoft.2010.01.007

Mulholland, P. J., C. S. Fellows, J. L. Tank, and others. 2001. Inter-biome comparison of factors controlling stream metabolism. Freshw. Biol. 46: 1503–1517.

Odum, H. T. 1956. Primary production in flowing waters. Limnol. Oceanogr. 1: 102–117.

Ortega-Pieck, A., A. K. Fremier, and C. H. Orr. 2017. Agricultural influences on the magnitude of stream metabolism in humid tropical headwater streams. Hydrobiologia 799: 49–64. doi:10.1007/s10750-017-3204-5

Paaby, P., and C. R. Goldman. 1992. Chlorophyll, primary productivity, and respiration in a lowland Costa Rican stream. Rev. Biol. Trop. 40: 185–198.

Padfield, D., C. Lowe, A. Buckling, R. Ffrench-Constant, S. Jennings, F. Shelley, J. S. Ólafsson, and G. Yvon-Durocher. 2017. Metabolic compensation constrains the temperature dependence of gross primary production. Ecol. Lett. 20: 1250–1260. doi:10.1111/ele.12820

Paerl, H. W., J. T. Scott, M. J. McCarthy, and others. 2016. It Takes Two to Tango: When and Where Dual Nutrient (N & P) Reductions Are Needed to Protect Lakes and Downstream Ecosystems. Environ. Sci. Technol. 50: 10805–10813. doi:10.1021/acs.est.6b02575

Palmer, M. A., and C. M. Febria. 2012. The heartbeat of ecosystems. Science (80-. ). 336: 1393–1394. doi:10.1126/science.1223250

Polato, N. R., B. A. Gill, A. A. Shah, and others. 2018. Narrow thermal tolerance and low dispersal drive higher speciation in tropical mountains. Proc Natl Acad Sci U S A. doi:10.1073/pnas.1809326115

Pringle, C. M., and T. Hamazaki. 1997. Effects of fishes on algal response to storms in a tropical stream. Ecology 78: 2432–2442.

Pringle, C. M., and T. Hamazaki. 1998. The role of omnivory in a Neotropical stream: separating diurnal and nocturnal effects. Ecology 79: 269–280.

Pringle, C. M., P. Paaby-Hansen, P. D. Vaux, and C. R. Goldman. 1986. In situ nutrient assays of periphyton growth in a lowland Costa Rican stream. Hydrobiologia 134: 207–213.

Quay, P. D., D. 0. Wilbur, J. E. Richey, A. H. Devol, R. Benner, and B. R. Forsberg. 1995. The 18O:16O of dissolved oxygen in rivers and lakes in the Amazon Basin: Determining the ratio of respiration to photosynthesis rates in freshwaters. Limnol. Oceanogr. 40: 718–729. doi:10.4319/lo.1995.40.4.0718

R Core Team. 2019. R: A language and environment for statistical computer.

Ramírez, A., M. Ardón, M. Douglas, and M. Graça. 2015. Tropical freshwater sciences: an overview of ongoing tropical research. Freshw. Sci. 34: 606–608.

Ramírez, A., C. M. Pringle, and L. Molina. 2003. Effects of stream phosphorus levels on microbial respiration. Freshw. Biol. 48: 88–97.

Raymond, P. A., C. J. Zappa, D. Butman, and others. 2012. Scaling the gas transfer velocity and hydraulic geometry in streams and small rivers. Limnol. Oceanogr. Fluids Environ. 2: 41–53. doi:10.1215/21573689-1597669

Richey, J. E., J. M. Melack, A. K. Aufdenkampe, V. M. Ballestter, and L. L. Hess. 2002. Outgassing from Amazonian rivers and wetlands as a large tropical source of atmospheric CO2. Nature 416: 617–620.

Ritz, C., F. Baty, J. C. Streibig, and D. Gerhard. 2015. Dose-response analysis using R. PLoS One 10: e0146021.
Riveros-Iregui, D. A., T. P. Covino, and R. González-Pinzón. 2018. The importance of and need for rapid hydrologic assessments in Latin America. Hydrol. Process. 32: 2441–2451. doi:10.1002/hyp.13163

Roberts, B. J., P. J. Mulholland, and W. R. Hill. 2007. Multiple scales of temporal variability in ecosystem metabolism rates: results from 2 years of continuous monitoring in a forested headwater stream. Ecosystems 10: 588–606.

Rohatgi, A. 2019. WebPlotDigitizer.

Rosemond, A. D., C. M. Pringle, A. Ramírez, M. J. Paul, and J. L. Meyer. 2002. Landscape variation in phosphorus concentration and effects on detritus-based tropical streams. Limnol. Oceanogr. 47: 278–289.

Rüegg, J., C. C. Conn, E. P. Anderson, and others. 2020. Thinking like a consumer: linking aquatic basal metabolism and consumer dynamics. Limnol. Oceanogr. Lett. doi:10.1002/lol2.10172

Sager, J. C., and J. C. McFarlane. 1997. Radiation, p. 1–29. In R.W. Langhans and T.W. Tibbitts [eds.], Plant Growth Chamber Handbook. Iowa State University.

Saha, S., S. Moorthi, X. Wu, and others. 2014. The NCEP climate forecast system version 2. J. Clim. 27: 2185–2208. doi:10.1175/JCLI-D-12-00823.1

Savoy, P., A. P. Appling, J. B. Heffernan, E. G. Stets, J. S. Read, J. W. Harvey, and E. S. Bernhardt. 2019. Metabolic rhythms in flowing waters: An approach for classifying river productivity regimes. Limnol. Oceanogr. doi:10.1002/lno.11154

Song, C., W. K. Dodds, J. Rüegg, and others. 2018. Continental-scale decrease in net primary productivity in streams due to climate warming. Nat. Geosci. 11: 415–420. doi:10.1038/s41561-018-0125-5

Taylor, B. W., A. S. Flecker, and R. O. Hall Jr. 2006. Loss of a harvested fish species disrupts carbon flow in a diverse tropical river. Science (80-. ). 313: 833–6.

Townsend, A. R., G. P. Asner, and C. C. Cleveland. 2008. The biogeochemical heterogeneity of tropical forests. Trends Ecol. Evol. 23: 424–431. doi:10.1016/j.tree.2008.04.009

Townsend, A. R., C. C. Cleveland, B. Z. Houlton, C. B. Alden, and J. W. C. White. 2011. Multi-element regulation of the tropical forest carbon cycle. Front. Ecol. Environ. 9: 9–17. doi:10.1890/100047

Vannote, R. L., G. W. Minshall, K. W. Cummins, J. R. Sedell, and C. E. Cushing. 1980. The river continuum concept. Can. J. Fish. Aquat. Sci. 37: 130–137.
Vlah, M., and Berdanier. 2020. StreamPULSE: Run Stream Metabolism Models on StreamPULSE data.

Ward, N. D., R. G. Keil, P. M. Medeiros, and others. 2013. Degradation of terrestrially derived macromolecules in the Amazon River. Nat. Geosci. 6: 530–533. doi:10.1038/ngeo1817

Webster, J. R., and J. L. Meyer. 1997. Organic matter budgets for streams: a synthesis. J. North Am. Benthol. Soc. 16: 141–161.

Welter, J. R., J. P. Benstead, W. F. Cross, J. M. Hood, A. D. Huryn, P. W. Johnson, and T. J. Williamson. 2015. Does N2 fixation amplify the temperature dependence of ecosystem metabolism? Ecology 96: 603–610. doi:10.1890/14-1667.1

Whiles, M. R., R. O. Hall, W. K. Dodds, and others. 2013. Disease-Driven Amphibian Declines Alter Ecosystem Processes in a Tropical Stream. Ecosystems 16: 146–157. doi:10.1007/s10021-012-9602-7

Williamson, T. J., W. F. Cross, J. P. Benstead, G. M. Gíslason, J. M. Hood, A. D. Huryn, P. W. Johnson, and J. R. Welter. 2016. Warming alters coupled carbon and nutrient cycles in experimental streams. Glob. Chang. Biol. 22: 2152–2164. doi:10.1111/gcb.13205

Yvon-Durocher, G., J. M. Caffrey, A. Cescatti, and others. 2012. Reconciling the temperature dependence of respiration across timescales and ecosystem types. Nature 487: 472–476. doi:10.1038/nature11205

# Chapter 3: Partitioning inorganic carbon fluxes using paired $O_2$-$CO_2$ gases in a headwater stream, Costa Rica

## 3.1 Introduction

Inland waters play an important role in the global carbon (C) cycle and estimates of C fluxes between inland waters, the atmosphere, and terrestrial ecosystems are being revised at a rapid rate (Cole et al. 2007; Raymond et al., 2013; Drake et al. 2018; Tank et al. 2018). Streams, wetlands, and lakes transform, export, and store terrestrial C prior to delivery downstream to the ocean (Cole et al. 2007) and contribute $CO_2$ to the atmosphere (Battin et al. 2009). These processes are particularly important in headwaters and small flowing water bodies, which comprise 79% of stream length (Colvin et al. 2019) and disproportionately contribute to evasion of $CO_2$ to the atmosphere on an areal basis (Raymond et al. 2013; Borges et al. 2019). However, these findings represent the synthesis from predominantly temperate systems, whereas tropical streams have not received similar study (Aufdenkampe et al. 2011). Tropical streams, as a result of higher year-round temperatures, high and continuous organic matter inputs, and drain soils with high respiration rates, are likely to be hotspots of greenhouse gas emissions and fluxes (Borges et al. 2019). In-stream production of $CO_2$ from processing of organic matter can further contribute to high $CO_2$ fluxes (Richey et al. 2002; Mayorga et al. 2005; Hotchkiss et al. 2015).

Streams are generally supersaturated with respect to atmospheric $CO_2$ (Wetzel and Likens 2000), reflecting large fluxes of $CO_2$ into headwater streams of both terrestrially derived and internally produced $CO_2$. Terrestrially derived $CO_2$ enters via subsurface groundwater as the result of respiration in soils. In contrast, $CO_2$ from internal processes is the result of respiration by in-stream heterotrophs minus uptake as gross primary productivity, represented as net ecosystem production (NEP) (Odum 1956). In headwater streams, the influence of terrestrially

derived $CO_2$ is greater than internal production and decreases in importance in larger streams and rivers (Hotchkiss et al. 2015). Losses of $CO_2$ from streams include evasion to the atmosphere, uptake through photosynthesis, and hydrologic export downstream. Evasion from freshwaters is a large flux of C largely unaccounted for in terrestrial budgets (Genereux et al. 2013) and is important at global scales (Raymond et al. 2013). Hydrologic export of dissolved inorganic carbon (DIC) includes all forms of C in equilibrium with the carbonate system, as $CO_2$, $HCO_3^-$, or $CO_3^{2-}$-, which speciate according to pH (Stumm and Morgan 1996). High concentrations of $CO_2$ can act as a weak acid and reduce pH, depending on the buffering capacity of the receiving water (Wetzel and Likens 2000; Small et al. 2012) and accelerate dissolution of carbonate minerals (Stoddard et al. 1999).

Advances in sensor technology allows for measurement of $CO_2$ in addition to $O_2$ at high frequency in freshwaters (Johnson et al. 2010), permitting estimation of fluxes across hydrologic conditions and as drivers of physicochemical processes in streams. Results from discrete sampling of evasion and lateral inputs of $CO_2$ reveal important understanding of underlying processes and estimates of upscaled fluxes (Oviedo-Vargas et al. 2015). Aquatic sensors allow partitioning into sources and sinks at higher frequency and under conditions hard to capture using discrete sampling (e.g. floods). Further, coupling $CO_2$ sensor data with $O_2$ data to determine NEP using methods to estimate stream C fixation and production allows for finer parsing of $CO_2$, variability across the hydrologic conditions, and evaluate processes that affect concentrations of both gases together (e.g. gas exchange, respiration) and separately (e.g. anaerobic respiration) (Vachon et al. 2020). Previous studies spanning various stream types across the continental US identified temporal patterns in headwater stream $CO_2$, from diel to annual and influenced by biology, physics, and hydrology (Crawford 2017). While combining

$CO_2$ and $O_2$ sensor data in headwater streams to partition and account for various sources and sinks has been applied in Arctic and temperate streams (Lupon et al. 2019; Rocher-Ros et al. 2019), these methods have not been applied in tropical streams. Last, deploying $CO_2$ sensors into shallow riparian wells reveals a novel approach to estimate $CO_2$ from groundwater and documenting higher concentrations (>15000 ppm $CO_2$) observed in these environments (Leith et al. 2015) and reflect the low pH observed in subsurface water (Small et al. 2012).

In this paper, we present the results of continuous deployment of $O_2$ and $CO_2$ sensors in a lowland Neotropical rainforest headwater stream in La Selva Biological Station, Costa Rica. We supplemented in stream sensors with a riparian well $CO_2$ sensor well to measure groundwater inputs of $CO_2$ ($GW_{CO2}$). We combined sensor data to estimate $CO_2$ fluxes into and out of the study reach, including hydrologic export, NEP from $O_2$ sensors, evasion, and groundwater inputs. The duration of our monitoring period allowed evaluation of $CO_2$ fluxes across short-term (i.e. individual rainfall events) and seasonal hydrologic patterns (i.e. the transition from dry to wet season) in a tropical wet forest stream. We hypothesized that 1) $CO_2$ would be supersaturated and $O_2$ undersaturated with respect to atmospheric equilibrium and the variation in paired gas concentration over time would reflect inputs from groundwater, 2) all $CO_2$ fluxes ($H_{CO2}$, $H_{HCO3}$, NEP, $F_{CO2}$, and $GW_{CO2}$) would increase during the wet season, 3) evasion would be greater fate of $CO_2$ compared to hydrologic loss, 4) discharge will drive increases in $CO_2$ fluxes, and 5) higher fluxes of $GW_{CO2}$ will decrease stream pH.

## 3.2 Methods

### 3.2.1 Site description

La Selva Biological Station, Costa Rica (LSBS), is a 1600 ha tropical wet forest reserve, with elevation ranging from 22 to 146 meters above sea level (Fig 3.1). LSBS is located at the

transition from the upland foothills of the Cordillera Central of Costa Rica and the Caribbean lowlands, and is the lowland terminus of the altitudinal transect in the Braulio Carrillo National Park (Fig 3.1). Mean annual rainfall from is 4300 mm, with dry season January to April and wet season July to December (Sanford et al., 1994).

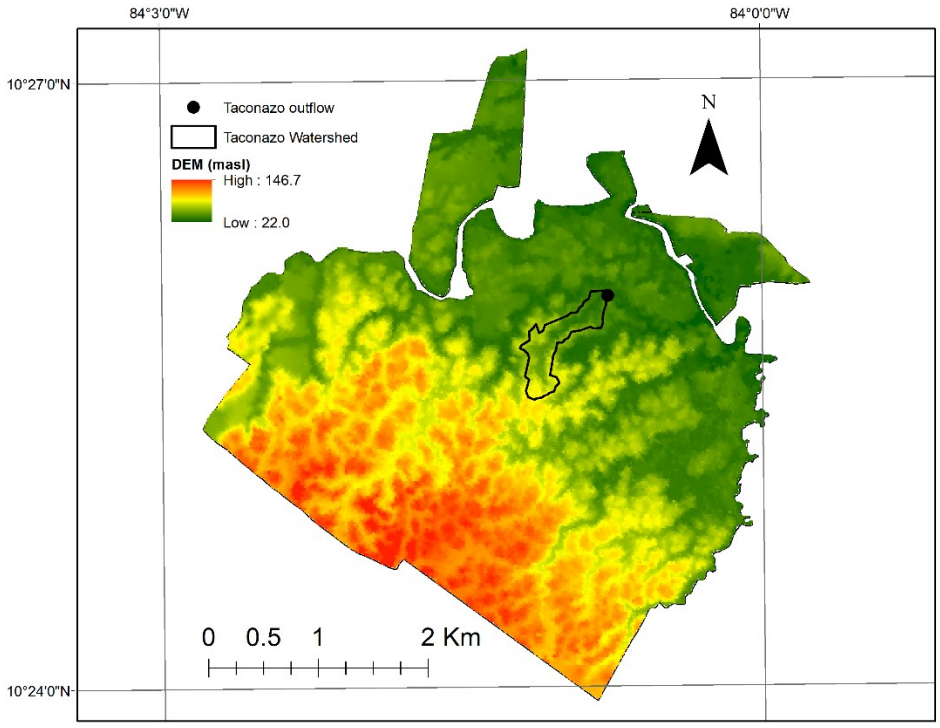


**Figure 3.1** Map of La Selva Biological Station filled with a 1 m digital elevation model. The Taconazo watershed (0.28 km2) is outlined in black and outflow designated at the black circle.

We focused on the lower 75 m reach of the Taconazo stream (10.432, -84.013) to partition $CO_2$ between inputs (NEP and $GW_{CO2}$) and outputs ($F_{CO2}$, $H_{CO2}$, $H_{HCO3}$). The Taconazo watershed area is 0.28 $km^2$, all of which is forested with a closed canopy (Table 3.1). The Taconazo is a low solute stream at LSBS, with long-term (1997 - 2015) mean water temperature is 25.1 ˚C, pH of 5.5, discharge of 0.06 $m^3 s^{-1}$, and $NO_3^-$ and SRP of 192.4 µg $L^{-1}$ and 4.9 µg $L^{-1}$, respectively (Ganong et al. 2015). The Taconazo has received significant study as a model

headwater forested tropical stream. Numerous studies from the Taconazo have contributed to better understand of the hydrology (Genereux et al. 2005; Genereux and Jordan 2006), biogeochemistry (Small et al. 2012; Osburn et al. 2018), and ecology (Ardón et al., 2006; Ramírez et al., 2003; Rosemond et al., 2002) of tropical headwater streams.

**Table 3.1** Reach characteristics from the Taconazo and summary statistics for physicochemical data during the study period. High frequency data is presented as the median (range) during the monitoring period.

| Characteristic (unit) | Value |
|---|---|
| Reach length (m) | 75 |
| Mean reach width (m) | 1.3 |
| Mean reach velocity (m $s^{-1}$) | 0.014 |
| Travel time (min) | 82.5 |
| Gradient (m $m^{-1}$) | 0.0024 |
| Temperature (˚C) | 24.5 (21.2 – 29.6) |
| DO (mg $L^{-1}$) | 5.94 (0.26 – 8.32) |
| pH | 5.32 (4.02 – 6.91) |
| $pCO_2$ (ppm) | 6443.6 (773.8 – 11994) |
| Discharge ($m^3$ $s^{-1}$) | 0.017 (0 – 1.378)[1] |

[1]excludes backflooding events when the downstream Rio Puerto Viejo floods its tributaries, including the Taconazo (Zanon et al., 2014).

3.2.2. Data collection

We collected stream data from April 1, 2013 - September 30, 2013. Discharge ($m^3$ $s^{-1}$) was continuously measured from the V-notch weir constructed near the outflow of the Taconazo; further descriptions of the weir in Zanon et al. (2014). Rainfall (mm) was collected from the

LSBS weather station, located ~900 m from the Taconazo. Meteorological data are available at: https://archive.tropicalstudies.org/meteoro/default.php?pestacion=201.

Groundwater discharge into the 75 m study reach has previously been measured using conservative tracer injections. In the dry season (April), groundwater flux into the reach was 20% of total stream discharge (Oviedo-Vargas et al. 2015), compared to the wet season (May-September) flux of 9% (Oviedo-Vargas et al. 2015, Ardón et al. 2013). For the dry and wet season, we multiplied discharge by the respective percentages as an estimate of groundwater discharge into the study reach.

A YSI 600xlm multiprobe sonde was secured 5 cm above the stream bottom in a PVC tube with holes drilled to allow for exchange of stream water. The multiprobe continuously measured temperature (˚C), pH, and DO (mg $L^{-1}$ and %-saturation) at hourly intervals. The sonde was retrieved every two weeks for recalibration and to clean fouling on the sensor heads. Partial pressure of $CO_2$ (ppm) was measured using a Vaisala GMT221 infrared gas analyzer (IRGA) in the stream and in a riparian well. The sensors were prepared for submerged deployment as described in Johnson et al. (2010) and $pCO_2$ was logged hourly using a Campbell CR1000 datalogger. *p*CO2 data were processed according to Johnson et al. (2010) for depth and temperature. We removed data from all sensors when the water level fell below the height of the sonde (e.g. conductivity < 0.005, DO near air saturation). Sensor data underwent further QAQC following the guidance of Taylor and Loescher (2013), inspecting or removing data that were flagged.

### 3.2.3 Gas departure variability and hysteresis

We evaluated the departure of $O_2$ and $CO_2$, measured as the difference of gas concentration relative to atmospheric equilibrium, and the change of gas departure over time. Processes that mediate $O_2$ and $CO_2$ departure in freshwaters include biochemical reactions that directly link $O_2$ and $CO_2$ (e.g. aerobic metabolism), water temperature, bicarbonate chemistry, and gas exchange (Vachon et al. 2020). Departure of $O_2$ and $CO_2$ is calculated as the difference between the measured gas concentration and the concentration at atmospheric saturation. For $CO_2$, we assumed atmospheric concentration of 400 ppm and for $O_2$, we calculated saturation as a function of temperature and barometric pressure at each time step, following the outline in Hall and Hotchkiss (2017). To reflect the stoichiometry between $O_2$ and $CO_2$ in biochemical reactions, gas concentrations were converted to molar units.

Paired $O_2$ and $CO_2$ departure were plotted as a data cloud. To evaluate movement of the cloud over time, we estimated 95% confidence interval ellipses for each month of the data collection using the ellipse v0.4.2 R package (Murdoch and Chow 2020). In each ellipse, we calculated the: 1) centroid, which indicates the quadrant location in Cartesian space and the average net effect on both $O_2$ and $CO_2$; 2) 1/[slope] through each ellipse, which details the efficiency of metabolism between $O_2$ and $CO_2$, interpreted as the moles of $CO_2$ produced per moles of $O_2$ consumed through ecosystem respiration. See Vachon et al. (2020) for more details on these metrics.

To examine the role of individual rainfall events (2067 mm over 180 days) on $pCO_2$, we selected three storm events in each the dry season, early wet season (June), and late wet season (August). In each of these events, we examined the hysteresis response of $pCO_2$ to discharge during these events. For each event, we subset the dataset to 1 hour prior to the rising limb,

through the peak in discharge, and for 5 hours following return to pre-storm discharge and before the next rising limb in the hydrograph (Evans and Davies 1998; Dinsmore and Billett 2008). We evaluated each hysteresis response for diagnostics describing the solute-discharge rotation (clockwise vs. counterclockwise vs. 'figure 8') and trend (positive vs. negative) (Evans and Davies 1998).

### 3.2.4 $CO_2$ flux calculations

$CO_2$ losses from the reach were defined as $F_{CO2}$ and hydrologic export, as $H_{CO2}$ and $E_{CO3}$. We calculated aqueous $CO_2$ ($[CO_2]_{aq\text{-}stream}$ and $[CO_2]_{aq\text{-}well}$) from the in-stream and riparian well stations from *p*CO2 using Henry's Law, using the temperature-corrected Henry's Law constant from Plummer and Busenberg (1982). Stream $CO_2$ saturation ($[CO_2]_{sat}$) was determined using the same method, substituting 400 ppm as the assumed atmospheric $CO_2$ concentration (Rocher-Ros et al. 2019). $CO_2$ evasion ($F_{CO2}$, g C $m^{-2}$ $h^{-1}$) was calculated as

$$F_{CO2} = ([CO_2]_{aq-stream} - [CO_2]_{sat}) * K_{CO2} * \bar{z} * 12.01 \quad (1)$$

Where $K_{CO2}$ is the dry (1.13 $h^{-1}$) or wet season (0.43 $h^{-1}$) gas exchange coefficient reported in Oviedo-Vargas et al. (2015), and z is depth in meters measured at the weir.

We defined $CO_2$ inputs to the lower reach as the groundwater $CO_2$ flux and from in-stream net ecosystem production (NEP). Groundwater $CO_2$ flux ($GW_{CO2}$) was estimated by multiplying the groundwater flux into the reach by $[CO_2]_{aq\text{-}well}$. We estimated hourly NEP using the instantaneous metabolism method outlined in Hall and Hotchkiss (2017). Briefly, NEP was estimated from the volumetric $O_2$ mass balance equation:

$$NEP_i = \left(\frac{O_i - O_{i-\Delta t}}{\Delta t} - K_O\left(O_{sat,i} - O_i\right)\right) * \bar{z} \quad (2)$$

Where $NEP_i$ is hourly instantaneous metabolism, $O_i$ is the $O_2$ concentration at each timepoint, $O_{sat,i}$ is the concentration of $O_2$ at saturation for the same timepoint, z is stream depth, and $K_O$ is the gas exchange coefficient for $O_2$. We converted $K_O$ from $K_{CO2}$ via Schmidt scaling (Raymond et al. 2012). Hourly NEP was converted to g C $m^{-2}$ assuming a 1:1 respiratory quotient (Rocher-Ros et al. 2019). We selected this direct metabolism method for determining NEP for two reasons: 1) the lack of a diel $O_2$ signal (Appendix 3), and 2) relatively high reaeration, make the Taconazo ill-suited to alternative stream metabolism methods (Appling et al. 2018).

Hydrologic export included both $[CO_2]_{aq}$ and $[HCO_3^-]$. $[HCO_3^-]$ was calculated from pH data combined with carbonate equilibrium dissociation constants, $\alpha_0$ and $\alpha_1$

$$\alpha_0 = \left(1 + \frac{K_1}{[H^+]} + \frac{K_1 K_2}{[H^+]^2}\right)^{-1} \quad 3$$

$$\alpha_1 = \left(1 + \frac{[H^+]}{K_1} + \frac{K_2}{[H^+]}\right)^{-1} \quad 4$$

Where $K_1$ is $10^{-6.3}$ and $K_2$ is $10^{-10.3}$. From these dissociation constants, we calculated total DIC as

$$DIC = \frac{[CO_2]_{aq}}{\alpha_0} \quad 5$$

And $[HCO_3^-]$ as

$$[HCO_3^-] = DIC * \alpha_1 \quad 6$$

Hydrologic export, $H_{CO2}$ and $H_{HCO3}$, as daily flow-weighted export, using hourly discharge and $[CO_2]_{aq}$ and $[HCO_3^-]$ following equations detailed by Birgand et al. (2010). Exports were converted to units of g C $d^{-1}$ and total DIC export as the daily sum of $H_{CO2}$ and $H_{HCO3.}$ The highest pH was 7.5, rendering DIC as $[CO_3^{2-}]$ negligible (<0.2% of total DIC) and not considered.

We compared sensor estimates of DIC to DIC estimates from syringe samples of stream water. Samples were collected in 10 mL syringe and 4 mL of water was injected into an inverted sealed serum vial with a 22-gauge needle and 0.45 μm pore filter. Samples were equilibrated on a shaker table, and 250 μL headspace was removed and $pCO_2$ analyzed on an SRI Instruments gas chromatograph (Las Vegas, Nevada, USA). Conversions from $pCO_2$ to DIC were calculated as described above. We matched the dates of syringe samples with sensor derived estimates and compared the two methods using the Student's t-test.

### 3.2.5 Drivers of $CO_2$ fluxes

Sub-daily fluxes were aggregated to daily rates. Daily fluxes were the sum of hourly fluxes, daily rainfall the sum of hourly rainfall, and discharge summarized as mean daily discharge. To evaluate univariate control of $CO_2$ fluxes by discharge, we used the Kendall rank correlation, $\tau$, on $\log_{10}$ transformed daily aggregated data. To evaluate multivariate control of the calculated $CO_2$ fluxes by discharge, rainfall, and the other fluxes, we used principal component analysis (PCA) on $\log_{10}$ transformed daily aggregated data. We lagged rainfall by one day to demonstrate the aggregated hydrologic fluxes in the preceding day will manifest changes in the fluxes the following day. We selected one day as the hydrologic events in the small Taconazo generally occur with that period (Genereux et al. 2005), though there are alternative methods to derive lags (Dinsmore and Billett 2008). To account for the broad ranges in the fluxes and different units for discharge, input data were scaled such that each flux had mean = 0 and variance = 1.

We evaluated the relationship of groundwater inputs of $CO_2$ as a driver of stream acidification events in the Taconazo. We used lm() to fit daily aggregated data in R v4.0.3 (R Core Team 2020).

## 3.3 Results

### 3.3.1 Field data

Total rainfall during the 180-day monitoring period was 2067 mm, with median daily rain of 2.29 mm (range: 0 – 107 mm) and 49 days with no rainfall recorded (Fig 3.2, a). April had the lowest rainfall (104.1 mm) and June had the most rainfall (498.6 mm). Median hourly discharge was 0.004 $m^3\ s^{-1}$ (0 – 1.378 $m^3\ s^{-1}$ range). Median discharge was lowest in April (0.0002 $m^3\ s^{-1}$) and greatest in July (0.0160 $m^3\ s^{-1}$). Median estimated groundwater flux into the reach was 0.0003 $m^3\ s^{-1}$ (0 – 0.0346 $m^3\ s^{-1}$ range) and followed temporal patterns as stream discharge, as expected (Fig 3.2, b). $pCO_2$ in the stream had median pressure of 6343.6 ppm (range 773 – 11994 ppm), lower than the measured in the riparian well (median $pCO_2$ 46924 ppm, range 28663 – 48683 ppm). Over the monitoring period, 13.8% of hourly $pCO_2$ measurements were missed in the stream, the largest missing section corresponding with the highest flows in late July and early August (Fig 3.2, d). In the riparian well, 26.7% of timepoints were missing, including the same period missing from the stream time-series, but also a period in May, during the likely transition from dry to wet season (Fig 3.2, e).

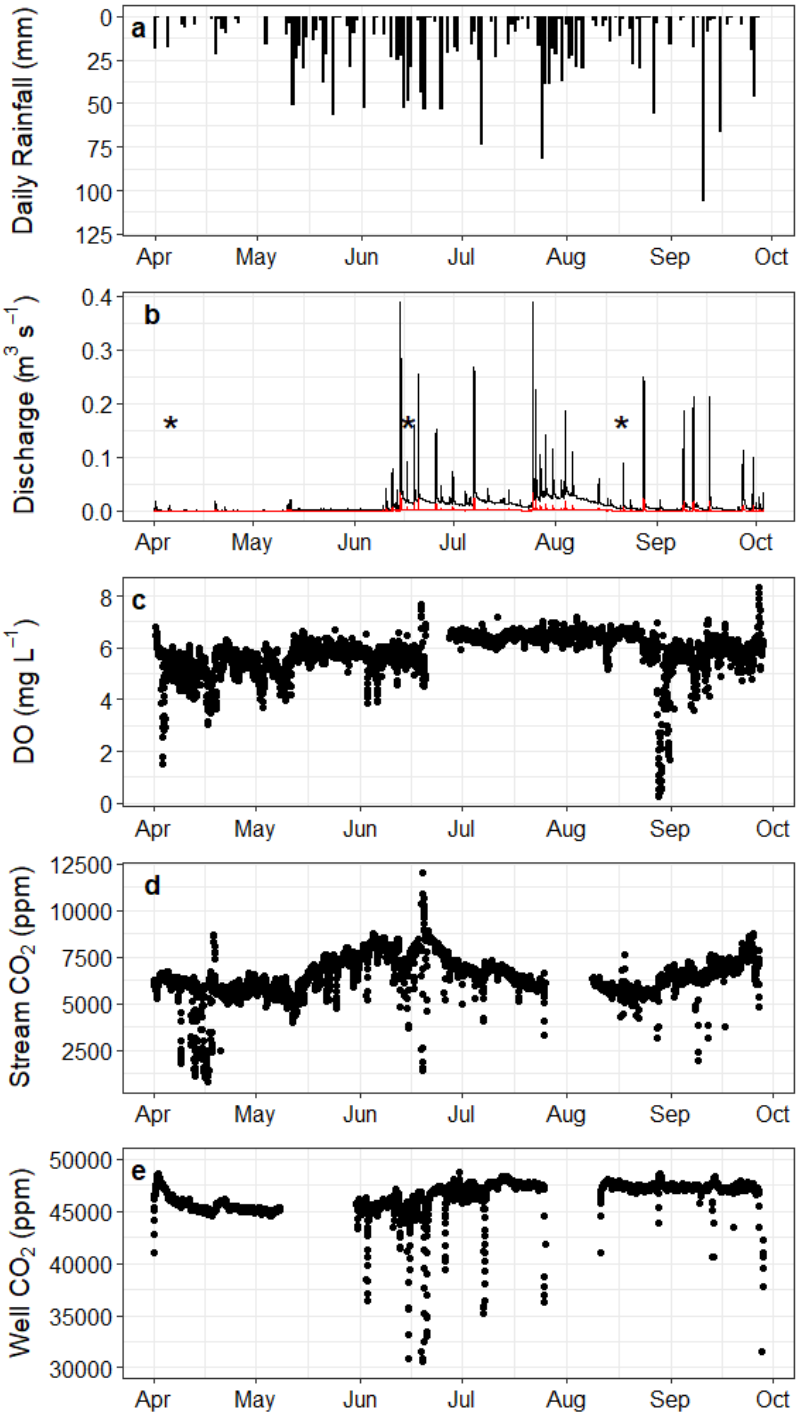


**Figure 3.2** a) Daily rainfall, b) hourly stream (black line) and groundwater (red line) discharge in the Taconazo, and hourly c) dissolved oxygen (mg $L^{-1}$), d) stream and e) riparian well $CO_2$ (ppm). Asterisk (*) in panel b) correspond to events used in to explore hysteresis.

3.2 Gas dynamics

In departure space, all data points show extreme $CO_2$ super-saturation and $O_2$ undersaturation. $CO_2$ departure was ~3100-times greater than $O_2$ departure (Fig 3.3, a). While the mean centroids and large overlap of the monthly ellipses showed little variation (Fig 3.3, b; Table 2), there is slight clockwise movement in departure space (Fig 3, c). Movement from April to May to June towards the bottom right exacerbates the supersaturation of $CO_2$ and undersaturation in $O_2$. From June to July, both $CO_2$ and $O_2$ departure slightly decreases. Ellipse centroid location varied little over time. The orientation of the ellipses, 1/[slope] for each month, was greatest in April (56938) and lowest in August (2055), showing a 27.7-fold decrease (Fig 3.3, b), indicating 92-times more mol $CO_2$ produced per mol $O_2$ consumed in April than in August.

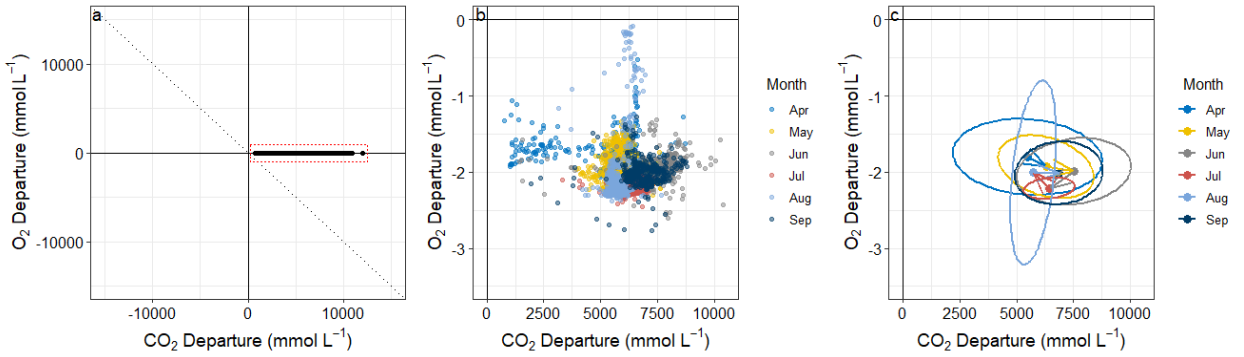


**Figure 3.3** Paired $O_2$ and $CO_2$ departure from atmospheric equilibrium clouds. a) All data plotted on equal axes, highlighting the $CO_2$ supersaturation and slight $O_2$ undersaturation, with the 1:-1 line representing gas concentrations are mediated by aerobic metabolism. The outlined area in red represents the plotting area in panels b) and c). b) All hourly data collected, with points colored by month. c) 95% CI ellipsoids of each month's data cloud, with mean as squares and arrows showing movement of centroids from one month to the next. Note the 1:-1 line is not visible in panels b) and c).

**Table 3.2** Paired $O_2$ - $CO_2$ metrics for ellipses for each month of the monitoring period. Mean $CO_{2\text{-Dep}}$ and $O_{2\text{-Dep}}$ correspond to the x and y coordinates for the squares in Fig 3b, and 1/[slope] is the slope of the linear model fit through each ellipse

| Month | Mean $CO_{2\text{-Dep}}$ (SD) | Mean $O_{2\text{-Dep}}$ (SD) | 1/[Slope] (mmol $L^{-1}$/mmol $L^{-1}$) |
|---|---|---|---|
| April | 5482.1 (1339.0) | -1.80 (0.21) | 56938 |
| May | 6292.8 (856.2) | -1.93 (0.17) | 16044 |
| June | 7516.8 (1025.4) | -1.99 (0.18) | 35499 |
| July | 6436.3 (457.3) | -2.21 (0.06) | 36330 |
| August | 5737.5 (411.0) | -2.01 (0.49) | 2055 |
| September | 6856.3 (793.6) | -2.01 (0.17) | 61458 |
| All Dates | 6272.0 (1273.5) | -1.98 (0.27) | 40578 |

3.3.2. $CO_2$ fluxes

Estimates of DIC from both discrete sampling (mean 2.78 ± 0.68 mg C $L^{-1}$) and from the sensor (mean = 2.94 ± 0.45 mg C $L^{-1}$) were similar ($p = 0.34$). For $CO_2$ inputs, median $GW_{CO2}$ (4.9 g C $m^{-2}$ $d^{-1}$, range 0 – 389) was 5.2-times greater than median NEP (0.67 g C $m^{-2}$ $d^{-1}$, range -3.8 – 6.1). $GW_{CO2}$ increased in June, while NEP decreased from April through mid-August, concurrent with the peak of the rainfall during the wet season (Fig 3.4, a). For 179 of the 180 days, NEP was a positive C flux. $F_{CO2}$ had median 5.4 g C $m^{-2}$ $d^{-1}$ (range 0.3 – 39.8, Fig 3.4, b). Flow-weighted hydrologic export was large, with $H_{CO2}$ (median 16.1 g C $ha^{-1}$ $d^{-1}$, range 0 – 463.6) and $H_{HCO3}$ (median 1.85 g C $ha^{-1}$ $d^{-1}$, range 0 – 158.2, Fig 3.4, c).

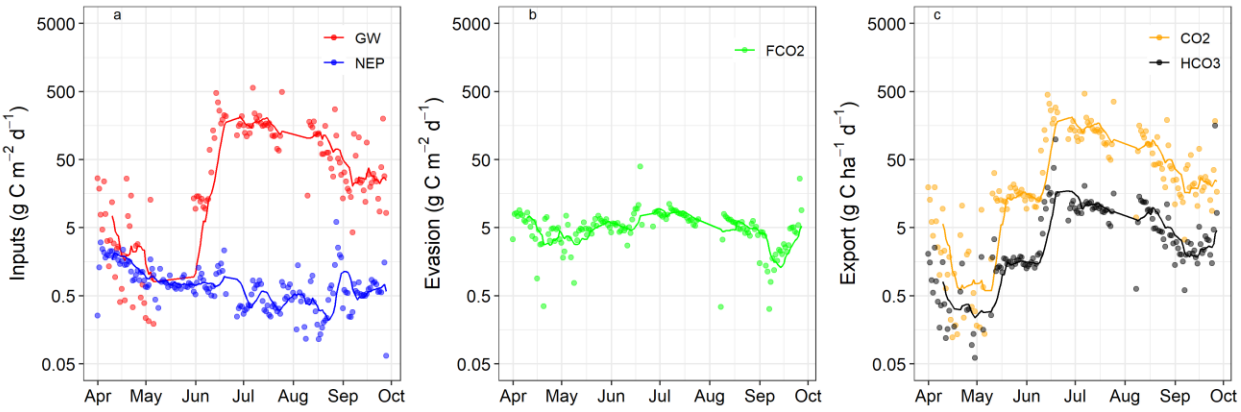


**Figure 3.4** $CO_2$ a) inputs and b) evasion, and c) flow-weighted hydrologic export in the Taconazo. Points in red are $CO_2$ from groundwater and points in blue are from NEP. In b) green points are $F_{CO2}$. In c) orange points are $H_{CO2}$ and black are $H_{HCO3}$. Lines are 10-day moving average. Note benthic areal flux units for $GW_{CO2}$, NEP, and $F_{CO2}$, compared to hydrologic exports expressed as loads normalized by watershed area.

### 3.3.3. Drivers of $CO_2$ fluxes

PCA explained 67.2% of the variation in the first two principal components and identified PC1 along $CO_2$ fluxes influenced by the hydrology of the Taconazo (Fig 3.5). Fluxes tied to hydrology, $GW_{CO2}$ and $H_{CO2}$, positively aligned with PC1, particularly for days in June, July, and August, and in opposition to points from April and September. PC2 oriented along an axis defined by lagged rainfall and NEP. Using the Kendall rank correlation statistic, $\tau$, non-hydrologic fluxes, $F_{CO2}$ ($\tau$ = -0.10, p = 0.05) and NEP ($\tau$ = -0.31, $p < 0.01$), were negatively correlated with discharge.

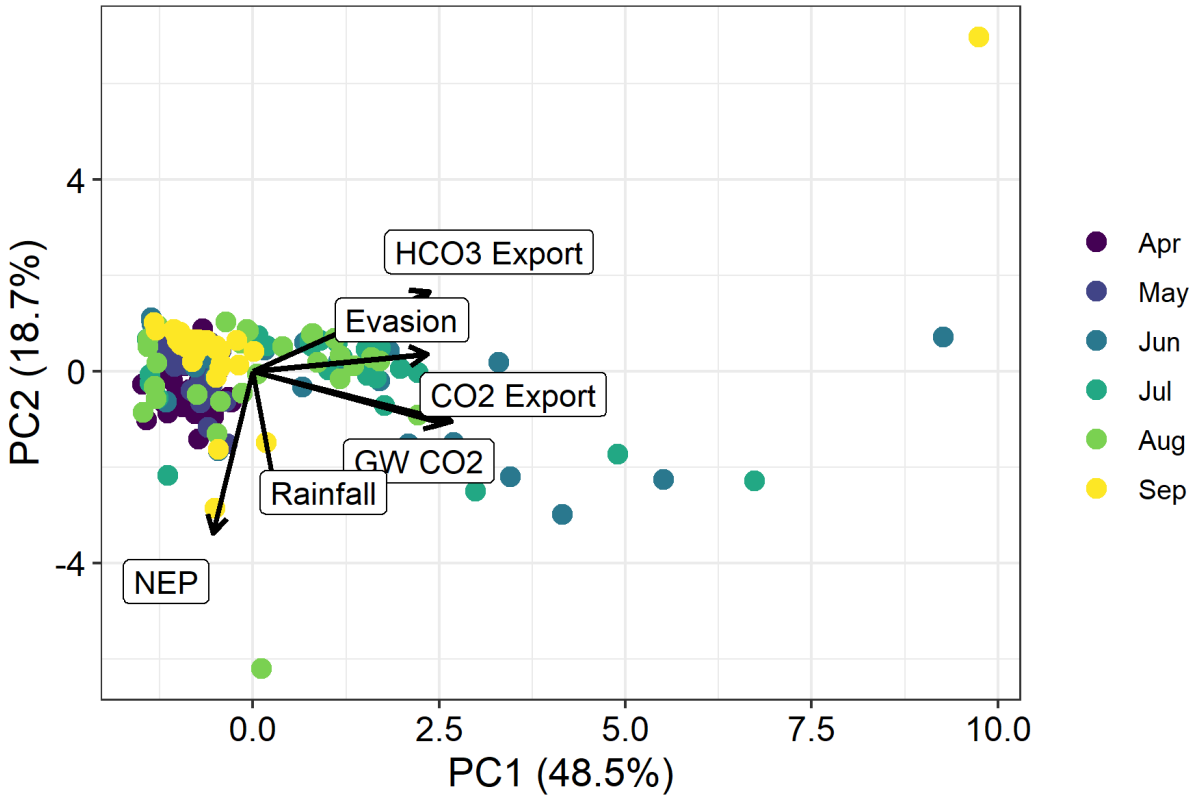


**Figure 3.5** Principal component analysis on $CO_2$ fluxes and discharge in the Taconazo. Points are colored for the months during the data collection. Variation explained in principal components 1 and 2 are in parentheses of each axis title.

3.4 $pCO_2$ hysteresis and influence on pH

There is little evidence of hysteresis between $pCO_2$ and discharge in the three storm events we examined. In the dry season, $pCO_2$ varies little across the rise in discharge, though during the falling limb, there is slight 'figure 8' rotation (Fig 3.6, a). Similarly, during the wet season events, $pCO_2$ varied little preceding, during, and during the falling limb, $pCO_2$ decreases before returning to pre-storm concentration (Fig 3.6 b). In the late wet season, $pCO_2$ stays relatively constant during the rising limb, before oscillating during the falling limb (Fig 3.6, c). Of note, during the early wet season event, overall $pCO_2$ was greater than during the dry and late

wet season events, and peak event discharge during the dry season (0.01 $m^3$ $s^{-1}$) was less than the early (0.08 $m^3$ $s^{-1}$) and late (0.08 $m^3$ $s^{-1}$) wet season events.

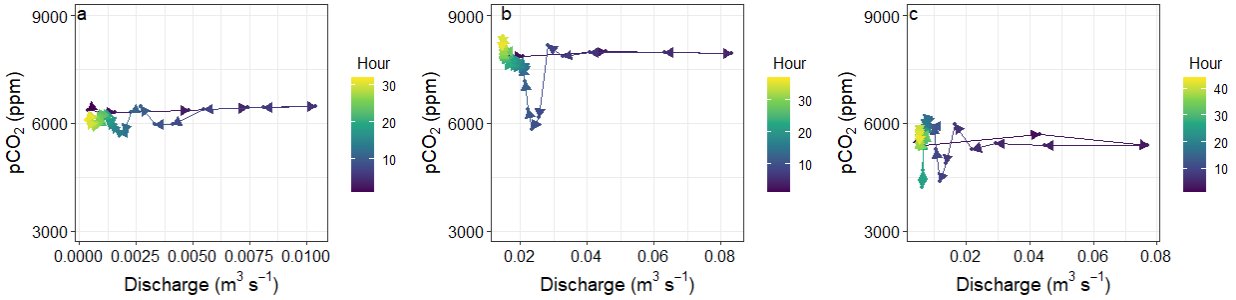


**Figure 3.6** Concentration - discharge plots of three storm events in the Taconazo during the a) dry season, b) early wet season (June), and c) late wet season (August). Point and line segment colors indicate the hour of the storm event, with dark colors showing early in the event and lighter later in the event.

Mean daily pH was lower when preceding day had greater $GW_{CO2}$ (Fig 3.7), fitting a logarithmic model ($F_{1,134} = 3.59$, $p = 0.06$, $R^2 = 0.02$). There were differences in pH response between months and seasons. In the dry season (April), mean daily pH fell to 4.50 at $GW_{CO2}$ of 1.69 g C $m^{-2}$ $d^{-1}$. During the peak of the wet season (July), $GW_{CO2}$ was 388 g C $m^{-2}$ $d^{-1}$, a 224-fold increase in $GW_{CO2}$, but corresponded to a mean daily pH of 5.4.

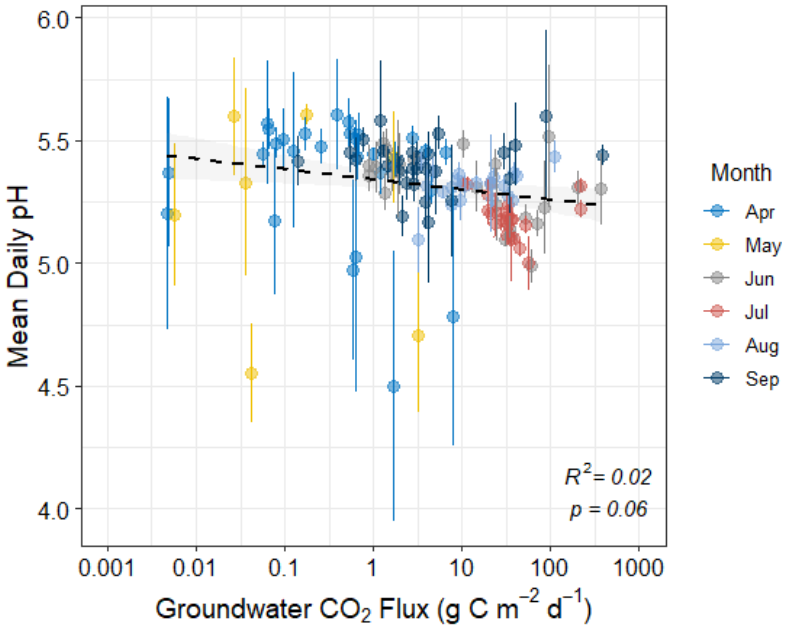


**Figure 3.7** Groundwater $CO_2$ flux as a driver of the next day mean stream pH. Dashed line is logarithmic line-of-best fit (p = 0.06). Point color indicates the month and vertical bars for each point represent the pH daily standard deviation.

## 3.4 Discussion

We showed that a combined sensor approach in stream combined with riparian well $CO_2$ sensors can be used to estimate inputs of terrestrial C into streams and atmospheric and hydrologic losses of C. Further, we showed $CO_2$ fluxes responded to changes in seasonality, defined by changes in rainfall and discharge. We find hydrologic export of inorganic C is an important loss of C from the Taconazo, revealing an important flux in headwater streams to consider in reach scale C assessments and budgets. Evasion in the Taconazo is a large flux compared to streams of similar sizes, reflecting an important fate in tropical headwater streams.

4.1. Temporal variability of gases and $CO_2$ fluxes

*p*$CO_2$ measured in the Taconazo is relatively high compared to *p*$CO_2$ in other streams. Compared to a cross-biome monitoring study, Taconazo *p*$CO_2$ was higher than 6 of the 7 streams monitored, only less than a site in a southern hardwood forest and greater than a tropical stream in Puerto Rico (Crawford et al. 2017). We observe little diel variability in *p*$CO_2$ or $O_2$ (Appendix 3), indicating gross primary productivity (GPP) is low in the Taconazo, and supported by the NEP estimates > 0 g C $m^{-2}$ $d^{-1}$ (Fig 3.3). Further, the paired $O_2$ - $CO_2$ cloud (Fig 3.3, a) is located far from the 1:-1 line for all time points, indicating aerobic metabolism is not a dominant process in the Taconazo and is not responsible for driving $O_2$ and *p*$CO_2$. In tundra headwater streams, the location of the $CO_2$-$O_2$ departure cloud was closer to the 1:-1 line and reflected the greater influence of in-stream NEP on $F_{CO2}$ (Rocher-Ros et al. 2019).

Over the monitoring period, we spanned one month of the dry season and the remainder during the wet season, following the seasonality reported at LSBS (Sanford Jr. et al. 1994). The transition from dry to wet season shows as increased rainfall in mid-May. The dry to wet transition coincides with an increase in stream *p*$CO_2$. Unfortunately, the well sensor did not collect data during this transition, but we hypothesize a similar increase in *p*$CO_2$ in the riparian groundwater stimulates the increase in stream *p*$CO_2$ via $GW_{CO2}$. During the wet season, along with an increase in stream *p*$CO_2$ there was greater variability in both stream *p*$CO_2$ and well $CO_2$. The variability is apparent in the wet season events (Fig 3.6 b, c), where *p*$CO_2$ shows little change on the rising limb of the hydrograph, but on the falling limb, either decreases (Fig 3.6, b) or shows little variation (Fig 3.6, c) before returning to pre-storm *p*$CO_2$. The increase in *p*$CO_2$ in the wet season reflects higher $GW_{CO2}$ flux corresponding to higher discharge and groundwater

flux into the Taconazo and lower fluxes in the late wet season, following the peak of the wet season in July and August.

$CO_2$ evasion showed little temporal variability (Fig 3.3). We attribute the lack of variability to the sustained high $pCO_2$ relative to the atmosphere despite concentration increases (Fig 3.2) and small difference between gas exchange during the dry and wet season. However, we lack $pCO_2$ and gas exchange estimates, and therefore $F_{CO2}$, at the highest discharges. In a British Columbia headwater stream, gas exchange was positively correlated with discharge (McDowell and Johnson 2018). Theory predicts gas exchange to increase with turbulence and morphological parameters, such as width, depth and velocity, and therefore with discharge (Raymond et al. 2012; Ulseth et al. 2019). However, there is substantial variability among these predictions, and, for the Taconazo, $F_{CO2}$ remains unclear during the largest discharge events, as observed in late July and August. Our $F_{CO2}$ estimates (mean dry season 5.2 ± 2.2, mean wet season 5.0 ± 4.1 g C $m^{-2}$ $d^{-1}$) are lower than discrete estimates from the same reach during the same year (dry 10.8 ± 4.8, wet 7.2 ± 3.6 g C $m^{-2}$ $d^{-1}$, Oviedo-Vargas et al. 2015). However, Oviedo-Vargas et al. (2015) report greater $F_{CO2}$ during the dry season (10.8 g C $m^{-2}$ $d^{-1}$) compared to the wet season (7.2 g C $m^{-2}$ $d^{-1}$), a result of lower $[CO_2]_{aq}$ in the study reach during the wet season, contrary to the increase measured in this study during the wet season. The difference in fluxes described above between these two studies in the same section of the Taconazo may stem from differences in sampling frequency or sensor error, as the gas exchange rates are the same. Mean daily $F_{CO2}$ from the Taconazo (5.0 ± 4.1 g C $m^{-2}$ $d^{-1}$) was greater than the average of six Arctic streams (1.6 g C $m^{-2}$ $d^{-1}$, Rocher-Ros et al. 2019), reflecting the predictions in Cole et al. (2007) and Raymond et al. (2013) that tropical streams are hotspots of $CO_2$ evasion to the atmosphere.

Hydrologic export appears to be an important fate of $CO_2$ in the Taconazo, both as $H_{CO2}$ and $H_{HCO3}$. As expected, the export of each species reflects patterns in stream discharge: low during the dry season with an increase during the transition to the wet season that is sustained throughout our monitoring period (Fig 3.3, c). Stream DIC estimated here (mean = 3.15 ± 2.2 mg $L^{-1}$) is slightly lower than measured from 2007 - 2009 (mean = 4.8 mg $L^{-1}$, Genereux et al. 2013), and results in a 4.5-times lower estimate of mean daily flow-weighted DIC export from sensor data alone in this study (59 x $10^{-3}$ g C $ha^{-1}$ $d^{-1}$) compared to Genereux et al. (2013) (260 x $10^{-2}$ g C $ha^{-1}$ $d^{-1}$).

4.2. Drivers of $CO_2$ fluxes

The location of the $O_2$ - $CO_2$ cloud represents $CO_2$ supersaturation and slight $O_2$ undersaturation and based on the predictions in Vachon et al. (2020), we conclude groundwater $CO_2$ inputs are largely responsible for this discrepancy. Further, the 1/[slope] for each monthly cloud (Table 3.2) suggests the ecosystem respiratory quotient, as mol $CO_2$ produced for mol of $O_2$ consumed in aerobic processes, is >>1, further contributing to the supersaturation of $CO_2$ measured. We conclude that $pCO_2$ and the fluxes that affect $pCO_2$ in the Taconazo are mediated primarily by groundwater inputs (Appendix 4), at broad timescales and is true for similar headwater streams in tropical wet forests.

Rainfall and discharge explained moderate variation in $CO_2$ fluxes. Preceding day rainfall was aligned strongest with NEP, but in the same quadrant as hydrologic fluxes (Fig 3.5). The negative correlation between discharge and NEP is informative. As NEP estimates from streams increases (Appling et al. 2018), so are the efforts to quantify the effect of discharge on NEP. In temperate streams, ecosystem respiration increased during higher flows due to increased

dissolved organic C (DOC) from soils (Demars 2019). In La Selva streams, DOC increases during storms, and is derived from plant leachates or organic rich surface soils (Osburn et al. 2018). Alternatively, high flow events lead to scour small streams, removing organic matter, macroinvertebrates, and microbial mats (Grimm and Fisher 1989) and, theoretically reducing respiration due to removal of heterotrophs in the stream. The 92-fold decrease in 1/[slope] from April to August (Table 3.2), which indicates more efficient respiration (i.e. fewer mol $CO_2$ produced per mol $O_2$ consumed), may reflect increasing DOC or higher quality DOC that is respired in the stream. Decreased NEP during high flow events is likely not a result of increased GPP offsetting $CO_2$ production via respiration. Light limitation under the closed canopy in the Taconazo inhibits GPP (Marzolf and Ardón 2021), and storm flows with elevated DOC and sediments further attenuates light to aquatic primary producers.

Our hypothesis that $F_{CO2}$ would increase with discharge was not supported. We show weak correlation ($\tau$ = -0.10) overall (Fig 3.4), but a slight increase through the transition through the wet season. $pCO_2$ increases during the wet season, and we observe a concurrent rise in $F_{CO2}$. Our estimates may underestimate the total $F_{CO2}$ during the highest flow events. Storm events generally span less than one day (Genereux et al. 2005), and our aggregation to the daily scale may be masking sub-daily processes; in contrast, the greater frequency of low discharges make the correlation susceptible to outlier high flow events (e.g. the flood at the end of July, Fig 3.2). We can use the hysteresis of $pCO_2$ with discharge to inform the relationship of $F_{CO2}$ with discharge (Fig 3.6). In the three storm events, there is little evidence for clockwise hysteresis, suggesting $pCO_2$ evasion during peak flows is small, as a decrease in $pCO_2$ would indicate. There is slight 'figure 8' hysteresis in the wet season storm events, potentially revealing a disequilibrium between inputs of $CO_2$ from $GW_{CO2}$ and losses via $F_{CO2}$ or $H_{CO2}$.

4.3. Influence on pH

Small et al. (2012) suggested that $CO_2$ from terrestrial sources enter streams with low solutes and reduce pH through carbonic acid creation, primarily during the early wet season. Our results provide some support for this hypothesis. We show $GW_{CO2}$ has a weak negative correlation with stream pH (Fig 3.7). In the late dry and early wet season (April – May, Fig 2), small inputs of $GW_{CO2}$ (<100 g C $m^{-2}$ $d^{-1}$) can reduce a mean daily pH as low as 4.5. However, greater $GW_{CO2}$ measured at the peak and late wet season (June onward) reduce pH to between 5 and 5.5. The Taconazo has low alkalinity (<5 mg $L^{-1}$ as $CaCO_3$, unpub. data), therefore the acid neutralizing capacity is overcome by small inputs of $CO_2$. $CO_2$ is supplemented by increased DOC during storm events (mean stormflow DOC = 2.25 mg $L^{-1}$, Ganong et al. 2015; Osburn et al. 2018) and redox reactions (e.g. iron oxidation) which can collectively reduce pH. During the wet season, DOC inputs to the Taconazo are disproportionately organic acids (Osburn et al. 2018) which have a lower $pK_a$ and contribute to lower pH.

The lowest hourly pH measured during our study was 4.0 and is similar to lowest pH measured in the long-term record from the Taconazo, which occurred following the global El Niño Southern Oscillation event in 1997-98 (Small et al. 2012). During this event at LSBS, tree growth was decreased (Clark et al. 2003, 2010) and root mortality increased (Espeleta and Clark 2007). Small et al. (2012) hypothesize the stock of labile C in the soil increased and soil respiration causes high soil $CO_2$ (Schwendenmann and Veldkamp 2006). When soil moisture increased during the early wet season, soil $CO_2$ is quickly flushed from groundwater into streams. While acidification events are common in low solute headwater streams at La Selva, where pH ranges from 4 – 6 in the span of days, the negative effects on organisms and ecosystem

processes are limited (Ganong 2015), though there is evidence of short term behavior modification in macroinvertebrates and fish (Ardón et al. 2013).

## 4.4. Conclusion

We deployed a trio of sensors, both in stream and in a riparian well, to simultaneously estimate external and internal fluxes of $CO_2$ in a headwater tropical stream. We found terrestrial flux of $CO_2$ is greater than internal production as NEP, high $F_{CO2}$ was sustained, and hydrologic export is an important loss of C. In a global synthesis of efflux from inland waters, both Cole et al. (2007) and Raymond et al. (2013) stress the importance of evasion estimates from headwater tropical streams, which exhibit higher reaeration velocities and higher $pCO_2$. We document sustained high $pCO_2$ results in higher $F_{CO2}$ compared to similar streams across the globe (Raymond et al. 2013). Hydrologic C export, as the sum of $H_{CO2}$ and $H_{HCO3}$ to yield DIC export, was an important loss of C (6.56 kg C $ha^{-1}$ $yr^{-1}$), but is low compared to its adjacent watershed, the Arboleda (6800 kg C $ha^{-1}$ $yr^{-1}$, Genereux et al. 2013) and similar to the Mengong (7.5 kg C $ha^{-1}$ $yr^{-1}$), a small stream (watershed area = 0.6 $km^2$) in the Nyong basin, Cameroon (Brunet et al. 2009). Our study provides estimates of globally relevant C fluxes from a stream type with disproportionate influence among inland waters and provides a sensor-based approach to estimate C fluxes.

3.5 References

Appling, A. P., R. O. Hall, C. B. Yackulic, and M. Arroita. 2018. Overcoming Equifinality: Leveraging Long Time Series for Stream Metabolism Estimation. J. Geophys. Res. Biogeosciences 123: 624–645. doi:10.1002/2017jg004140

Ardón, M., J. H. Duff, A. Ramírez, G. E. Small, A. P. Jackman, F. J. Triska, and C. M. Pringle. 2013. Experimental acidification of two biogeochemically-distinct neotropical streams: buffering mechanisms and macroinvertebrate drift. Sci. Total Environ. 443: 267–277. doi:10.1016/j.scitotenv.2012.10.068

Ardón, M., L. A. Stallcup, and C. M. Pringle. 2006. Does leaf quality mediate the stimulation of leaf breakdown by phosphorus in Neotropical streams? Freshw. Biol. 51: 618–633. doi:10.1111/j.1365-2427.2006.01515.x

Aufdenkampe, A. K., E. Mayorga, P. A. Raymond, J. M. Melack, S. C. Doney, S. R. Alin, R. E. Aalto, and K. Yoo. 2011. Riverine coupling of biogeochemical cycles between land, oceans, and atmosphere. Front. Ecol. Environ. 9: 53–60. doi:10.1890/100014

Battin, T. J., S. Luyssaert, L. A. Kaplan, A. K. Aufdenkampe, A. Richter, and L. J. Tranvik. 2009. The boundless carbon cycle. Nat. Geosci. 2: 598–600. doi:10.1038/ngeo618

Birgand, F., C. Faucheux, G. Gruau, B. Augeard, F. Moatar, and P. Bordenave. 2010. Uncertainties in assessing annual nitrate loads and concentration indicators: Part 1. Impact of sampling frequency and load estimation algorithms. Trans. Am. Soc. Agric. Biol. Eng. 53: 437–446.

Borges, A. V, F. Darchambeau, T. Lambert, and others. 2019. Variations in dissolved greenhouse gases (CO2, CH4, N2O) in the Congo River network overwhelmingly driven by fluvial-wetland connectivity. Biogeosciences 16: 3801–3834.

Brunet, F., K. Dubois, J. Veizer, G. R. Nkoue Ndondo, J. R. Ndam Ngoupayou, J. L. Boeglin, and J. L. Probst. 2009. Terrestrial and fluvial carbon fluxes in a tropical watershed: Nyong basin, Cameroon. Chem. Geol. 265: 563–572. doi:10.1016/j.chemgeo.2009.05.020

Clark, D. A., S. C. Piper, C. D. Keeling, and D. B. Clark. 2003. Tropical rain forest tree growth and atmospheric carbon dynamics linked to interannual temperature variation during 1984-2000. Proc. Natl. Acadademy Sci. United States Am. 13: 5852–5857.

Clark, D. B., D. A. Clark, and S. F. Oberbauer. 2010. Annual wood production in a tropical rain forest in NE Costa Rica linked to climatic variation but not to increasing CO2. Glob. Chang. Biol. 16: 747–759. doi:10.1111/j.1365-2486.2009.02004.x

Cole, J. J., Y. T. Prairie, N. F. Caraco, and others. 2007. Plumbing the Global Carbon Cycle: Integrating Inland Waters into the Terrestrial Carbon Budget. Ecosystems 10: 172–185. doi:10.1007/s10021-006-9013-8

Collins, M., R. Knutti, J. Arblaster, and others. 2013. Long-term climate change: Projections, commitments and irreversibility, In T.F. Stocker, D. Qin, G.-K. Plattner, et al. [eds.], Climate Change 2013 the Physical Science Basis: Working Group I Contribution to the Fifth Assessment Report of the Intergovernmental Panel on Climate Change. Cambridge University Press.

Colvin, S. A. R., S. M. P. Sullivan, P. D. Shirey, and others. 2019. Headwater Streams and Wetlands are Critical for Sustaining Fish, Fisheries, and Ecosystem Services. Fisheries 44: 73–91. doi:10.1002/fsh.10229

Crawford, J. T., E. H. Stanley, M. M. Dornblaser, and R. G. Striegl. 2017. CO2 time series patterns in contrasting headwater streams of North America. Aquat. Sci. 79: 473–486. doi:10.1007/s00027-016-0511-2

Demars, B. O. L. 2019. Hydrological pulses and burning of dissolved organic carbon by stream respiration. Limnol. Oceanogr. 64: 406–421. doi:10.1002/lno.11048

Dinsmore, K. J., and M. F. Billett. 2008. Continuous measurement and modeling of CO2 losses from a peatland stream during stormflow events. Water Resour. Res. 44: 1–11. doi:10.1029/2008WR007284

Drake, T. W., P. A. Raymond, and R. G. M. Spencer. 2018. Terrestrial carbon inputs to inland waters: A current synthesis of estimates and uncertainty. Limnol. Oceanogr. Lett. **3**: 132–142. doi:10.1002/lol2.10055

Espeleta, J. F., and D. A. Clark. 2007. Multi-scale variation in fine-root biomass in a tropical rain forest: a seven-year study. Ecol. Monogr. 77: 377–404. doi:10.1890/06-1257.1

Evans, C., and T. D. Davies. 1998. Causes of concentration/discharge hysteresis and its potential as a tool for analysis of episode hydrochemistry. Water Resour. Res. 34: 129–137. doi:10.1029/97WR01881

Ganong, C. N. 2015. Effects of Precipitation Regime on Neotropical Streams: Biogeochemical Drivers of Stream Physicochemistry and Macroinvertebrate Tolerance to pH Shifts. University of Georgia.

Ganong, C. N., G. E. Small, M. Ardón, W. H. McDowell, D. P. Genereux, J. H. Duff, and C. M. Pringle. 2015. Interbasin flow of geothermally modified ground water stabilizes stream exports of biologically important solutes against variation in precipitation. Freshw. Sci. 34: 276–286. doi:10.1086/679739

Genereux, D. P., and M. Jordan. 2006. Interbasin groundwater flow and groundwater interaction with surface water in a lowland rainforest, Costa Rica: A review. J. Hydrol. 320: 385–399. doi:10.1016/j.jhydrol.2005.07.023

Genereux, D. P., M. T. Jordan, and D. Carbonell. 2005. A paired-watershed budget study to quantify interbasin groundwater flow in a lowland rain forest, Costa Rica. Water Resour. Res. 41. doi:10.1029/2004wr003635

Genereux, D. P., L. A. Nagy, C. L. Osburn, and S. F. Oberbauer. 2013. A connection to deep groundwater alters ecosystem carbon fluxes and budgets: Example from a Costa Rican rainforest. Geophys. Res. Lett. 40: 2066–2070. doi:10.1002/grl.50423

Gómez-Gener, L., G. Rocher-Ros, T. Battin, and others. Enhanced nocturnal emissions of carbon dioxide amplify the role of streams in the global carbon cycle. Nat. Geosci.

Grimm, N. B., and S. G. Fisher. 1989. Stability of periphyton and macroinvertebrates to disturbance by flash floods in a desert stream. J. North Am. Benthol. Soc. 8: 293–307.

Hall, R. O., and E. R. Hotchkiss. 2017. Stream Metabolism, p. 219–233. In G.A. Lamberti and F.R. Hauer [eds.], Methods in Stream Ecology, Vol 2: Ecosystem Function, 3rd Edition. Academic Press Ltd-Elsevier Science Ltd.

Hotchkiss, E. R., R. O. Hall, R. A. Sponseller, D. Butman, J. Klaminder, H. Laudon, M. Rosvall, and J. Karlsson. 2015. Sources of and processes controlling CO2 emissions change with the size of streams and rivers. Nat. Geosci. 8: 696–699. doi:10.1038/ngeo2507

Johnson, M. S., M. F. Billett, K. J. Dinsmore, M. Wallin, K. E. Dyson, and R. S. Jassal. 2010. Direct and continuous measurement of dissolved carbon dioxide in freshwater aquatic systems-method and applications. Ecohydrology 68–78. doi:10.1002/eco.95

Leith, F. I., K. J. Dinsmore, M. B. Wallin, M. F. Billett, K. V. Heal, H. Laudon, M. G. Öquist, and K. Bishop. 2015. Carbon dioxide transport across the hillslope-riparian-stream continuum in a boreal headwater catchment. Biogeosciences 12: 1881–1902. doi:10.5194/bg-12-1881-2015

Lupon, A., B. A. Denfeld, H. Laudon, J. Leach, J. Karlsson, and R. A. Sponseller. 2019. Groundwater inflows control patterns and sources of greenhouse gas emissions from streams. Limnol. Oceanogr. doi:10.1002/lno.11134

Marzolf, N. S., and M. Ardón. 2021. Ecosystem metabolism in tropical streams and rivers: a review and synthesis. Limnol. Oceanogr. lno.11707. doi:10.1002/lno.11707

Mayorga, E., A. K. Aufdenkampe, C. A. Masiello, A. V. Krusche, J. I. Hedges, P. D. Quay, J. E.

Richey, and T. A. Brown. 2005. Young organic matter as a source of carbon dioxide outgassing from Amazonian rivers. Nature 436: 538–541. doi:10.1038/nature03880

McDowell, M. J., and M. S. Johnson. 2018. Gas transfer velocities evaluated using carbon dioxide as a tracer show high streamflow to be a major driver of total CO2 evasion flux for a headwater stream. J. Geophys. Res. Biogeosciences 123: 2183–2197. doi:10.1029/2018jg004388

Murdoch, D., and E. D. Chow. 2020. ellipse: Functions for Drawing Ellipses and Ellipse-Like Confidence Regions.

Odum, H. T. 1956. Primary production in flowing waters. Limnol. Oceanogr. 1: 102–117.

Osburn, C. L., D. Oviedo-Vargas, E. Barnett, D. Dierick, S. F. Oberbauer, and D. P. Genereux. 2018. Regional groundwater and storms are hydrologic controls on the quality and export of dissolved organic matter in two tropical rainforest streams, Costa Rica. J. Geophys. Res. Biogeosciences. doi:10.1002/2017JG003960

Oviedo-Vargas, D., D. P. Genereux, D. Dierick, and S. F. Oberbauer. 2015. The effect of regional groundwater on carbon dioxide and methane emissions from a lowland rainforest stream in Costa Rica. J. Geophys. Res. Biogeosciences 120: 2579–2595. doi:10.1002/

R Core Team. 2020. R: A language and environment for statistical computer.

Ramírez, A., C. M. Pringle, and L. Molina. 2003. Effects of stream phosphorus levels on microbial respiration. Freshw. Biol. 48: 88–97.

Raymond, P. A., J. Hartmann, R. Lauerwald, and others. 2013. Global carbon dioxide emissions from inland waters. Nature 503: 355–359. doi:10.1038/nature12760

Raymond, P. A., C. J. Zappa, D. Butman, and others. 2012. Scaling the gas transfer velocity and hydraulic geometry in streams and small rivers. Limnol. Oceanogr. Fluids Environ. 2: 41–53. doi:10.1215/21573689-1597669

Richey, J. E., J. M. Melack, A. K. Aufdenkampe, V. M. Ballestter, and L. L. Hess. 2002. Outgassing from Amazonian rivers and wetlands as a large tropical source of atmospheric CO2. Nature 416: 617–620.

Rocher-Ros, G., R. A. Sponseller, A. Bergstr, M. Myrstener, and R. Giesler. 2019. Stream metabolism controls diel patterns and evasion of CO2 in Arctic streams. Glob. Chang. Biol. 0–3. doi:10.1111/gcb.14895

Rocher-Ros, G., R. A. Sponseller, W. Lidberg, C. Mörth, and R. Giesler. 2019. Landscape process domains drive patterns of CO2 evasion from river networks. Limnol. Oceanogr. Lett. doi:10.1002/lol2.10108

Rosemond, A. D., C. M. Pringle, A. Ramírez, M. J. Paul, and J. L. Meyer. 2002. Landscape variation in phosphorus concentration and effects on detritus-based tropical streams. Limnol. Oceanogr. 47: 278–289.

Sanford Jr., R. L., P. Paaby, J. C. Luvall, and E. Phillips. 1994. Climate, geomorphology, and aquatic systems, p. 19–33. In L.A. McDade, K.S. Bawa, H.A. Hespenheide, and G.S. Hartshorn [eds.], La Selva: Ecology and natural history of a Neotropical rain forest. University of Chicago Press.

Sawakuchi, H. O., V. Neu, N. D. Ward, and others. 2017. Carbon Dioxide Emissions along the Lower Amazon River. Front. Mar. Sci. 4. doi:10.3389/fmars.2017.00076

Schwendenmann, L., and E. Veldkamp. 2006. Long-term CO2 production from deeply weathered soils of a tropical rain forest: evidence for a potential positive feedback to climate warming. Glob. Chang. Biol. 12: 1878–1893. doi:10.1111/j.1365-2486.2006.01235.x

Schwendenmann, L., E. Veldkamp, T. Brenes, J. J. O'Brien, and J. Mackensen. 2003. Spatial and temporal variation in soil CO2 efflux in an old-growth neotropical rain forest, La Selva, Costa Rica. Biogeochemistry 64: 111–128. doi:10.1023/A:1024941614919

Small, G. E., M. Ardón, A. P. Jackman, J. H. Duff, F. J. Triska, A. Ramírez, M. Snyder, and C. M. Pringle. 2012. Rainfall-driven amplification of seasonal acidification in poorly buffered tropical streams. Ecosystems 15: 974–985.

Stubbins, A., L. M. Silva, T. Dittmar, and J. T. Van Stan. 2017. Molecular and Optical Properties of Tree-Derived Dissolved Organic Matter in Throughfall and Stemflow from Live Oaks and Eastern Red Cedar. Front. Earth Sci. 5: 22. doi:10.3389/feart.2017.00022

Stumm, W., and J. J. Morgan. 1996. Dissolved Carbon Dioxide, In Aquatic chemistry: chemical equilibria and rates in natural waters. Wiley.

Tank, S. E., J. B. Fellman, E. Hood, and E. S. Kritzberg. 2018. Beyond respiration: Controls on lateral carbon fluxes across the terrestrial-aquatic interface. Limnol. Oceanogr. Lett. **3**: 76–88. doi:10.1002/lol2.10065

Taylor, J. R., and H. L. Loescher. 2013. Automated quality control methods for sensor data: a novel observatory approach. Biogeosciences 10: 4957–4971. doi:10.5194/bg-10-4957-2013

Ulseth, A. J., R. O. Hall, M. Boix Canadell, H. L. Madinger, A. Niayifar, and T. J. Battin. 2019. Distinct air–water gas exchange regimes in low- and high-energy streams. Nat. Geosci. doi:10.1038/s41561-019-0324-8

Vachon, D., S. Sadro, M. J. Bogard, and others. 2020. Paired O2–CO2 measurements provide emergent insights into aquatic ecosystem function. Limnol. Oceanogr. Lett. 5: 287–294. doi:10.1002/lol2.10135

Wetzel, R. G., and G. E. Likens. 2000. The Inorganic Carbon Complex: Alkalinity, Acidity, CO 2, pH, Total Inorganic Carbon, Hardness, Aluminum, p. 113–135. In Limnological analyses. Springer.

Zanon, C., D. P. Genereux, and S. F. Oberbauer. 2014. Use of a watershed hydrologic model to estimate interbasin groundwater flow in a Costa Rican rainforest. Hydrol. Process. 28: 3670–3680. doi:10.1002/hyp.9917

# Chapter 4: Do experimental pH increases alter the structure and function of a lowland tropical stream?

## 4.1 Introduction

Ecosystems are subject to disturbances that stress biological assemblages. Broadly, disturbances are defined as discrete events that cause structural changes in natural communities that move ecosystems away from equilibrium (Sousa 1984, Resh et al. 1988) and have a biological consequence (Townsend 1989, Poff 1992, Stanley et al. 2010). Beyond viewing disturbance as a discrete event, disturbances can the viewed as a process (Grimm et al. 2017), with legacy effects as subsequent drivers of successional processes and influencing ecosystem response (Peters et al. 2011, Graham et al. 2020). The type, magnitude, frequency, and duration of disturbances drive changes in both ecosystem structure (e.g. biotic assemblage) and function (e.g. chemical cycling, organic matter decomposition, organismal growth). Disturbances vary over temporal and spatial scales (Lake 2000), from high frequency-low magnitude events to low frequency-high magnitude events (Sousa 1984). For example, infrequent and large magnitude events are floods caused by hurricanes while frequent, low magnitude events are seasonal floods or episodic acidification events. High frequency low magnitude events, in some cases, are not considered disturbances, but rather regular features of the ecosystem, such as spates in snow-fed mountain streams (Poff 1992), tidal changes (Sousa 1984), and fire in longleaf pine ecosystems (Palik et al. 2002) to which the biota have developed adaptions (Lytle and Poff 2004).

In stream ecosystems, the definition of disturbance has evolved to account for spatial, temporal, and ecological variability (Pickett and White 1985, Resh et al. 1988, Poff 1992, Lake 2000, Stanley et al. 2010). Disturbances in streams are defined by 1) quantifiable metrics of the disturbance (e.g. intensity, frequency, and duration); and 2) a biological consequence.

Disturbances in streams centers around changes in flow or discharge as discrete hydrologic (e.g. flooding from hurricanes) events (Poff 1992, Poff et al. 1997) or across a continuum of pulses (e.g. seasonal floods), presses (e.g. barrier effects of dams), and ramps (e.g. droughts) (Lake 2000, Graham et al. 2020). Expanding beyond hydrologic disturbances, changes in stream physicochemistry across temporal and spatial scales can be considered disturbance but understanding the variability of physicochemical changes and how they drive stream ecosystem structure and function remain understudied. Non-hydrologic disturbance events in streams (Lake 2000, Stanley et al. 2010), include temperature (Harper and Peckarsky 2006), incident light (Steinman et al. 1991), and pollutants and chemicals (Steinman et al. 1992, Harper and Peckarsky 2005).

Stream pH, which varies as a result of concentrations of dissolved solutes, inorganic carbon, and rainfall chemistry (Stumm and Morgan 1996), is an important parameter that directly affects the of the ecosystem and its biota, particularly at low pH. We define acidification events as periods of rapid and temporary pH declines or loss of acid neutralizing capacity (Laudon et al. 2004), resulting in a wide range of consequences on both structure and function of stream ecosystems. For example, Mulholland et al. (1987) measured slower rates of leaf litter decomposition, microbial respiration, and bacterial production in streams with naturally occurring low pH (<6) compared to streams with higher pH (>6). Long-term stream and lake acidification due to acid-rain inputs and reduced acid neutralizing capacity had detrimental effects on fish, macroinvertebrate, and algal assemblages (Bernard et al. 1990, Baker et al. 1996). In certain tropical streams, there is a linkage between acidification events and rainfall, which is driven by variation in El Niño Southern Oscillation (Small et al. 2012). In these streams in Costa Rica, macroinvertebrate drift increased in response to experimental acidification (Ardón et al.

2013), providing support for low pH events as disturbances that elicit changes in behavior of stream biota. Further study of structure and function responses to pH regimes is needed in the face of intensifying El Niño cycles under climate change (Rauscher et al. 2008).

In this paper, we experimentally evaluated the response of tropical stream structure and function to episodic acidification events, defining ~1 unit pH decreases as disturbances in headwater streams. We took advantage of naturally occurring differences in acidification event frequency between a stream reach with low acidification return interval due to high buffering capacity, and three reaches with high acidification return interval which experience acidification at both daily and seasonal time scales. We experimentally increased the buffering capacity of a short reach to prevent acidification events and mimic the infrequent acidification events of the buffered stream reach. We measured structural and functional responses at the individual, assemblage, and ecosystem scale to empirically test how acidification propagates through the ecosystem hierarchy. We hypothesized that increasing the buffering capacity would 1) stimulate individual growth rates of dominant taxa, 2) shift the macroinvertebrate assemblage to be more similar to the naturally buffered reach; and 3) accelerate decomposition rates of leaf litter and coarse woody debris.

## 4.2 Methods

### 4.2.1 Study Site

This study was conducted at La Selva Biological Station (LSBS, 10° 26’ N, 84° 01’ W), Costa Rica (Fig 4.1). La Selva, area = 1536 ha, has predominantly primary and secondary tropical wet forest, and receives, on average, 4000 mm of rainfall per year (Sanford Jr. et al. 1994). Streams at LSBS can be distinguished by two sources of groundwater inputs. Local

groundwater inputs, which originate within the streams' watershed, are present in all streams. Certain streams below ~50 m above sea level receive inputs of inter-basin modified groundwater (IMG) (Pringle and Triska 1991, Pringle et al. 1993, Genereux et al. 2005). Streams with IMG inputs are characterized by higher solute concentrations, including soluble reactive phosphorus (SRP), cations, and carbonate species (Pringle et al. 1990, Pringle 1991, Oviedo-Vargas et al. 2015). Streams with IMG exhibit faster microbial respiration (Rosemond et al. 2002, Ramírez et al. 2003), faster macroinvertebrate turnover (Ramírez and Pringle 2006), faster leaf litter decomposition rates (Ardón et al. 2006), and higher and more stable pH as a result of higher buffering capacity (Small et al. 2012).

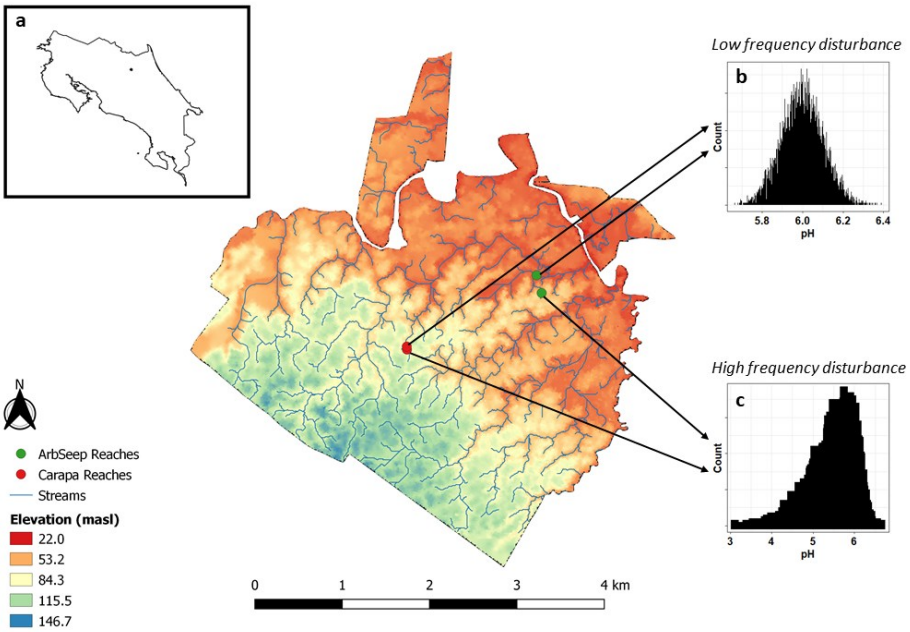


**Figure 4.1** Location of the Carapa and ArbSeep study reaches within the property of La Selva Biological Station, and a) location of La Selva in Costa Rica. The side panels identify the pH histograms from b) downstream buffered reaches, and c) upstream, unbuffered reaches, respectively. Data in the histograms are from long-term monitoring (1997-2019, STREAMS project).

### 4.2.2 Experimental design

We selected two headwater streams to test the effects of episodic acidification on both structure and function: the Carapa and the Arboleda Seep (hereafter ArbSeep) (Table 4.1). The Carapa is a characteristic low-solute, headwater stream at LSBS, experiencing seasonal and episodic acidification (Small et al. 2012). The ArbSeep is a headwater tributary to the Arboleda, and the downstream reach of ArbSeep receives IMG, resulting in different physicochemical characteristics between the upstream and downstream sections of the ArbSeep. We selected two 5-10 m reaches within each of the two streams, resulting in a total of four study reaches: two

upstream low buffering capacity and frequently acidified reaches, one downstream higher buffering capacity reach in the ArbSeep capacity reach (due to natural IMG inputs), and one downstream low-buffering capacity reach in the Carapa that we chose for experimental carbonate amendments to simulate IMG inputs (Fig 4.1). To facilitate experimental logistics, the Carapa experiment occurred from 15 June 2018 – 20 July 2018, and the ArbSeep occurred from 18 June 2018 – 23 July 2018. Rainfall data was collected from this period using a tipping bucket rain gauge located ~1 km from our streams and are available at https://anetium.ots.ac.cr/meteoro/default.php?pestacion=1.

**Table 4.1** Morphology and long-term data from the two study streams.

| Stream | Watershed Area (ha) | Wetted Width (m) | Velocity (m $s^{-1}$) | Mean Discharge (L $s^{-1}$)[1] | Mean Temp (°C)[1] | Mean pH[1] |
|---|---|---|---|---|---|---|
| Carapa | 4.26 | 1.44 | 0.17 | 11.1 ± 0.00 | 24.4 ± 0.92 | 5.52 ± 0.53 |
| Arboleda Seep | 4.65 | 2.50 | 0.08 | 9.10 ± 0.00 | 25.2 ± 0.61 | 6.18 ± 0.32 |

[1] From long-term data collection, 1997-2019 (STREAMS project)

4.2.3 Buffering capacity addition

To mimic IMG inputs and prevent episodic acidification from occurring in the experimental downstream reach of the Carapa, we continuously added buffering capacity, in the form of carbonate species in two phases for five weeks (15 June 2018 – 20 July 2018). For the first two weeks of the experiment, we dissolved 1,920 g of $NaHCO_3$ in a 220 L barrel of stream water and pumped this solution (~0.1 M $HCO_3^-$) into the stream above the downstream reach at a

rate of 25 mL $min^{-1}$, refilling and amending the barrel with upstream water as needed. The $NaHCO_3$ pumping addition was not as effective as anticipated in preventing episodic acidification; therefore, for the remainder of the experiment, we added 500 g of solid $CaCO_3$ in coarse mesh bags directly in the stream immediately upstream of the downstream reach so it would dissolve in water. $CaCO_3$ bags were replaced every 2-3 days for the remaining three weeks of the experiment.

4.2.4 Stream physicochemistry

We deployed a YSI EXO1 multiprobe sonde (Xylem Inc., Yellow Springs, OH) in the two downstream reaches during the five-week experiment. Sondes measured temperature (°C) and pH every 15 minutes and were calibrated weekly. Due to sensor error, we only collected data in the Carapa for the final three weeks of the experiment. As the sondes were deployed in the downstream reach during the experiment, we deployed the sondes in the upstream reaches for five weeks the following summer to collect the same data from the upstream reaches from August 13, 2019 - September 24, 2019. While these dates do not overlap with the dates of the 2018 experiment, the 2019 dates are still in the wet season at LSBS and we expect similar weather in this period. To examine the frequency of acidification, we used the Shaprio-Wilks test of normality to assess the distributions of pH data in each of the four study reaches, assuming that buffered reaches would exhibit normal distributions and unbuffered reaches would not.

We measured discharge and nutrients weekly during the experiment. Discharge was measured in the downstream reaches using the cross-sectional area method with a velocity meter (Marsh-McBirney, Frederick, MA). Triplicate nutrient ($NO_3^-$, $NH_4^+$, and SRP) samples were collected in 60 mL bottles, filtered in the lab (0.45 µm), and frozen. Samples were transported to

North Carolina State University frozen, where $NH_4^+$ and SRP were analyzed on an AA3 Segmented Flow Analyzer (Seal Analytical, Mequon, WI) and $NO_3^-$ analyzed on a Metrohm 930 ion chromatograph (Metrohm, Ionenstrasse, Switzerland).

4.2.5 Macroinvertebrate assemblage and ecosystem function response

In the four stream reaches, we deployed coarse mesh (3 mm) and fine mesh (300 μm) litter bags to measure leaf litter (LL) and coarse woody debris (CWD) decomposition. Fine mesh litter bags were used to exclude macroinvertebrates and estimate microbial decomposition rates, whereas coarse mesh bags allow macroinvertebrates access and contribute to decomposition (Woodward et al. 2012). Litter bags of each mesh size and organic matter type were deployed for each collection date and type of organic matter, and triplicate litter bags were collected following one and five weeks of deployment in the stream (total n of decomposition bags = 96). Leaves from *Luehea seemannii* Triana & Planch. (Tiliaceae) (5 g) and CWD segments from *Pentaclethra macroloba* (Willd.) Kuntze (Fabaceae) (50 g) were added to each litter bag, respectively. On the pre-assigned collection date, litter bags were removed from the stream using a dip net, transferred to a 4 L plastic bag, and transported to the lab. In the lab, leaf and wood matter were washed over a 250 μm sieve for all sediment and biota. Leaf litter and CWD material were placed into paper bags, dried at 40 ˚C for 48 h, and subsamples placed in a muffle furnace at 500 ˚C for 1 h to calculate dry mass (DM) and ash-free dry mass (AFDM), respectively. We calculated the decomposition rate constant for LL and CWD, $k_{LL}$ or $k_{CWD}$, using the negative exponential model. Material collected in the sieve was preserved in 95% ethanol for macroinvertebrate identification. Macroinvertebrates were identified to the lowest taxonomic rank possible and are presented at family level.

### 4.2.6 Individual organism response

We measured the growth of chironomid larvae (Diptera: Chironomidae) in the four reaches of the buffering experiment. Chironomids are the dominant detritivores in streams at La Selva and have comprised >50% of invertebrate biomass in previous leaf litter decomposition experiments (Rosemond et al. 2001, Ardón et al. 2006). Coarse mesh bags filled with *Ficus insipida* Willd. leaves were incubated in each of the four reaches for 10 d, allowing colonization by chironomids, and returned to the lab. Chironomid larvae were picked from the colonized leaf packs and measured to the nearest 0.2 mm. We selected six larvae between 2 and 5 mm for growth experiments. Groups of six larvae were placed into six replicate plastic tea strainers with six *Ficus* leaf discs (100 mm diameter) and deployed into the respective stream reach for 48 hr. After deployment, we counted surviving individual chironomids and re-measured the length of each individual. We estimated individual chironomid initial and final biomass using length-mass relationships (Small et al. 2011), and calculated percent change in biomass and survivorship for each tea strainer.

### 4.2.7 Statistics

Decomposition rates for LL and CWD were analyzed using two-way ANOVA across the four reaches and two litter bag mesh sizes. We used a post-hoc Tukey test to determine significant groups among the four reaches. Macroinvertebrate abundance from litter bags was evaluated after one and five weeks of deployment. Abundance data failed the normality assumptions for ANOVA, therefore we evaluated macroinvertebrate abundance across the four study reaches, mesh bag size, and organic matter type using the non-parametric Aligned Rank Transform test in the ARTool v0.10.8 (Kay and Wobbrock 2020) and post-hoc evaluation in the

emmeans v1.5.3 R packages (Lenth 2020). To evaluate macroinvertebrate diversity, we calculated family richness for each litter bag.

To document changes in the diversity of the macroinvertebrate assemblage at the end of the experiment, we used non-metric multidimensional scaling (NMDS). In the NMDS, we used the Bray-Curtis dissimilarity index in three dimensions on $\log_{10}$ transformed abundance data and visualized the ordination across our experimental treatments (study reaches, mesh bag size, and type of organic matter) to assess influence of each treatment. To statistically assess the diversity of the assemblages, we used analysis of similarity (ANOSIM) using the Bray-Curtis dissimilarity index and 9999 permutations for the treatments in the experiment. We used the ANOSIM R statistic to evaluate diversity across the experimental treatments (reaches, mesh size, organic matter), where R values closer to 0 indicate similarity versus values closer to 1 indicating dissimilarity. Macroinvertebrate assemblage analysis used the vegan v2.5-7 R package (Oksanen et al. 2019).

Chironomid survival and growth rates were evaluated across the four study reaches. We used one-way Aligned Rank Transform test non-normally distributed chironomid survival across the four reaches. Percent biomass change was non-normally distributed and were $\log_{10}$ transformed prior to one-way ANOVA and post-hoc Tukey test across the four reaches. Finally, we performed an ANCOVA of $\log_{10}$ transformed final chironomid biomass, using reach as a fixed effect for the experimental reach and $\log_{10}$ transformed initial biomass as covariate. We used the Tukey post-hoc test to determine groups across the four reaches using the agricolae v1.3-3 R package (de Mendiburu 2017).

We calculated the effect size statistic Hedge's g to assess the experimental treatments for macroinvertebrate abundance, richness, chironomid growth rate and survival, and $k_{LL}$ and $k_{CWD}$.

Hedge's g is the preferred metric for small sample sizes ($n < 20$). Hedge's g was calculated using the effsize v0.8.1 R package (Torchiano 2020).

## 4.3 Results

### 4.3.1 Stream chemistry and buffering capacity additions

Mean discharge was greater in the two Arboleda reaches, but there was large variation in each of the four reaches and discharge increased over the duration of the experiment (Table 4.2). Nutrient concentrations varied across the four study reaches. $NO_3$-N was highest in the ArbSeep upstream (mean 243.0 µg $NO_3$-N $L^{-1}$) and lowest in the Carapa reaches (upstream = 150.2 µg $NO_3$-N $L^{-1}$, downstream = 158.2 µg $NO_3$-N $L^{-1}$) (Table 4.2). $NH_4$-N was greatest in the downstream Arboleda (45.8 µg $NH_4$-N $L^{-1}$) and lowest in the upstream reaches (Carapa = 25.7 µg $NH_4$-N $L^{-1}$, ArbSeep = 17.2 µg $L^{-1}$) (Table 4.2). SRP was greatest in the downstream ArbSeep (36.8 µg $L^{-1}$), with low concentrations in the remaining three reaches (<5 µg $L^{-1}$ in each) (Table 4.2). Nutrient ratios, DIN:SRP, in the ArbSeep downstream reach was 10.7 - 17.9-times lower than the other three reaches, reflecting higher SRP concentrations in the ArbSeep downstream reach.

**Table 4.2** Stream discharge and nutrient concentrations from the four experimental reaches during the five-week experiment. Discharge is the mean with range in parentheses, and concentrations are means ± standard error across the five weeks of sampling. Values in parentheses are Kendall tau correlation coefficient which describes the trend of the analyte during the experiment.

| Reach | Discharge (L $s^{-1}$) | $NO_3$ -N (µg $L^{-1}$) | $NH_4$-N (µg $L^{-1}$) | $PO_4$-P (µg $L^{-1}$) | DIN:SRP (Molar) |
|---|---|---|---|---|---|
| Carapa Upstream | 6.3 (3.0 - 15.7) | 150.2 ± 6.0 (-0.22) | 25.7 ± 3.5 (-0.12) | 4.02 ± 0.3 (-0.29) | 105.7 ± 8.6 (0.30) |
| Carapa Downstream | 8.5 (3.3 - 24.0) | 158.2 ± 6.8 (-0.22) | 32.0 ± 9.4 (0.03) | 4.61 ± 0.5 (0.05) | 103.1 ± 9.0 (-0.12) |
| ArbSeep Upstream | 13.3 (3.5 - 23.1) | 243.0 ± 7.7 (0.12) | 17.2 ± 1.5 (-0.01) | 3.58 ± 0.2 (-0.07) | 172.2 ± 11.6 (0.10) |
| ArbSeep Downstream | 16.2 (8.0 - 31.2) | 197.7 ± 6.7 (0.17) | 45.8 ± 3.2 (-0.17) | 36.8 ± 4.1 (-0.30) | 18.45 ± 2.4 (0.22) |

Rainfall totals slightly differed across the four reaches due to logistics and start date of the experiments. Total rainfall in the downstream Carapa reach (15 June - 20 July) was 1068 mm (Fig 4.2, c). Mean pH in the experimental Carapa reach was 5.66 (range 4.85 - 7.90). We documented 36 events where pH, measured every 15 minutes, dropped ≤ 0.3 pH units (1.7% of all measurements). Conversely, there were 38 instances where the pH increased ≥ 0.3 units

(1.8%), indicating a halving of hydrogen ion concentration, [$H^+$]. Mean daily pH followed a normal distribution in the experimental Carapa reach (Shapiro-Wilks $p = 0.36$).

During the ArbSeep experiment (18 June - 23 July), total rainfall was 1280 mm, more than during the Carapa experiment due to different start dates of the experiments. Mean pH in the ArbSeep downstream was 6.23 (range 5.87 - 6.39). The pH in the ArbSeep downstream was less variable compared to the Carapa (Fig 4.2, d), with no increase in pH of more than 0.3 units through the entire experiment. pH was reduced during a large storm event on 14 July, which caused the downstream Arboleda to 'backflood' into the study reach. However, the magnitude of pH reduction during the backflooding event was relatively small, with a mean pH during the event of 6.08 compared to mean pH preceding the event of 6.25. pH in the ArbSeep fell below 6.08 during three separate occasions preceding the backflooding event, coinciding with increased rainfall (Fig 4.2, b, d). Mean daily pH was left-skewed (Shapiro-Wilks $p = 0.01$), but removal of backflooding days reveals normally distributed pH data (Shapiro Wilks $p = 0.31$). Backflooding events in the Arboleda are common events, recurring annually and usually lasting less than a day (Genereux et al. 2005), although it persisted longer during our experiment (Fig 4.2, d, black highlighted area).

Rainfall was much greater during the 2018 experimental period compared to 2019. In 2019, total rainfall was 514.3 mm, ~500 mm less than during the experiment duration in 2018. Mean pH was 5.27 (range 4.28 - 5.56) in the ArbSeep upstream and 5.39 (range 4.74 - 5.69) in the Carapa upstream reach. In the ArbSeep upstream, there were six pH declines of ≤ 0.3 pH units, which corresponds to a doubling of [$H^+$], while four instances were measured in the Carapa upstream. There were no instances in either upstream reach of pH changes ≥ 0.3.

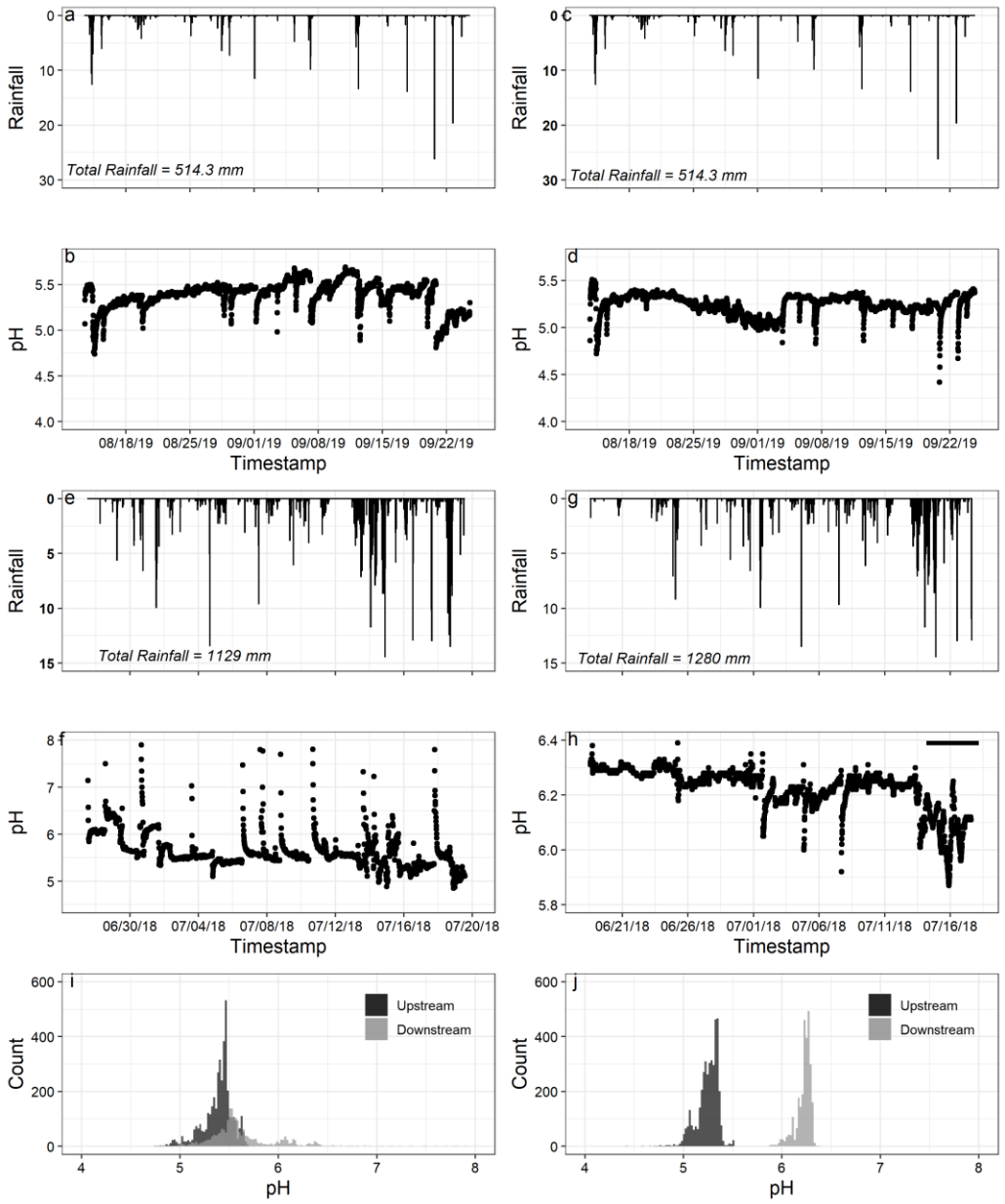


**Figure 4.2** Rainfall (a, c, e, g) and pH (b, d, f, h) time-series from the four experimental reaches. Upstream reaches from the Carapa (a ,b) and ArbSeep (c, d) represent data collected in 2019 and downstream reaches from Carapa (e, f) and ArbSeep (g, h) are from the experiment in 2018 (see text for details). Paired pH histograms from the Carapa (i) and ArbSeep (j), with the data from upstream (dark grey) and downstream (light grey) plotted on equal axes to highlight the differences in regimes. Area under the black bar in h) coincide with the backflooding event.

4.3.2 Structure and ecosystem function- assemblage and decomposition rates

Leaf litter decomposition ($k_{LL}$) was similar across the four study reaches. Decomposition rates ranged from 0.028 to 0.052 $d^{-1}$ across all litter bags, and mean rates from the four reaches spanned a narrower range (0.037 - 0.046 $d^{-1}$). Neither reach ($F_{3,14}$, $p = 0.34$) nor mesh size ($F_{1,14}$, $p = 0.28$) affected $k_{LL}$ (Fig 4.3, a). In contrast, CWD decomposition varied between the four reaches. Woody debris rates spanned a wide range (0.24 - 3.30 $yr^{-1}$) and was 3.12-times greater in the ArbSeep reaches ($F_{3, 13}$, $p = 0.001$) (Fig 4.3, b). However, there was no difference in $k_{CWD}$ between the upstream and downstream reaches in both streams or among the two bag mesh sizes ($F_{1, 13}$, $p = 0.30$).

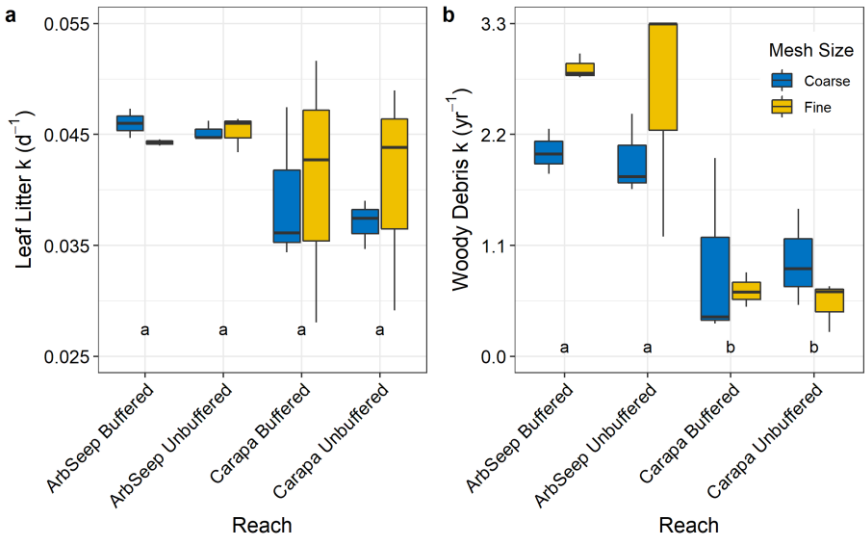


**Figure 4.3** Decomposition rates for a) leaf litter and b) coarse woody debris across the four study reaches. Blue boxplots represent coarse mesh bags and yellow boxplots represent fine mesh bags. Letters indicate Tukey post-hoc groupings across the experimental reaches.

We documented 6053 individual macroinvertebrates across the two sampling weeks, four reaches, LL and CWD litter bags, and litter bag mesh sizes. Fine mesh bags were unsuccessful at excluding macroinvertebrates, but coarse mesh bags hosted a greater number of families than fine mesh bags (12.3 vs 9.4 mean number of families per bag, Fig 4.4). There was no difference in the number of families ($p = 0.53$) or in total abundance ($p = 0.17$) across the four reaches. There was no difference in the number of families ($p = 0.87$) between LL and CWD litter bags, but abundance per g AFDM was much greater in LL (mean = 30.3 insects g $AFDM^{-1}$) than in CWD (mean = 0.66 insects g $AFDM^{-1}$) (Fig 4.5, Student's $t = 4.5$, $p < 0.01$). We observed a greater number of macroinvertebrates in Week 1 (n = 3573) than Week 5 (n = 2480), but the mean richness in Week 5 was 6.1 ± 2.7 ($p < 0.01$) (Fig 4.4), compared to a mean richness of 3.5 ± 2.0 in Week 1.

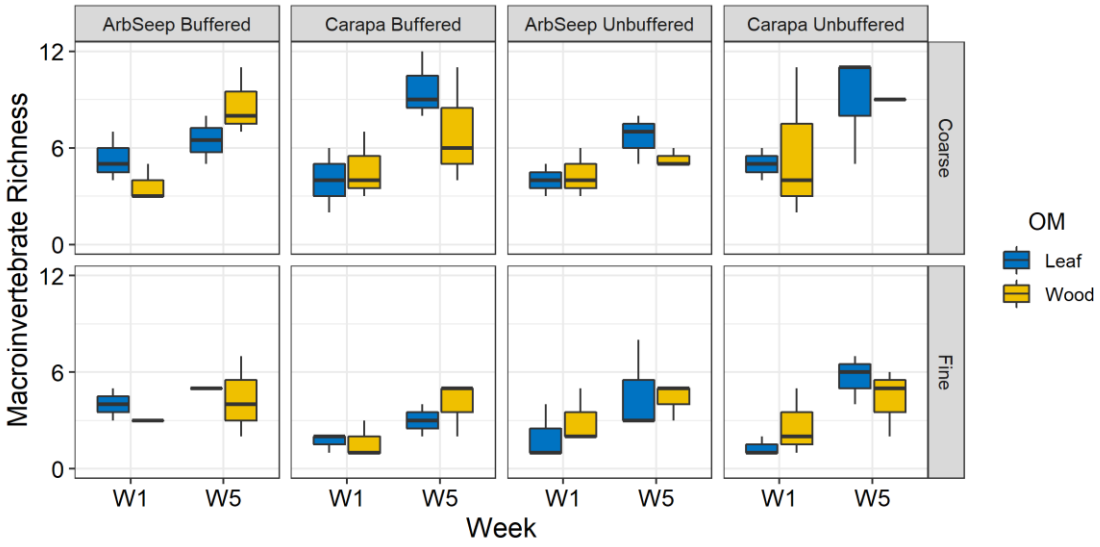


**Figure 4.4** Mean macroinvertebrate abundance per g AFDM remaining in a) leaf litter and b) coarse woody debris decomposition bags. Error bars are standard error.

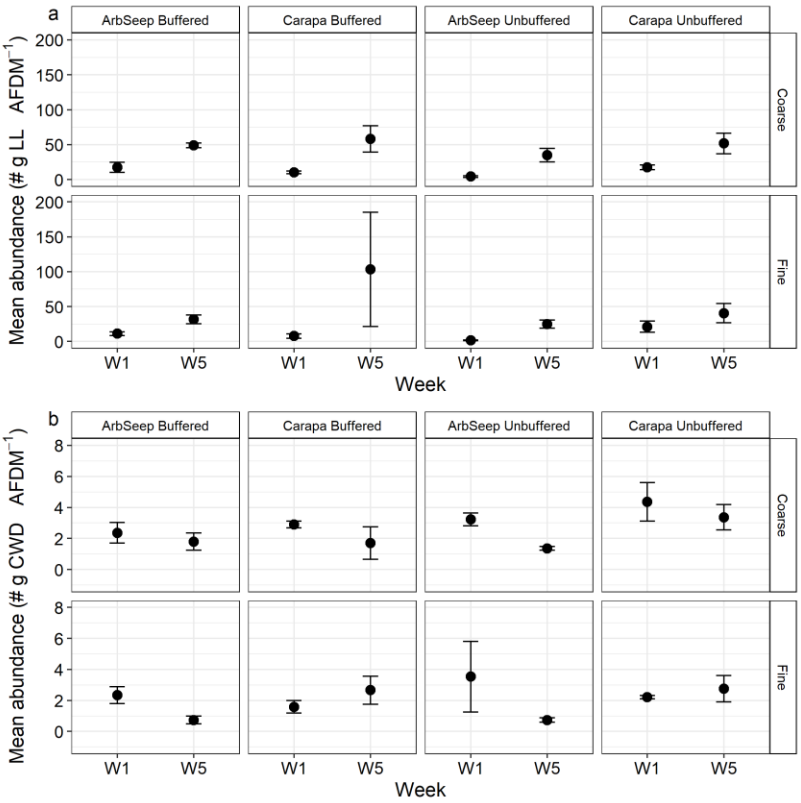


**Figure 4.5** Macroinvertebrate richness across the four study reaches, organic matter, and mesh size treatments in the buffering experiment. Boxplots represent triplicate samples from each week, with yellow boxes identifying coarse woody debris (CWD) litter bags and blue identifying leaf litter (LL) bags. The top row indicates coarse mesh bags and the bottom row fine mesh bags.

Macroinvertebrate assemblages were similar across our experiment as measured by NMDS. Overall, there was mild ordination stress (0.17), indicating overall similarity across the assemblages by the end of the experiment, but examination of the family vectors driving the ordination (Fig 4.6, a) and experimental factors in ordination space revealed several differences. Among the four reaches, the downstream ArbSeep assemblage was most distinct and showed little overlap with the other three reaches, including the ArbSeep upstream reach. Strongest assemblage similarity was shown between the two Carapa reaches, with the buffered downstream reach less similar than the ArbSeep reaches (Fig 4.6, b). There was strong overlap

between LL and CWD organic matter groups, though the assemblages from CWD litter bags spanned a wider range in ordination space (Fig 4.6, c). Finally, there was strong assemblage dissimilarity between fine and coarse mesh bags (Fig 4.6, d), likely a result of the greater diversity present in coarse mesh bags (Fig 5). Analysis of similarity further emphases these findings. There was greatest dissimilarity across the four reaches (ANOSIM R = 0.14, $p < 0.01$), and more similarity across mesh bag sizes (ANOSIM R = 0.02, $p = 0.10$) and organic matter types (ANOSIM R = 0.08, $p < 0.01$).

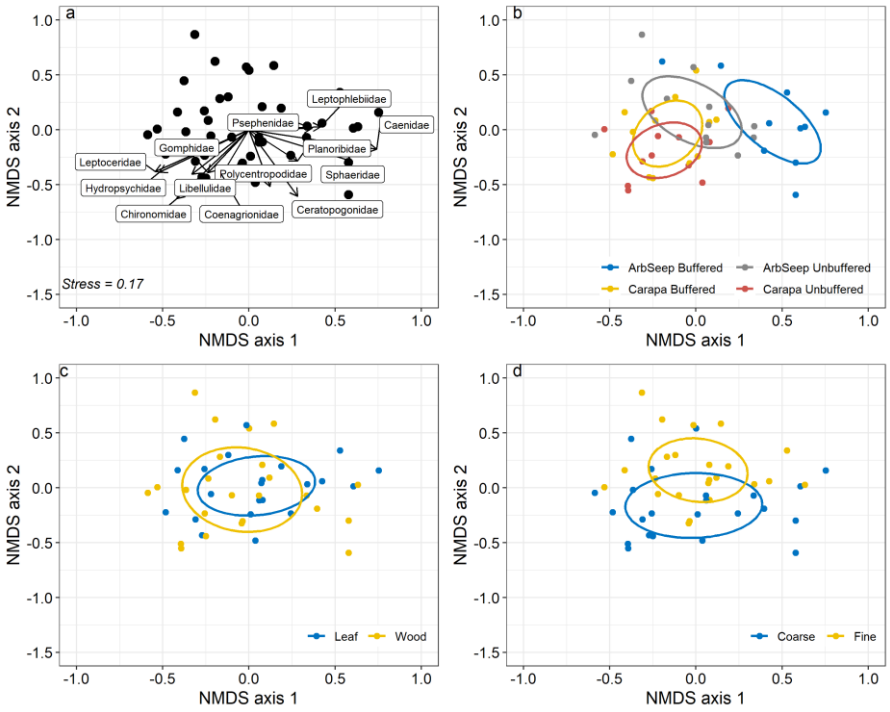


**Figure 4.6** Non-metric dimensional scaling of macroinvertebrate assemblage during Week 5 of the buffering experiment. Each point represents the assemblage of an individual litter bag collected in Week 5 and ellipses are 95% confidence intervals for the different components of the experiment. a) Family-level vectors driving the ordination; b) colors of ellipses and points represent the four study reaches of the experiment; c) colors distinguish leaf litter (LL) and coarse woody debris (CWD) assemblages; d) colors distinguish between fine and coarse mesh bags.

### 4.3.3 Individual- Chironomid growth rate

Mean chironomid survival was 56.4%, with range from 0% to 100% but no differences in survival across the four study reaches ($F_{3, 35}$, $p = 0.08$) (Table 4.3). Mean percent change in chironomid biomass was 89.5%, ranging from -33.8 to 649.2% and was not different across the

four study reaches ($F_{3, 24}$, $p = 0.07$), though growth in the ArbSeep downstream reach was 2.3 - 3.7-times greater than the other three reaches. Final chironomid biomass was 2.2 - 2.5-times greater in the ArbSeep downstream reach, but there were no effects of reach ($F_{3, 29}$, $p = 0.26$), initial biomass ($F_{1,29}$, $p = 0.28$), or their interaction ($F_{3, 29}$, $p = 0.40$).

**Table 4.3** Chironomid growth experiment results. Superscript letters indicate post-hoc groups.

| Reach | Final Biomass (mg) ± SE | %Biomass Change ± SE | %Survival ± SE |
|---|---|---|---|
| Carapa Up | 0.032 ± 0.004[a] | 53.6 ± 17.1[a] | 50.0 ± 7.9[a] |
| Carapa Down | 0.031 ± 0.006[a] | 65.4 ± 34.2[a] | 72.9 ± 7.0[a] |
| ArbSeep Up | 0.030 ± 0.007[a] | 41.7 ± 27.5[a] | 64.3 ± 10.6[a] |
| ArbSeep Down | 0.091 ± 0.019[b] | 155.8 ± 50.9[a] | 47.6 ± 6.5[a] |

### 4.3.4 Effect sizes

Using Hedge's g effect size statistic to evaluate the factors in the experiment (Table 4.4), we interpret the effects of the two reaches in our unmodified study stream (ArbSeep) and our experimental study stream (Carapa). In the ArbSeep moving from upstream to downstream, $k_{LL}$ was slower, $k_{CWD}$ faster, macroinvertebrate abundance and diversity were greater, and chironomid growth was greater (Table 4.4). In contrast, the same longitudinal movement in the experimental Carapa showed faster $k_{LL}$ and $k_{CWD}$, a less abundant, and less diverse macroinvertebrate assemblage, and lower chironomid growth rates (Table 4.4).

**Table 4.4** Hedges' g effect sizes in the buffering experiment and the treatments. Effect sizes for Stream are calculated as ArbSeep vs Carapa, and effect sizes for Reach are calculated as downstream vs upstream.

| Comparison | $k_{LL}$ | $k_{CWD}$ | Macroinvertebrate abundance | Macroinvertebrate richness | Chironomid % Growth |
|---|---|---|---|---|---|
| ArbSeep Down vs Up | -0.08 | 0.22 | 0.03 | 0.20 | 0.68 |
| Carapa Down vs Up | 0.14 | 0.07 | -0.06 | -0.16 | -0.15 |

## 4.4 Discussion

We present an experimental approach to understand the effects of episodic acidification on the structure and function in headwater streams, measuring responses at individual, assemblage, and ecosystem scales. Our hypotheses were largely unsupported: in the experimentally buffered reach, individual chironomid growth was not stimulated, the macroinvertebrate assemblage was less abundant and less diverse compared to the unamended reaches, and organic matter decomposition rates were similar to rates in the other reaches. Our results suggest that, rather than preventing an episodic disturbance, increasing the buffering capacity was a disturbance. We conclude that stream biota in streams with low buffering capacity are adapted to some degree of episodic acidification and slightly increasing the pH presented conditions that inhibited biotic function. The acidification events inhibited in this experiment are relatively small in magnitude, though there is evidence for prolonged and stronger acidification events related to climate variability, and may be more common in the future.

4.4.1 Drivers and experimental modification of episodic acidification

Our experimental manipulation of the downstream Carapa reach was moderately successful. The goal was to reduce the frequency of acidification events and mimic the pH regime in reaches where IMG buffers against acidification. We prevented acidification events in the downstream Carapa reach and slightly increased pH events as a result of our additions (Fig 4.2, e). In comparison, the upstream reach showed a higher frequency of acidification events and a lower mean pH across during the experiment. However, we did not achieve complete mimicry, as, the downstream ArbSeep reach pH regime varied little over time and was 0.92 units higher than the upstream reach. In contrast, pH in the Carapa downstream reach was only 0.25 units greater than its corresponding upstream reach.

Rainfall appears to be an important driver of acidification events in headwater streams at La Selva. Even with a ~500 mm difference in total rainfall between the five-week periods in 2018 and 2019, the high frequency of small rainfall events can be observed in stream pH. The monitoring period in 2018 had >1000 mm rainfall and was among the wettest periods at La Selva since 2015 (STREAMS project, http://www.streamslaselva.net/). Even in the naturally buffered reach, elevated rainfall was responsible for slight pH decreases in the ArbSeep downstream reach on 2 July 2018, 5 July 2018, and 8 July 2018. Extreme rainfall starting on 14 July 2018 resulted in the downstream Arboleda stream backflooding into the ArbSeep downstream reach, located <20 m from the confluence. The backflood of water from the Arboleda and high rainfall resulted in a three-day period of relatively low pH in the reach.

The synchrony of rainfall and pH in streams at La Selva has been documented in previous studies (Small et al. 2012, Ardón et al. 2013) and may be a driving physicochemical disturbance mechanism. At short time scales (sub-daily to daily), in streams without IMG inputs,

pH quickly decreases during rainfall events, with the magnitude of the decrease as large as 0.75 units (Fig 4.2, a, b). In stream reaches with IMG, pH decreases are smaller in magnitude and less frequent. At longer time scales (seasonal to multi-year), stream pH responds to monthly rainfall. During the wet season following extreme dry periods during the global El Niño event in 1998, pH was reduced (<5) in streams without IMG (Ramírez et al. 2006, Small et al. 2012). In general, stream pH increases during the dry season, and decreases during the wet season, concurrent with $CO_2$ and Fe fluxes from riparian soils and groundwater (Small et al. 2012, Ganong 2015, Chapter 3).

### 4.4.2 Individual response to acidification

Our results on chironomid growth reveal effects of pH regimes on individual macroinvertebrate function. Percent chironomid growth was fastest in the downstream ArbSeep reach, compared to similar rates across the remaining three reaches (Table 4.3). In addition, chironomids grown in the ArbSeep downstream were ~3-times larger than chironomids from other reaches, as measured by final biomass (Table 4.3). Higher growth and better survival among macroinvertebrates in reaches with IMG is supported by previous work at LSBS, where macroinvertebrates have faster growth rates in response to higher P concentrations (Ramírez and Pringle 2006). In our experimental reach, we measured a negative effect (Table 4.4) on chironomid growth and survival, suggesting pH is not limiting growth. The similarities in chironomid growth in the unmodified reaches provide similar conclusions to Small et al. (2011), which shows local adaptation by chironomids to their native reach. The strong negative effect size of chironomid growth between the experimentally modified reach and its upstream counterpart gives evidence that our experiment was itself a disturbance to which the chironomids

were not adapted which negatively affected their growth. Further, Ganong (2015) showed local adaptation and tolerance in macroconsumers to acidic conditions, suggesting that multiple levels in the food webs at La Selva are adapted to localized pH regimes.

### 4.4.3 Assemblage response to acidification

Macroinvertebrate assemblages were dominated by larval Chironomids (Appendix 5). While we attempted to distinguish microbial and macroinvertebrate influences on organic matter decomposition using the coarse and fine mesh bag approach (Woodward et al. 2012), fine mesh bags were ineffective in excluding chironomids. For this reason, we present decomposition across the mesh types rather than attributing effects to microbes and macroinvertebrates. However, while abundance was similar in the two mesh bag types, there were differences in the assemblages (Fig 4.6, c). Coarse mesh hosted a more diverse assemblage, notably Trichoptera and Odonata (Fig 4.6). Previous studies at LSBS documented Chironomidae as important contributors in decomposition of LL (Ramírez and Pringle 1998, Rosemond et al. 1998, Ardón et al. 2006), though this study is the first to examine CWD as habitat and resource for macroinvertebrates. Specialization (e.g. mining, xylophagy) of chironomids on CWD has been previously reported across the globe (Cranston and McKie 2006), including from tropical streams (Ferrington et al. 1993), suggesting CWD could be important to specialized chironomids and other macroinvertebrates at LSBS.

Our results provide insight on the role of CWD in the food webs of streams at La Selva. There were fewer macroinvertebrates per g AFMD found in CWD litter bags (Fig 4.4), likely reflecting the poorer quality of CWD as a food resource. Previous studies in temperate forested streams reveal CWD and CWD associated biofilms to be an important resource for specialized

taxa (i.e. those with appropriate mouth parts to use CWD (Eggert and Wallace 2007)). The scarcity of shredders in tropical streams (Boyero et al. 2011) suggest a larger role on microbially-mediated processing of organic matter (Rosemond et al. 1998, Ardón and Pringle 2008) or a macroinvertebrate assemblage with generalist feeding strategies (Cheshire et al. 2005, Boyero et al. 2021). While we were unable to distinguish microbial vs macroinvertebrate driven decomposition rates, it is possible $k_{CWD}$ is driven by microbes or CWD-specialized macroinvertebrates, as we observed fewer macroinvertebrates in CWD bags. However, more research is needed to explore the role of CWD in food webs at La Selva.

### 4.4.4 Ecosystem response to acidification

Decomposition rates were similar across the four reaches and were not affected by different mesh bag sizes. Leaf litter decomposition rates (Fig 4.3, a) are similar to previously measured rates of fast-decomposing litter from La Selva streams (Appendix 6, Ardón et al. 2006). However, unlike previous work at La Selva, our results do not show faster decomposition rates at higher SRP concentrations and at higher pH (Rosemond et al. 2002, Ramírez et al. 2003, Ardón et al. 2006). Previous studies have examined a gradient of SRP concentrations, whereas only one of our four reaches had elevated SRP (ArbSeep downstream). However, mean SRP concentration in the ArbSeep downstream (36.8 $\mu g\ L^{-1}$) is greater than the half-saturation constant reported for leaf litter decay rate (6.6 $\mu g\ L^{-1}$; Rosemond et al. 2002). Coarse woody debris decomposition rates were faster in both reaches of the ArbSeep compared to the rates measured in the Carapa (Fig 4.3, b), and overall, mean decomposition rates in fine mesh bags were faster than in coarse mesh bags. While fine mesh bags were not entirely successful in

excluding macroinvertebrates, the abundance of chironomids and biofilms in fine mesh bags (Table 4.4) may be responsible for the faster rates measured.

A second explanation for faster decomposition rates in the ArbSeep is elevated discharge. While the four reaches had similar characteristics, as revealed by the long-term mean discharge (Table 4.1), we measured 2.0 and 2.7-times greater discharge in the ArbSeep downstream compared to the Carapa upstream and downstream reaches during the experiment, respectively (Table 4.2). Sites with faster flow have faster decomposition rates due to physical abrasion of organic matter (Ardón et al. 2006), and may contribute to faster $k_{LL}$ measured in the ArbSeep in this study. While the backflooding events in the downstream ArbSeep reach resulted in standing water and higher discharge, though it is unclear how, if at all, this event affected decomposition rates. We note that dissolved oxygen fell as low as 2.8 mg $O_2$ $L^{-1}$ during the backflooding event, indicating aerobic processes were stressed.

Overall, there appears to be little effect of frequent acidification at the ecosystem scale. The effect size of decomposition in the downstream versus the upstream reach is negligible to small (Table 4.4) for both LL (0.01) and CWD (0.10). However, within the ArbSeep, $k_{LL}$ was faster in the upstream reach than downstream, while $k_{CWD}$ was faster in the downstream than upstream reach. Conversely, decomposition rate was faster in the Carapa downstream reach than in upstream reach. Overall, there were small statistical differences in decomposition rates between the four reaches and the effect sizes are small (Table 4.4). We therefore conclude that the overarching effects of changing pH regime on ecosystem function are compensated for within each reach and the biota (i.e. microbes and macroinvertebrates) are adapted to the acidification recurrence interval.

4.4.5. Contextualizing acidification as a disturbance in headwater streams

This study presents an experimental test of short-term disturbance regimes on structure and function of tropical streams, with effects measured at the organismal, assemblage and ecosystem level. Our hypothesis that frequent acidification would inhibit structure and function at the individual, assemblage, and ecosystem scale was not supported Our results provide further evidence for adaptation at the reach scale to disturbance regimes that have likely existed for millennia (Small et al. 2011), allowing stream biota to adapt to acidification events (Graham et al. 2020). Our data suggest that by preventing acidification events from occurring naturally, we induced negative effects on macroinvertebrate abundance and diversity, and the growth of an important and abundant taxon (Table 4.2). However, the duration of our experiment was relatively short (five weeks), and our results should be extrapolated with caution to effects that scale over long time periods. In the hierarchy of temporal scaling as relates to disturbances (Poff and Ward 1990), we have answered questions at the diel to seasonal scale, but our experiment was unable to answer questions at the multiannual or geological scale.

Further, we explore the negative effects of short-term acidification in freshwater ecosystems within a stream ecosystem hierarchy. Several previous studies have documented negative effects of increased acidity on leaf litter decomposition, microbial respiration, fungal biomass, and bacterial production in streams with low pH (Mulholland et al. 1987, Dangles et al. 2004). Similarly, negative effects on ecosystem structure as an effect of acidification have been shown for macroinvertebrate density (Hall 1994), insect emergence and food web simplification (Hall et al. 1980), and macroinvertebrate drift (Ardón et al. 2013). An extension our experiment allows is comparison of the three unamended reaches, particularly the ArbSeep. In this stream, the downstream reach had faster $k_{CWD}$, more abundant and more diverse macroinvertebrate

assemblage, and faster chironomid growth compared to the upstream reach. The longitudinal increases in structure and function across individual, assemblage, and ecosystem scale processes observed in the ArbSeep but not in the Carapa (Table 4.4) suggest pH is not a main driver, but the additional solutes and nutrients (e.g. SRP) contribute to the difference in effect sizes.

Our study informs how stream structure and function respond to existing disturbance regimes, using an experimental method to reduce the frequency of the disturbance, and allows us to populate a conceptual framework for the effects of acidification, specific to the streams at LSBS (Fig 4.7). Episodic acidification during the wet season (Fig 4.2) and seasonal pH reduction during the wet season (Small et al. 2012) are phenomena that have likely existed for millennia as a result of the geology and hydrology of the region (Genereux et al. 2009), and represent a disturbance legacy in these streams (Grimm et al. 2017). The historical recurrence of acidification has induced adaptation of stream biota to episodic acidification events (Ganong 2015). However, we lack information on the response of stream biota to stream acidification events following multi-year El Niño cycles. Following the 1997-98 global El Niño event, stream pH across La Selva decreased by ~1 unit for months (Ramírez et al. 2006, Small et al. 2012). Acidification events of this magnitude are less frequent in this system, and therefore the biota are less likely to adapt to prolonged and stronger acidification events. Ardón et al. (2013) documented greater macroinvertebrate drift from experimentally acidified reaches, providing clues as to the response during less frequent and more intense acidification events. Recurrence intervals of stronger acidification events will likely be shorter in the face of climate change and intensifying and more frequent El Niño cycles. Correspondingly, results of a long-term monitoring study in the Carapa revealed that precipitation and El Niño cycles are important drivers of reduced macroinvertebrate abundance and diversity (Gutierréz-Fonseca et al. 2018).

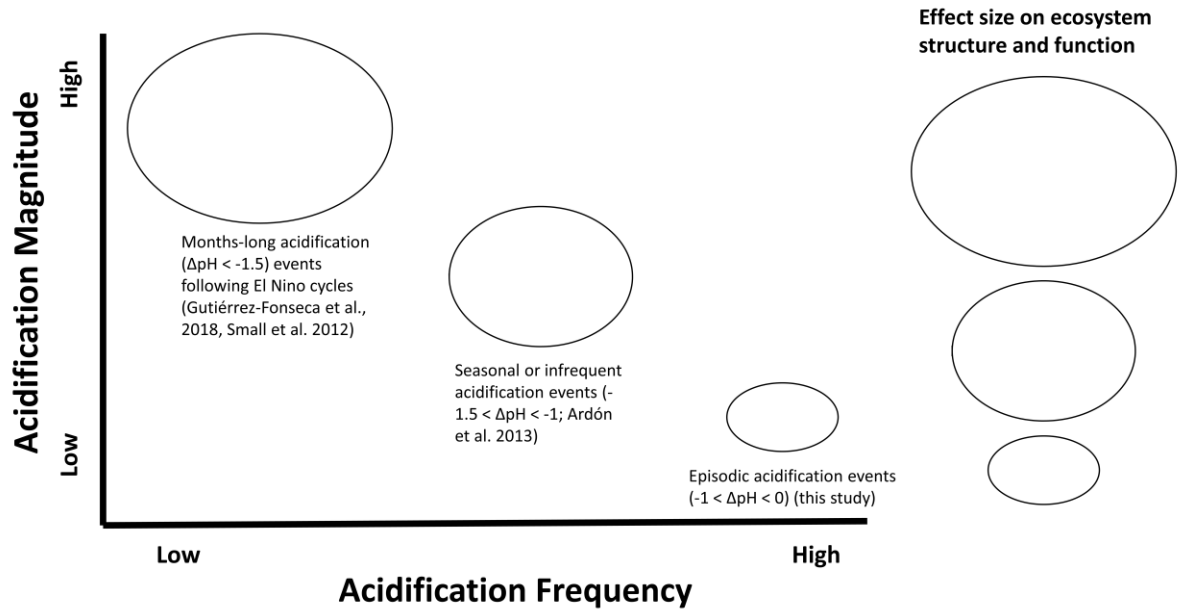


**Figure 4.7** Conceptual framework to explore acidification disturbance in streams, populated with results from streams at La Selva. Acidification frequency ranges from multi-year intervals to sub-daily intervals, and acidification magnitude ranges from strong acidification events ($\Delta pH < -1.5$) to small acidification events ($0 > \Delta pH > -1$). Ellipse sizes are proportional to the expected effects of an acidification event magnitude and frequency, with small effects measured for episodic events and large effects measured during infrequent events.

We conclude that understanding the effects of naturally occurring disturbances is necessary to better understand novel disturbances that are associated with climate change. The prevalence of regional groundwater inputs into streams, particularly in Central America (Pringle et al. 1993, Ganong et al. 2015), likely provide numerous cases where streams of high and low buffering capacity are adjacent and reflect the pH regimes that we explore here. If our results here are characteristic of streams across Central America regarding pH regimes, macroinvertebrates are resilient to low pH and the effects at the individual scale propagate

through the assemblage and ecosystem scale. Stream function may be adapted to changes in pH, but novel stressors or disturbances at novel recurrence intervals are likely to be stronger disturbances. Climate change projections in Central America predict warmer temperatures and more variable rainfall (Collins et al. 2013), with more extremes in seasonality and likely resulting in more frequent and stronger acidification events in low solute streams.

4.5 References

Ardón, M., J. H. Duff, A. Ramírez, G. E. Small, A. P. Jackman, F. J. Triska, and C. M. Pringle. 2013. Experimental acidification of two biogeochemically-distinct neotropical streams: buffering mechanisms and macroinvertebrate drift. Science of the Total Environment 443:267–277.

Ardón, M., and C. M. Pringle. 2008. Do secondary compounds inhibit microbial- and insect-mediated leaf breakdown in a tropical rainforest stream, Costa Rica? Oecologia 155:311–323.

Ardón, M., L. A. Stallcup, and C. M. Pringle. 2006. Does leaf quality mediate the stimulation of leaf breakdown by phosphorus in Neotropical streams? Freshwater Biology 51:618–633.

Baker, J. P., J. Van Sickle, C. J. Gagen, D. R. DeWalle, W. E. Sharpe, R. F. Carline, B. P. Baldigo, P. S. Murdoch, D. W. Bath, W. A. Krester, H. A. Simonin, and P. J. Wigington. 1996. Episodic Acidification of Small Streams in the Northeastern United States: Effects on Fish Populations. Ecological Applications 6:422–437.

Bernard, D. P., W. E. Neil, and L. Rowe. 1990. Impact of mild experimental acidification on short term invertebrate drift in a sensitive British Columbia stream. Hydrobiologia 203:63–72.

Boyero, L., R. G. Pearson, D. Dudgeon, M. A. S. Graça, M. O. Gessner, R. J. Albariño, V. Ferreira, C. M. Yule, A. J. Boulton, and M. Arunachalam. 2011. Global distribution of a key trophic guild contrasts with common latitudinal diversity patterns. Ecology 92:1839–1848.

Boyero, L., J. Pérez, N. López-Rojo, A. M. Tonin, F. Correa-Araneda, R. G. Pearson, J. Bosch, R. J. Albariño, S. Anbalagan, L. A. Barmuta, L. Beesley, F. J. Burdon, A. Caliman, M. Callisto, I. C. Campbell, M. Leal, K. Lehosmaa, R. Marchant, R. T. Martins, F. O. Masese, M. Camden, B. G. McKie, A. O. Medeiros, J. A. Middleton, T. Muotka, J. N. Negishi, J. Pozo, A. Ramírez, R. S. Rezende, J. S. Richardson, J. Rincón, J. Rubio-Ríos, C. Serrano, A. R. Shaffer, F. Sheldon, C. M. Swan, N. S. D Tenkiano, S. D. Tiegs, J. R. Tolod, M. Vernasky, A. Watson, M. J. Yegon, and C. M. Yule. 2021. Latitude dictates plant diversity effects on instream decomposition. Science Advances 7:53.

Cheshire, K., L. Boyero, and R. G. Pearson. 2005. Food webs in tropical Australian streams: shredders are not scarce. Freshwater Biology 50:748–769.

Collins, M., R. Knutti, J. Arblaster, J.-L. Dufresne, T. Fichefet, P. Friedlingstein, X. Gao, W. J. Gutowski, T. Johns, G. Krinner, M. Shongwe, C. Tebaldi, A. J. Weaver, and M. Wehner. 2013. Long-term climate change: Projections, commitments and irreversibility. Page in T. F. Stocker, D. Qin, G.-K. Plattner, M. Tignor, S. K. Allen, J. Boschung, A. Nauels, Y. Xia, V. Bex, and P. M. Midgley, editors. Climate Change 2013 the Physical Science Basis: Working Group I Contribution to the Fifth Assessment Report of the Intergovernmental Panel on Climate Change. Cambridge University Press, Cambridge, United Kingdom and New York, NY, USA.

Cranston, P. S., and B. McKie. 2006. Aquatic wood–an insect perspective. Page 9 Insect Biodiversity and Dead Wood: Proceedings of a Symposium for the 22nd International Congress of Entomology. US Department of Agriculture, Forest Service, Southern Research Station.

Dangles, O., M. O. Gessner, F. Guerold, and E. Chauvet. 2004. Impacts of stream acidification on litter breakdown: Implications for assessing ecosystem functioning. Journal of Applied Ecology 41:365–378.

Eggert, S. L., and J. B. Wallace. 2007. Wood biofilm as a food resource for stream detritivores. Limnology and Oceanography 52:1239–1245.

Ferrington, L. C., K. M. Buzby, and E. C. Masteller. 1993. Composition and temporal abundance of Chironomidae emergence from a tropical rainforest stream at El Verde , Puerto Rico. Journal of the Kansas Entomological Society 66:167–180.

Ganong, C. N. 2015. Effects of Precipitation Regime on Neotropical Streams: Biogeochemical Drivers of Stream Physicochemistry and Macroinvertebrate Tolerance to pH Shifts. University of Georgia, Athens, GA.

Ganong, C. N., G. E. Small, M. Ardón, W. H. McDowell, D. P. Genereux, J. H. Duff, and C. M. Pringle. 2015. Interbasin flow of geothermally modified ground water stabilizes stream exports of biologically important solutes against variation in precipitation. Freshwater Science 34:276–286.

Genereux, D. P., M. T. Jordan, and D. Carbonell. 2005. A paired-watershed budget study to quantify interbasin groundwater flow in a lowland rain forest, Costa Rica. Water Resources Research 41.

Genereux, D. P., M. Webb, and D. K. Solomon. 2009. Chemical and isotopic signature of old groundwater and magmatic solutes in a Costa Rican rain forest: Evidence from carbon, helium, and chlorine. Water Resources Research 45:1–14.

Graham, E., C. Averill, B. Bond-Lamberty, J. Knelman, S. Krause, A. Peralta, A. Shade, A. P. Smith, S. Cheng, N. Fanin, C. Freund, P. Garcia, S. Gibbons, M. Van Goethem, M. Ben Guebila, J. Kemppinen, R. Nowicki, J. Pausas, S. Reed, J. Rocca, A. Sengupta, D. Sihi, M. Simonin, M. Słowiński, S. Spawn, I. Sutherland, J. Tonkin, N. Wisnoski, S. Zipper, and C. Consortium. 2020. Towards a generalizable framework of disturbance ecology through crowdsourced science. Frontiers in Ecology and Evolution 9:76.

Grimm, N. B., S. T. A. Pickett, R. L. Hale, and M. L. Cadenasso. 2017. Does the ecological concept of disturbance have utility in urban social–ecological–technological systems? Ecosystem Health and Sustainability 3:1–18.

Gutierréz-Fonseca, P. E., A. Ramírez, and C. M. Pringle. 2018. Large-scale climatic phenomena drive fluctuations in macroinvertebrate assemblages in lowland tropical streams, Costa Rica: The importance of ENSO events in determining long-term (15y) patterns. PLoS One 13:e0191781.

Hall, R. J. 1994. Responses of benthic communities to episodic acid disturbances in a lake outflow stream at the Experimental Lakes Area, Ontario. Canadian Journal of Fisheries and Aquatic Sciences 51:1877–1892.

Hall, R. J., G. E. Likens, S. Fiance, and G. Hendrey. 1980. Experimental acidification of a stream in the Hubbard Brook Experimental Forest , New Hampshire. Ecology 61:976–989.

Harper, M. P., and B. L. Peckarsky. 2005. Effects of pulsed and pressed disturbances on the benthic invertebrate community following a coal spill in a small stream in northeastern USA. Hydrobiologia 544:241–247.

Harper, M. P., and B. L. Peckarsky. 2006. Emergence cues of a mayfly in a high-altitude stream ecosystem: Potential response to climate change. Ecological Applications 16:612–621.

Kay, M., and J. Wobbrock. 2020. ARTool: Aligned Rank Transform for Nonparametric Factorial ANOVAs.

Lake, P. S. 2000. Disturbance, patchiness, and diversity in streams. Journal of the North American Benthological Society 19:573–592.

Laudon, H., P. J. Dillon, M. C. Eimers, R. G. Semkin, and D. S. Jeffries. 2004. Climate-induced episodic acidification of streams in central Ontario. Environmental Science and Technology 38:6009–6015.

Lenth, R. 2020. emmeans: Estimated marginal means, aka Least-Squares means.
Lytle, D. A., and N. L. R. Poff. 2004, February 1. Adaptation to natural flow regimes. Elsevier Ltd.

Marzolf, N. S., G. E. Small, and M. Ardón. (n.d.). Partitioning inorganic carbon fluxes in a Neotropical headwater stream, Costa Rica. in prep.
de Mendiburu, F. 2017. agricolae: Statistical Procedures for Agricultural Research.

Mulholland, P. J., A. V Palumbo, J. W. Elwood, and A. D. Rosemond. 1987. Effects of acidification on leaf decomposition in streams. Journal of the North Americal Benthological Society 6:147–158.

Oksanen, J., F. G. Blanchet, M. Friendly, R. Kindt, P. Legendre, D. McGlinn, P. R. Minchin, R. B. O'Hara, L. S. Gavin, P. Solymos, H. H. Stevens, E. Szoecs, and H. Wagner. 2019. vegan: Community Ecology Package.

Oviedo-Vargas, D., D. P. Genereux, D. Dierick, and S. F. Oberbauer. 2015. The effect of regional groundwater on carbon dioxide and methane emissions from a lowland rainforest stream in Costa Rica. Journal of Geophysical Research: Biogeosciences 120:2579–2595.

Palik, B. J., R. J. Mitchell, and J. K. Hiers. 2002. Modeling silviculture after natural disturbance to sustain biodiversity in the longleaf pine (Pinus palustris) ecosystem : balancing complexity and implementation. Forest Ecology and Management 155:347–356.

Peters, D. P. C., A. E. Lugo, F. S. Chapin, S. T. A. Pickett, M. Duniway, A. V. Rocha, F. J. Swanson, C. Laney, and J. Jones. 2011. Cross-system comparisons elucidate disturbance complexities and generalities. Ecosphere 2:1–26.

Pickett, S. T. A., and P. S. White. 1985. The ecology of natural disturbance and patch dynamics. Aca, Orlando, Florida.

Poff, N. L. 1992. Why Disturbances Can Be Predictable : A Perspective on the Definition of Disturbance in Streams Author ( s ): N . LeRoy Poff Source : Journal of the North American Benthological Society , Vol . 11 , No . 1 ( Mar ., 1992 ), Published by : The University of. Journal of the North American Benthological Society 11:86–92.

Poff, N. L., J. D. Allan, M. B. Bain, J. R. Karr, K. L. Prestegaard, B. D. Richter, R. E. Sparks, and J. C. Stromberg. 1997. The natural flow regime. BioScience 47:769–784.

Poff, N. L. R., and J. V. Ward. 1990. Physical habitat template of lotic systems: Recovery in the context of historical pattern of spatiotemporal heterogeneity. Environmental Management 14:629–645.

Pringle, C. M. 1991. Geothermally modified waters surface at La Selva Biological Station, Costa Rica: volcanic processes introduce chemical discontinuities into lowland tropical streams. Biotropica 23:523–529.

Pringle, C. M., G. L. Rowe, F. J. Triska, J. F. Fernandez, and J. West. 1993. Landscape linkages between geothermal activity and solute composition and ecological response in surface waters draining the Atlantic slope of Costa Rica. Limnology and Oceanography 38:753–774.

Pringle, C. M., and F. J. Triska. 1991. Effects of geothermal groundwater on nutrient dynamics of a lowland Costa Rican stream. Ecology 72:951–965.

Pringle, C. M., F. J. Triska, and G. Browder. 1990. Spatial variation in basic chemistry of streams draining a volcanic landscape on Costa Rica's Caribbean slope. Hydrobiologia 206:73–85.

Ramírez, A., and C. M. Pringle. 1998. Structure and production of a benthic insect assemblage in a neotropical stream. Journal of the North American Benthological Society 17:443–463.

Ramírez, A., and C. M. Pringle. 2006. Fast growth and turnover of chironomid assemblages in response to stream phosphorus levels in a tropical lowland landscape. Limnology and Oceanography 51:189–196.

Ramírez, A., C. M. Pringle, and M. Douglas. 2006. Temporal and spatial patterns in stream physicochemistry and insect assemblages in tropical lowland streams. Journal of the North American Benthological Society 25:108–125.

Ramírez, A., C. M. Pringle, and L. Molina. 2003. Effects of stream phosphorus levels on microbial respiration. Freshwater Biology 48:88–97.

Rauscher, S. A., F. Giorgi, N. S. Diffenbaugh, and A. Seth. 2008. Extension and intensification of the Meso-American mid-summer drought in the twenty-first century. Climate Dynamics 31:551–571.

Resh, V. H., A. V Brown, A. P. Covich, M. E. Gurtz, H. W. Li, G. Wayne, S. R. Reice, A. L. Sheldon, J. B. Wallace, and R. C. Wissmar. 1988. The Role of Disturbance in Stream Ecology Journal of the North American Benthological Society. Journal of the North American Benthological Society 7:263–288.

Rosemond, A. D., C. M. Pringle, and A. Ramírez. 1998. Macroconsumer effects on insect detritivores and detritus processing in a tropical stream. Freshwater Biology 39:515–523.

Rosemond, A. D., C. M. Pringle, A. Ramírez, and M. J. Paul. 2001. A test of top-down and bottom-up control in a detritus-based food web. Ecology 82:2279–2293.

Rosemond, A. D., C. M. Pringle, A. Ramírez, M. J. Paul, and J. L. Meyer. 2002. Landscape variation in phosphorus concentration and effects on detritus-based tropical streams. Limnology and Oceanography 47:278–289.

Sanford Jr., R. L., P. Paaby, J. C. Luvall, and E. Phillips. 1994. Climate, geomorphology, and aquatic systems. Pages 19–33 in L. A. McDade, K. S. Bawa, H. A. Hespenheide, and G. S. Hartshorn, editors. La Selva: Ecology and natural history of a Neotropical rain forest. University of Chicago Press.

Small, G. E., M. Ardón, A. P. Jackman, J. H. Duff, F. J. Triska, A. Ramírez, M. Snyder, and C. M. Pringle. 2012. Rainfall-driven amplification of seasonal acidification in poorly buffered tropical streams. Ecosystems 15:974–985.

Sousa, W. P. 1984. The role of disturbance in natural communities. Annual review of ecology and systematics. Vol. 15:353–391.

Stanley, E. H., S. M. Powers, and N. R. Lottig. 2010. The evolving legacy of disturbance in stream ecology: Concepts, contributions, and coming challenges. Journal of the North American Benthological Society 29:67–83.

Steinman, A. D., P. J. Mulholland, A. V. Palumbo, D. L. DeAngelis, and T. E. Flum. 1992. Lotic ecosystem response to a chlorine disturbance. Ecological Applications 2:341–355.

Steinman, A. D., P. J. Mulholland, A. V Palumbo, T. F. Flum, and D. L. DeAngelis. 1991. Resilience of lotic ecosystems to a light-elimination disturbance. Ecology 72:1299–1313.

Stumm, W., and J. J. Morgan. 1996. Acids and Bases. Pages 172–177 Aquatic chemistry: chemical equilibria and rates in natural waters. 3rd editio. Wiley, New York.

Torchiano, M. 2020. effsize: Efficient Effect Size Computation.

Townsend, C. R. 1989. The Patch Dynamics Concept of Stream Community Ecology. North Am. Benthol. Soc. **8**: 36–50.

Woodward, G., M. O. Gessner, P. S. Giller, V. Gulis, S. Hladyz, A. Lecerf, B. Malmqvist, B. G. McKie, S. D. Tiegs, H. Cariss, M. Dobson, A. Elosegi, V. Ferreira, M. A. S. Graça, T. Fleituch, J. O. Lacoursière, M. Nistorescu, J. Pozo, G. Risnoveanu, M. Schindler, A. Vadineanu, L. B. M. Vought, and E. Chauvet. 2012. Continental-Scale Effects of Nutrient Pollution on Stream Ecosystem Functioning. Science 336:1438–1440.

## Chapter 5: Conclusions

The results of this research inform our understanding of ecosystem processes across the global tropics and important processes in headwater tropical streams. In Chapter 2, I present a synthesis of gross primary production (GPP) and ecosystem respiration (ER) from tropical streams and rivers and determine the rates in these ecosystems and drivers are similar to their temperate counterparts. However, tropical streams and rivers may be more susceptible to climate warming, changes in biodiversity, and land cover change than temperate streams and rivers. In Chapter 3, I estimate carbon fluxes in a headwater tropical stream, presenting a combination of sensor measurements of $CO_2$ to measure in stream processes and inputs of terrestrial $CO_2$ to the stream. I found terrestrial $CO_2$ fluxes are large, $CO_2$ evasion to the atmosphere is high, and export of C reflects high $CO_2$ concentrations sustained by terrestrial inputs. Terrestrial C inputs are correlated with stream pH, quantifying a driver of stream acidification events. In Chapter 4, I explored the effects of disturbance, as episodic acidification events, in headwater tropical streams using a field experiment at individual, assemblage, and ecosystem scale. We find acidification does not inhibit processes in the study reaches, providing evidence for biotic adaptation to episodic acidification events in these streams and episodic acidification is a process-based disturbance rather than a discrete event.

# APPENDICES

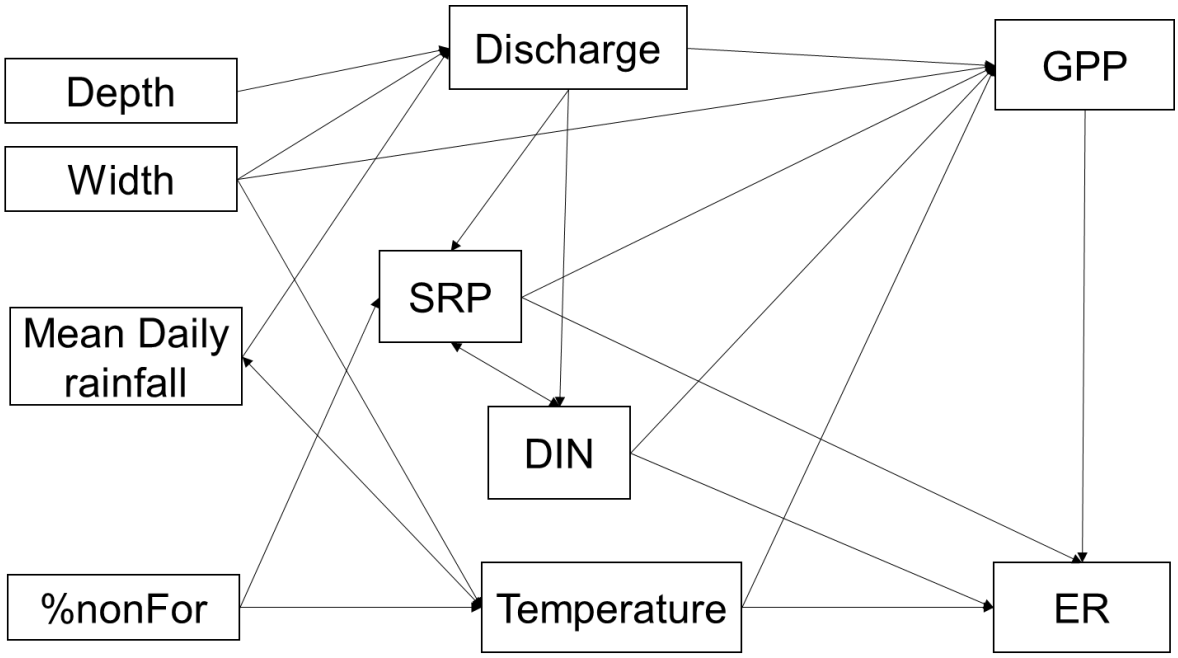

Appendix 1) meta-model for multivariate control of GPP and ER in tropical streams.

Appendix 2) Summary of structural equation model output. Standardized estimates correspond to values of linkages in Figure 6.

| Response | Predictor | Unstandardized Estimate | Standardized Estimate | Standard Error | *n* | *p* value | $r^2$ |
|---|---|---|---|---|---|---|---|
| ER | GPP | 0.27 | 0.45 | 0.07 | 83 | **<0.01** | 0.74 |
| | SRP | -0.50 | -0.76 | 0.08 | 61 | **<0.01** | |
| | DIN | 0.26 | 0.37 | 0.08 | 42 | **<0.01** | |
| | Rainfall | -1.61 | -0.65 | 0.34 | 83 | **<0.01** | |
| | Discharge | -0.18 | -0.47 | 0.08 | 76 | **0.04** | |
| | Width | 0.46 | 0.56 | 0.20 | 68 | **0.03** | |
| GPP | Discharge | 0.20 | 0.30 | 0.14 | 76 | 0.15 | 0.26 |
| | %Non-Forest | 0.81 | 0.51 | 0.23 | 70 | **<0.01** | |
| | Temperature | 1.40 | 0.16 | 1.20 | 77 | 0.25 | |
| Temperature | %Non-Forest | 0.04 | 0.22 | 0.03 | 64 | 0.13 | 0.19 |
| | Depth | 0.04 | 0.18 | 0.05 | 62 | 0.40 | |
| | Discharge | -0.07 | -0.87 | 0.02 | 72 | **<0.01** | |
| Discharge | Rainfall | -1.09 | -0.17 | 0.67 | 76 | 0.11 | 0.84 |
| | Width | 0.72 | 0.34 | 0.17 | 66 | **<0.01** | |
| | Depth | 1.88 | 0.65 | 0.28 | 66 | **<0.01** | |
| SRP | Depth | -1.17 | -0.68 | 0.40 | 51 | **<0.01** | 0.28 |
| | Rainfall | 2.03 | 0.53 | 0.71 | 61 | **0.01** | |
| | Discharge | 0.37 | 0.62 | 0.14 | 59 | 0.01 | |
| | Temperature | -0.66 | -0.08 | 1.24 | 59 | 0.60 | |
| DIN | Discharge | 0.24 | 0.43 | 0.14 | 42 | 0.09 | 0.30 |
| | Rainfall | 2.16 | 0.60 | 0.73 | 42 | **0.01** | |
| | Temperature | -2.85 | -0.38 | 1.43 | 42 | 0.06 | |
| DIN | SRP* | 0.49 | 0.49 | - | 42 | **<0.01** | - |
| Temperature | Rainfall* | 0.66 | 0.66 | - | 77 | **<0.01** | - |
| Width | Depth* | 0.68 | 0.68 | - | 58 | **<0.01** | - |

* Refers to correlated errors, not a direct pathway in the model

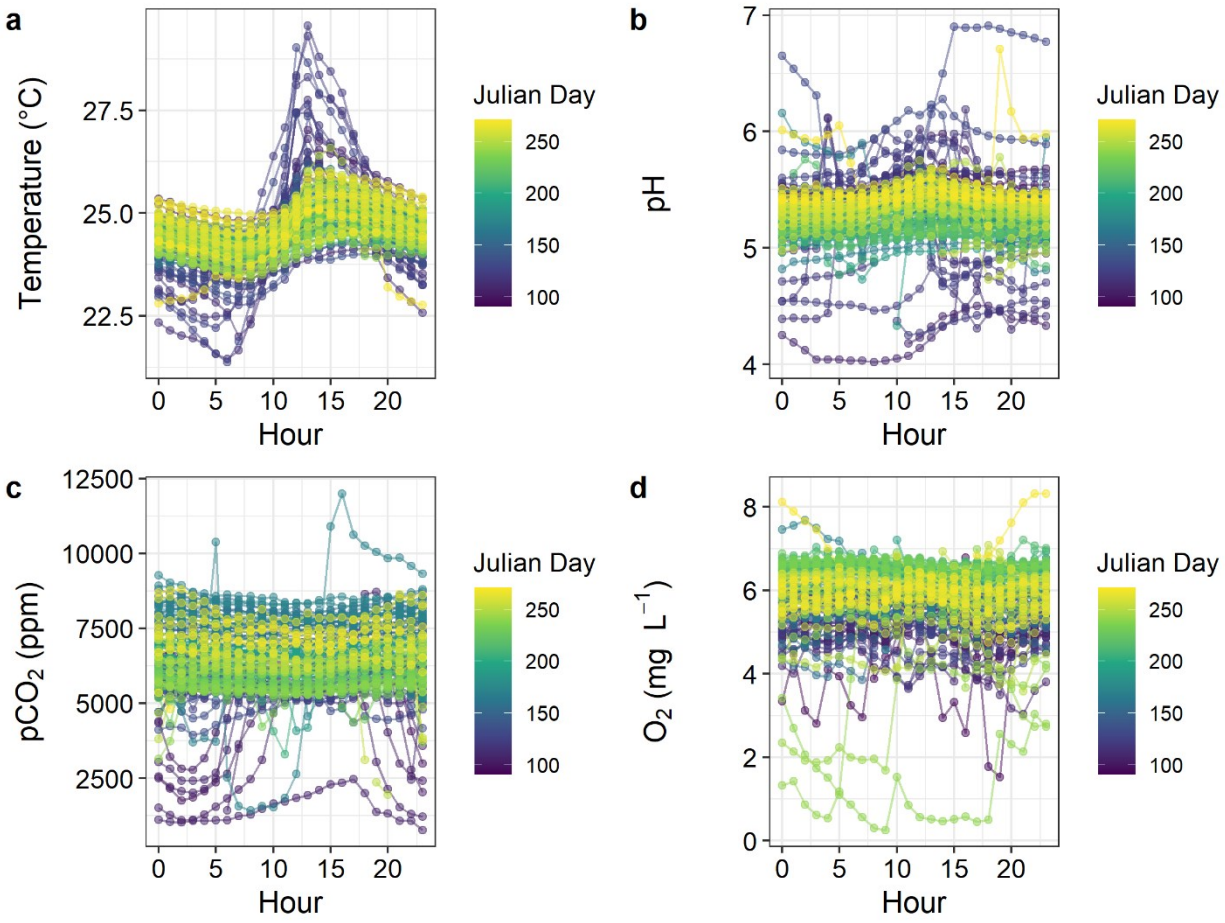


Appendix 3) Diel a) temperature, b) pH, c) $pCO_2$, and d) DO from the Taconazo. These plots highlight the variation observed within the span of each day of data collection, with blue colors representing the dry season (April) and lighter greens and yellows the wet season. We highlight: 1) diel temperature in the dry season that becomes muted during the wet season; 2) large pH variation, particular sustained low pH during the dry season; 3) little diel variation in $pCO_2$, though slight increases during night-time (6PM – 6AM) indicating aerobic respiration contributing to $pCO_2$; and 4) lack of diel variability, highlighting the lack of GPP in the Taconazo, and the small GPP that does occur is overcome by night-time increases in ER.

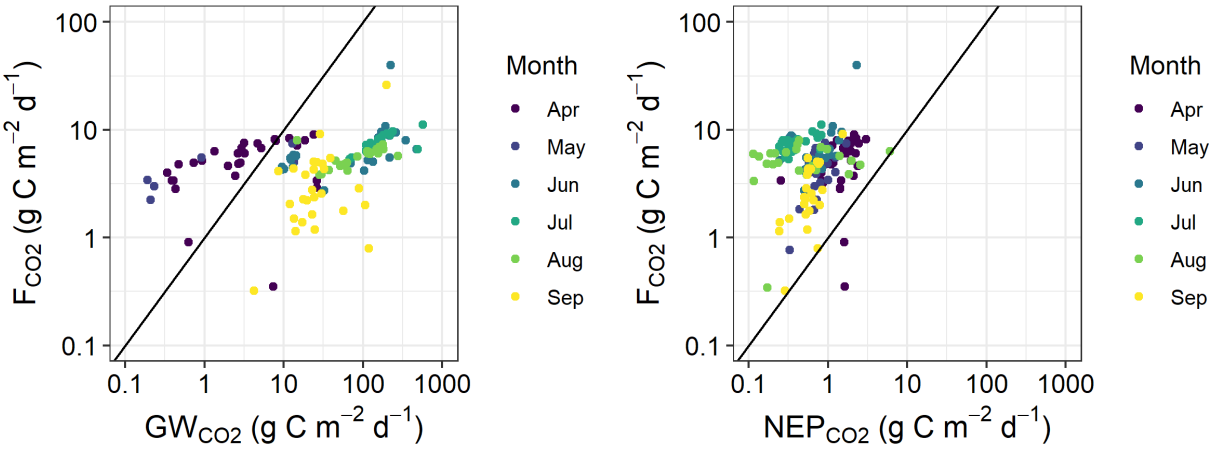


Appendix 4) Contributions of daily C inputs ($GW_{CO2}$ and NEP) to C evasion, $F_{CO2}$ in the Taconazo. Points are colored from the month of data collection. Solid line is the 1:1 line.

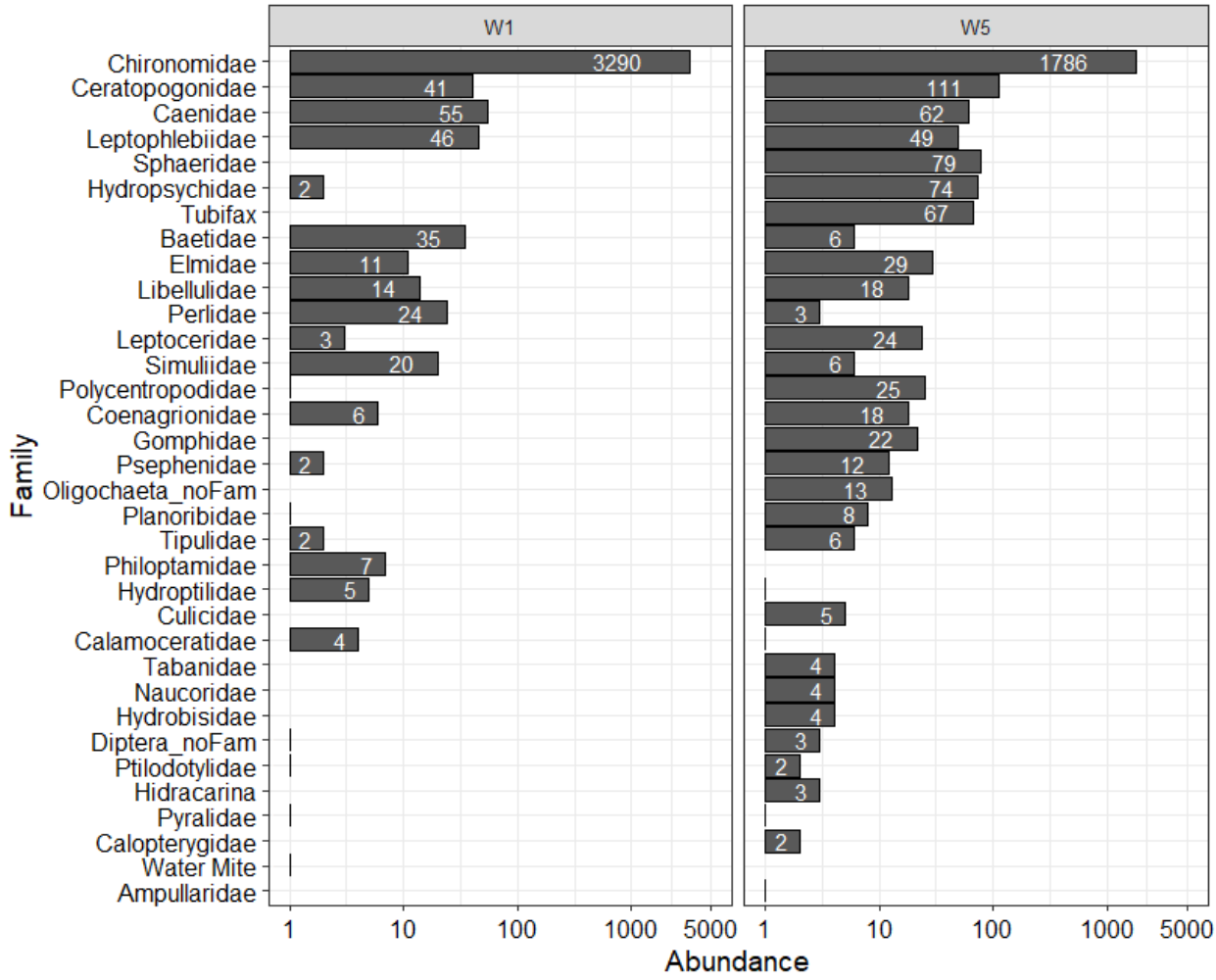


Appendix 5) Abundance of macroinvertebrate families identified from litter bags in Week 1 (left plot) and Week 5 (right plot) of the experiment, with values >1 in each bar. The subscript _noFam indicates no further taxonomic resolution could be identified. Note $\log_{10}$ x-axis.

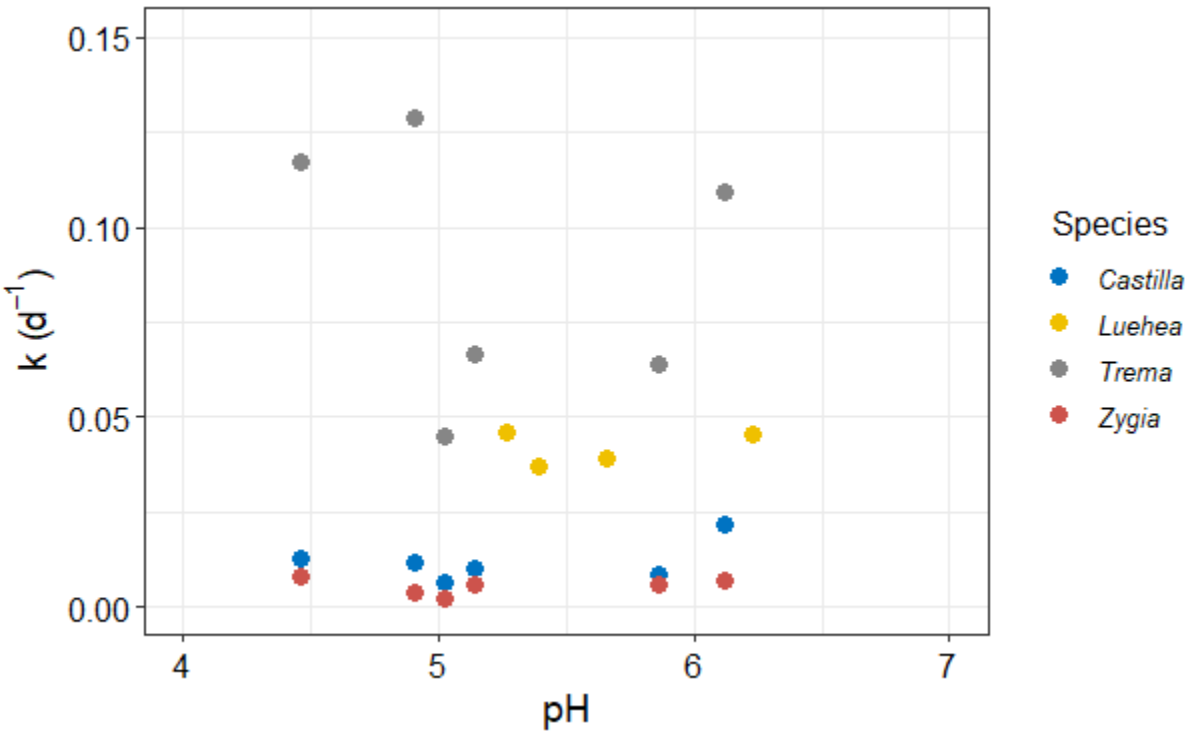


Appendix 6) Effect of stream pH on leaf litter decomposition rate, k ($d^{-1}$), across various streams at La Selva and species of leaf litter used. *Luehea* was used in this study and *Castilla, Luehea,* and *Zygia* data are from Ardón et al. (2006). Across multiples streams and leaf litter species, leaf litter decomposition varies little across pH at La Selva.